Sonochemical processes for the degradation of antibiotics in aqueous solutions: A review

Sonochemical processes for the degradation of antibiotics in aqueous solutions: a review

Pengyun Liu[1], Zhilin Wu[1], Anna V. Abramova[2], Giancarlo Cravotto[1,3]*

[1] Department of Drug Science and Technology, University of Turin, via P. Giuria 9, Turin, 10125, Italy.

[2] Federal State Budgetary Institution of Science N.S. Kurnakov Institute of General Inorganic Chemistry of the Russian Academy of Sciences, GSP-1, V-71, Leninsky Prospekt 31, 119991, Moscow, Russia.

[3] World-Class Research Center "Digital biodesign and personalized healthcare", Sechenov First Moscow State Medical University, 8 Trubetskaya ul, Moscow, Russia.

*Correspondence: giancarlo.cravotto@unito.it (G. Cravotto), Tel: +39.011.670.7183, Fax: +39.011.670.7162.

Abstract

Antibiotic residues in water are general health and environmental risks due to the antibiotic-resistance phenomenon. Sonication has been included among the advanced oxidation processes (AOPs) used to remove recalcitrant contaminants in aquatic environments. Sonochemical processes have shown substantial advantages, including cleanliness, safety, energy savings and either negligible or no secondary pollution. This review provides a wide overview of the different protocols and degradation mechanisms for antibiotics that either use sonication alone or in hybrid processes, such as sonication with catalysts, Fenton and Fenton-like processes, photolysis, ozonation, etc.

Keywords: Antibiotic degradation, Sonication, Sonocatalysis, Sono/Fenton, Sonophotocatalysis, Sonozonation.

Abbreviations of antibiotics:

AMP, ampicillin; AMX, amoxicillin; AZI, azithromycin;

CAP, chloramphenicol; CDX, cefadroxil; CEF, ceftriaxone; CEFX, cefalexin; CFX, Cefixime); CFZ, cefazolin; CIP, ciprofloxacin; CLA, clarithromycin; CLM, clindamycin; CLX, cloxacillin; CPD, cephadroxyl; CPX, cephalexin; CTC, chlortetracycline; CTX, cefotaxime;

DOXO, doxorubicin; DTC, deoxytetracycline; DXC, dicloxacillin;

EF, enrofloxacin;

FLU, flumequine;

GMF, gemifloxacin;

LEV, levofloxacin;

MNZ, metronidazole; MOX, moxifloxacin;

NAF, nafcillin; NOR, norfloxacin;

OFX, ofloxacin; OTC, oxytetracycline; OXA, oxacillin;

PG, penicillin G;

RIF, rifampin; RXM, Roxithromycin;

SA, sulfanilamide; SDZ, sulfadiazine; SMR, sulfamerazine; SMX, sulfamethoxazole; SMZ, sulfamethazine; SSZ, sulfasalazine;

TC, tetracycline; TNZ, tinidazole; TYL, tylosin.

1 Introduction

Antibiotics were first discovered in 1928 by Alexander Fleming and the term was first used in 1942 by Waksman and his collaborators [1, 2]. Initially, the classical definition of antibiotics was: chemotherapeutic agents that can eradicate or restrain the growth of microorganisms, including bacteria, fungi or protozoa [3, 4, 5]. Antibiotics have been widely used for the treatment of infectious diseases in humans and animals to the present day [4]. Macrolides, β-lactams, quinolones, tetracyclines, and sulfonamides are the most consumed antibiotics [6]. Since the 1990s, however, antibiotic residues have been broadly observed in aqueous matrices and soil as well as in microorganism, animal and human bodies over the world thanks to the appearance of the advance analytical technologies [5, 6].

The presence of antibiotic residues in the environment can either be caused by their continuous discharge or inherent high persistence [7]. For example, CEFX and CTX have attained levels surpassing 1000 μg/L in urban wastewater samples in Hong Kong and Shenzhen, South China [8]. 11 antibiotics in hospital wastewater and sewage treatment plants (STPs) have been identified in Beijing, China. Fluoroquinolones, in particular, were found to be the most abundant, with a highest concentration of 16.8 μg/L in the hospital samples. The maximum concentrations of antibiotics in STPs and hospital wastewater were 1-3 orders of magnitude higher than those in the surface water from the Wenyu River and groundwater [9].

Antibiotic concentrations in wastewater and environmental water bodies are obviously correlated with variations in annual consumption data [10]. Some antibiotics, such as penicillins, are easily degraded, whereas others, such as fluoroquinolones (e.g. CIP), macrolides (e.g. TYL) and tetracyclines, are considerably more persistent, resulting in their residues being found in the environment, spreading and accumulating in organisms [10]. Antibiotic occurrence in water is generally in the range of a few to hundreds ng/L [3, 5, 6, 10]. For examples, 77 antibiotics have been reported in Danjiangkou Reservoir in China, but most were present at lower than 5.0 ng/L and

77 SMX was the most abundant one [11]. 22 antibiotics, including eight quinolones, nine
78 sulfonamides and five macrolides, have been detected in the Huangpu River in
79 Shanghai, China, where the concentration of sulfonamides was in the range of 34–859
80 ng/L [12]. Sulfonamides (0.86–1563 ng/L) were also found to be the dominant
81 antibiotics in Baiyangdian Lake, China [13]. 9 antibiotics, including sulfonamides,
82 tetracyclines, quinolones and macrolides, have been investigated in 6 urban rivers in
83 Guangzhou, South China. NOR was the most abundant followed by CIP, and the highest
84 concentration was 2702 ng/L [14]. The concentrations of 4 quinolone antibiotics, OFX,
85 NOR, CIP and EF, ranged from 3.49-660.13 ng/L in the Qingshitan reservoir, South
86 China [15]. In addition, according to Ghernaout, *et al.* [8], an elevated number of
87 antibiotics, made up of sulfonamides, trimethoprim and macrolides, was found in
88 Japanese urban rivers.

89 As a side effect of antibiotic use, antibiotic-resistance genes and antibiotic-
90 resistant bacteria may be formed in microorganisms, causing a significant threat to
91 human health and ecological safety [5, 10, 16]. For example, OXA-resistant bacteria
92 are currently a serious problem in Latin American hospitals [17]. Meanwhile, other
93 adverse effects, such as endocrine disruption and aquatic toxicity, can also destroy
94 ecosystems [16].

95 Biological degradation [5], adsorption [18], reverse osmosis [18], ion exchange
96 [18] and advanced oxidation processes (AOPs), including ozonation [5], photocatalysis
97 [19-24], electrochemical degradation [23, 24], non-thermal plasma [25], Fenton/photo-
98 Fenton reaction [5], sonochemical degradation, and combination [26, 27], have been
99 extensively studied as means to remove antibiotics from aqueous matrices. Biological
100 processes are widely used in industrial effluent treatments with large effluent flow rates,
101 but the high concentration of pollutants in effluents with high toxicity are recalcitrant
102 to the microorganisms, resulting in limited antibiotic removal efficiency (RE) [5]. High-
103 concentration antibiotics can be transported from water matrices onto solid adsorbents
104 via adsorption, but the loaded adsorbents must be subsequently treated, causing higher

105 treatment costs [28, 29]. Reverse osmosis has been used to remove antibiotics with
106 larger molecules, it can efficient to reduce levels of dissolved salts. However, with this
107 process, the contaminants are slowly concentrated rather than removed. Besides, the
108 deterioration/fouling of the membrane structure caused by high-concentration
109 compounds is another drawback. Therefore, frequent back-washing and regeneration is
110 required [30].

111 Due to the limitations of physical and biological processes, AOPs have gradually
112 emerged as means for the degradation/mineralization of organic pollutants over recent
113 decades [31]. As non-selective oxidation technologies, AOPs have attained the total
114 removal of antibiotics, efficient reductions in toxicity and antimicrobial activity, and
115 have also increased biodegradability [17, 31-38]. The generation of reactive oxygen
116 species (ROS), such as $^{\bullet}O$, $^{\bullet}O^{2-}$, $^{\bullet}OH$, $^{\bullet}OOH$, H_2O_2, etc., via various methods was the
117 origin of AOPs [4, 10, 21, 22, 31, 33, 39-48].

118 Hydroxyl radicals ($^{\bullet}OH$) and other ROS are released by ozone (O_3) decomposition
119 in water during the ozonation process. Meanwhile, O_3 often selectively reacts with
120 nucleophilic molecules. However, the high costs of equipment, maintenance and
121 operation, the high quantities of energy required, lower mass transfer, extreme pH-
122 dependence and potential effluent ecotoxicity limit the application of ozonation [49,
123 50]. Photocatalysis has often been applied under ambient conditions and may gain
124 energy from sunlight with the advantages of simple operation and scale-up applicability,
125 but it also suffers from mass-transfer limitations, and is affected by catalyst amount,
126 light wavelength, radiation intensity, pH and water quality. Additionally, the catalysts
127 consumed need to be specially treated or recycled, causing high overall costs [19-22,
128 26, 27, 30]. Electrochemical degradation is an effective, versatile, cost-effective, easy
129 and clean technology, and is suitable for the treatment of toxic wastewater that contains
130 high-concentration antibiotics and COD. However, the RE depends on the nature and
131 structure of the electrode material, electrolyte composition, the applied current and the
132 diffusion rates of substrates to the active sites of the anode. The low flow rates and high

operating costs limit the application of electrochemical methods [23, 24]. Non-thermal plasma generated in electrical discharges in liquid or at the gas-liquid interface leads to the formation of ROS and the power introduced into the plasma is very high, leading to low energy yields [25]. The Fenton reaction is usually used in homogeneous and heterogeneous systems and in conjugation with UV radiation to enhance the oxidation process. However, the narrow acidic pH range of the operation and dissolved catalysts limits this process [5].

Sonochemical degradation (sonolysis), namely, degradation that is driven or enhanced by sonication, emerged in the 1990s. Ultrasound (US) is sound that exceeds the human hearing range, and has a wide frequency range of 18 kHz to 500 MHz [37, 45, 51-54]. Ultrasonic propagation, with cycles of compression and rarefaction, causes acoustic cavitation phenomena, which is defined as the sonochemical origin [52, 55-61]. Such numerous cavitation bubbles are also referred to as microreactors, since they act as the centre of chemical reactions [45, 62]. Gas-filled cavitation bubbles grow and extensively implode under the positive pressure that occurs during the compression cycle of US in water bulk [37, 45, 51, 52, 54]. Meanwhile, enormous local temperatures (ca. 5000 K) and high pressures (ca. 500 atm), microjets and shockwaves are produced [10, 27, 63, 64]. Subsequently, ROS are produced through the pyrolysis of water molecules at the collapsing bubbles (hotspots), and oxidize the substrates in water [45, 51]. Among these formed ROS, $^{\bullet}OH$ is a significantly important, very strong and nonspecific oxidizing species [45, 51, 54]. Besides, hydrophobic volatile compounds also suffer thermal decomposition at hotspots, and both the above actions contribute to the degradation of organic contaminants [65-67].

In theory, a large variety of organic pollutants are capable of being degraded by sonication without additional chemicals. Thus, sonication is usually seen as a green and safe technique to perform wastewater treatment. However, the sonolysis of organic contaminants has limited efficiency and consumes considerable amounts of energy [23, 45, 68]. To improve the RE and reduce energy consumption, sonication-based

combinations, such as sonocatalysis [69-73], Sono/Fenton [19, 21, 35, 43, 44, 74-77], sonication-ozonation (Sonozonation) [78-81], sonication-persulfate (Sono/PS) [82], sonophotocatalysis (Sono/Photo) [31, 39, 83-85], sonoelectrochemical degradation [86-88], sonication-microwaves [89], sonication-hydrodynamic cavitation [90], and ultrasound-assisted biological processes [91-93], have attracted great attention.

This review aims to provide an overview, and evaluate the REs, of the degradation of antibiotics in aqueous matrices by various sonochemical processes, including sonication alone [31, 36, 41, 46, 69, 71, 94-100], sonocatalysis [35, 40, 52, 72, 75, 101-110], Sono/Fenton [21, 22, 32, 33, 34, 35, 43, 44, 111, 112, 113], Sono/PS, Sono/Photo [20, 31, 39, 83, 84, 85, 114-119], sonozonation [78, 79, 80, 120-123], etc., and will focus on the degradation mechanisms and influence of operating conditions indicated in appriopriate studies that have been published in the last few years.

2 Antibiotic degradation by sonication alone

2.1 Mechanisms of sonolysis

In general, sonochemical degradation occurs in three reaction zones relative to the collapsing cavitation bubbles: inside the cavitation bubbles; in the interfacial region between cavitation bubbles and the bulk solution; and in the bulk solution [5, 10, 45]. Inside and around the collapsing cavitation bubbles, the thermal dissociation of water molecules and oxygen occurs to release ROS [45]. Moreover, hydrophobic volatile compounds around the hotspots are also thermally decomposed [10, 45, 62, 63, 64]. Hydrophilic and non-volatile compounds, such as LEV [42], that remain in the bulk solutions are oxidized by ROS. The sonochemical reaction with $^{\bullet}OH$ has been speculated to occur at the cavitation interface, where the maximum $^{\bullet}OH$ concentration is present [42]. Only ca. 10% of the radicals created in the interfacial region diffuse or escape to the bulk liquid [10, 41]. Therefore, antibiotic degradation is strongly dependent on the distance between non-volatile antibiotic molecules and the cavitation bubbles, and this distance is determined by hydrophobicity [4, 41, 42, 45].

Figure S1 clearly shows the HPLCs of SMT degradation and the appearance of intermediates with sonication time. In addition, LC/MS/MS analyses have indicated that the sonolytic degradation of SMT is mainly ascribed to OH oxidation. The sonolytic degradation pathway of SMT is shown in Scheme 1. As can be seen, SMT is first oxidized by •OH radicals, resulting in the formation of (OH)SMT and the cleavage of the N–S bond [41]. 4,6-dimethylpyrimidin-2-amine, sulfanilic acid and the mono-hydroxyl derivative of sulfanilic acid are probably produced by the cleavage of the N–S bond of SMT or (OH)SMT. The mono-hydroxyl derivative of sulfanilic acid may also be formed by the •OH radical that directly attacks the sulfanilic acid. Aniline is an intermediate product in SMT degradation via the breakage of the C–S bond in SMT or sulfanilic acid, and can be oxidized to phenol [41].

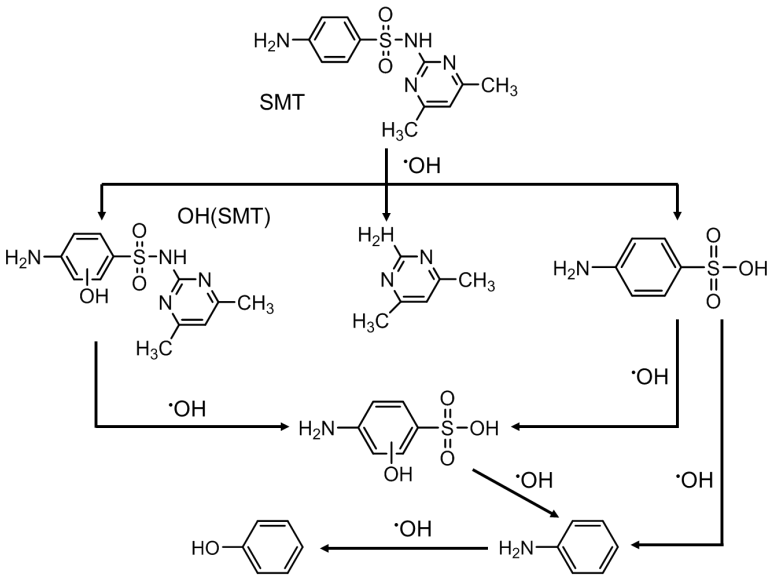

Scheme 1 *Pathway of intermediate formation in the sonolytic degradation of SMT [41].*

However, the sonochemical degradation products were rarely mineralized. About 100% of 180 μM SMT was decomposed, but only 8.31% TOC was reduced by sonication for 2 h at 800 kHz and 100 W. Fortunately, the effluent became much more biodegradable (BOD_5/COD was increased from 0.04 to 0.45), indicating that the toxicity of the effluent to microorganisms was obviously reduced [41].

Extensive investigation with the addition of a radical scavenger, such as isopropyl

alcohol, ethanol, methanol [41], *n*-butanol [97], terephthalate (TA) and Suwannee River Fulvic Acid (SRFA) [124], has revealed that reaction with •OH is the main degradation route for antibiotics during sonication [41, 97, 124, 125]. For example, with a hydrophobic character in the whole pH range, *n*-butanol diffuses to the gas/liquid interface of the microbubbles where it is able to scavenge •OH and quench the antibiotic degradation as a consequence [97]. In the presence of TA, CIP (a hydrophilic compound) degradation was inhibited by a factor of 40–1500 depending on the frequency and initial concentration, while degradation was slightly affected by SRFA [124]. TA reacts with •OH in bulk solution and accumulates around cavitation bubbles, greatly quenching •OH, while SRFA stays in bulk solution and catches •OH and competes with CIP [124].

In addition, the inhibition of DXC degradation via the addition of a radical scavenger (2-propanol or glucose) was observed [96]. DXC degradation was not affected significantly when low- or high-concentration glucose (high hydrophilicity) and low-concentration 2-propanol (miscible with water) were individually added. It was speculated that both glucose and low-concentration 2-propanol are dissolved in the bulk liquid far away from the bubbles, while DXC is relatively closer to the cavitation bubbles. As a result, no competing reactions between glucose or 2-propanol with •OH occurred around the hotspots. However, a significant decrease in the DXC degradation rate was observed in the presence of a high concentration of 2-propanol due to its relatively high volatility [126]. Therefore, the addition of the radical scavengers confirmed that •OH-mediated reactions either occur at the interface of the cavitation bubbles, or in the bulk liquid depending on the properties of the antibiotics [65, 97]. Unreacted •OH will be recombined into H_2O_2, for example, 77.6 and 57.3 μM of H_2O_2 have been observed as being generated after 30 min sonication in the presence of AMP and NAF, respectively [69].

Overall, two reaction mechanisms are presumably responsible for the sonolysis of antibiotics: pyrolysis and oxidation by the •OH generated in the system [27, 43, 52, 53].

2.2 Application of sonication for antibiotic degradation

Sonication systems used for the degradation of antibiotics mainly include ultrasonic horn-type and bath-type apparatus, as shown in Figure 1.

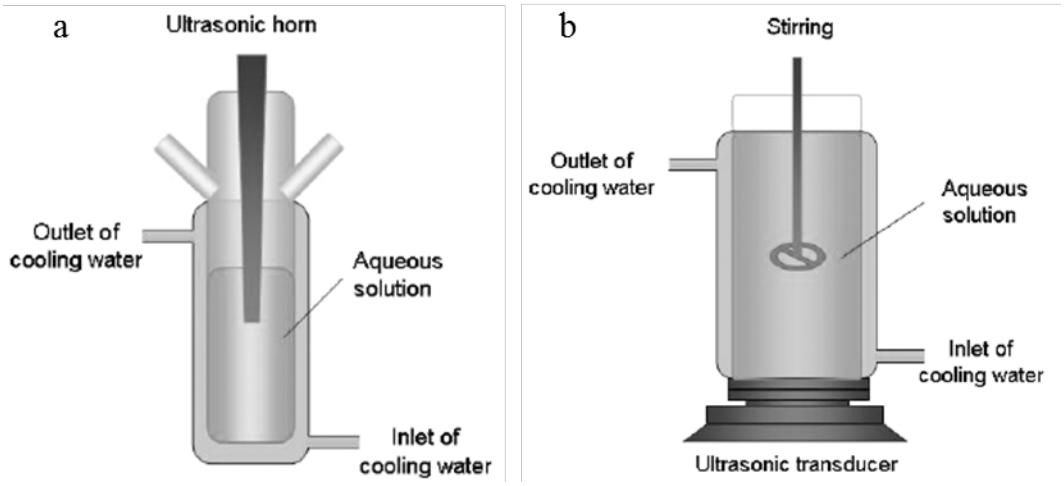

Figure 1 *Schematic diagram of ultrasonic horn-type (a) and bath-type (b) setups for degradation. Reprinted from ref. [68] Copyright (2006), with permission from Elsevier.*

Hapeshi, *et al.* have investigated the degradation of OFX using a 20 kHz horn-type ultrasonic reactor. The results showed that the RE of OFX increases with increasing US power density and decreasing initial OFX concentration. Under the optimal conditions, 27.7 μM OFX and 640 W/L of US power density, the RE of OFX in a 350 mL solution reached 31% after 240 min sonication [36]. As a result, 12.5 nmol of OFX was removed per minute by 20 kHz sonication, and the radical reactions are responsible for OFX degradation.

Villegas-Guzman, *et al.* have studied the degradation of DXC using a 600 kHz bath reactor [96]. 210 μM DXC was fully removed in 100 mL aqueous solution for 180 min under acid and neutral conditions. Thus, 117 nmol of DXC was removed per minute by 600 kHz sonication with 0.6 W/L of power density. However, no significant change in TOC concentration and a 30% reduction in COD were observed during 480 min of sonication, indicating that either no or less mineralization occurred under sonication alone.

To date, sonication has been extensively used to probe the RE of a large number of antibiotics, which are summarized in Table 1.

Table 1 *Summary of the degradation of antibiotics in water by sonication alone.*

Antibiotics	F_{US}/P_E (kHz/W)	P_{US}(W)	t (min)	C_0/V (mg/L)/mL	pH	RE (%)	Other results	Refs.
OFX	20/224	-	240	10/350	-	31	Mainly radical reactions.	[36]
LEV	20/400	-	20	20/50	5.9	9.4	BOD_5/COD increased.	[42]
CIP	20/-	20	-	-/50	8.5	-	CIP is far away from cavitation bubbles.	[124]
CPX	24/200	17.3	60	20/50	6.5	~52	BOD_5/COD ratio was raised.	[127]
PG	35/860	-	70	200/50	3.0	66.7	RE is pH dependent.	[95]
PG	40/100	-	60	50/1000	-	-	24.8% COD was removed.	[114]
CIP	205/-	13.5	35/70	10 μM/300	3.5	~65	Molar volume is critical.	[70]
PG	205/-	13.5	35/70	10 μM/300	3.5	<10	Molar volume is critical.	[70]
OXA	275/60	20.7	120	20/250	5.6	100	Mineralization is difficult	[128]
CIP/NOR/ CPX/CDX/ OXA/CLX	354/-	26.4	75-120	40 μM/300	6.5	-	Hydrophobicity was critical.	[129]
CIP	520/-	13.8	120	15/150	3.0-10.0	57	*RE* is pH-dependent.	[38]
CIP	544/200	-	150	15/<1000	7.0	~60	544 kHz>801/1081 kHz	[125]
SDZ	580/-	22	120	25/250	5.5	90	H_2O_2 affects negatively	[97]
DXC	600/60	34.8	300	0.21 mM/300	3.0	100	~ 0 mineralization was obtained.	[130]
DXC	600/60	34.8	480	98.8/100	5.5	100	30% of COD was eliminated.	[96]
SMZ	800/100	-	120	180 μM/-	-	100	8.31% TOC was reduced.	[41]

Note: F_{US}: ultrasonic frequency; P_E: electrical power input; P_{US}: the power dissipated by the reactor (calculated using the calorimetric method); t: sonication time; C_0: initial antibiotic concentration; V: volume of solution; RE: removal

efficiency; Refs.: references.

As listed in Table 1, the sonolysis of CIP, CPX, LEV, PG and OFX, etc., have been conducted at low US frequency (20-40 kHz) and high electrical power (200-860 W); their REs are lower, liying in the range of 9.4%-66.7% after 20-240 min sonication. In addition, COD was slightly removed, leading to an increasing BOD_5/COD ratio. By contrast, the sonolysis of CDX, CIP, CLX, CPX, DXC, NOR, OXA, PG, SDZ and SMZ, etc., was performed at medium US frequency (205-600 kHz) and lower electrical power (60-200 W), and their REs are relatively higher, lying in the range of 10%-100% after 35-300 min sonication. However, the mineralization of antibiotics is difficult under sonication alone.

2.3 Role of effective factors

Under sonication, the degradation of antibiotics mostly occurs via radical reactions in the bulk liquid and generally follows pseudo-first order (PFO) kinetics [38, 69, 96, 99]. The degradation rate and RE of antibiotics are dependent on many factors, such as US frequency [36, 42, 97, 129], power [36, 96, 97], and sonication mode (continuous or pulse) [70], chemical structure and physicochemical properties [129, 131], initial concentration [36, 129, 131], solution volume [36, 69, 132], pH value [38, 97], temperature [33, 40, 111, 125], and sonication time [36, 129, 131, 132], etc. The influence of the critical parameters on the sonochemical degradation of antibiotics is discussed below.

2.3.1 Effect of US frequency and power

As summarized in Table 1, the radical reactions that take place in the bulk liquid dominate antibiotic degradation, while more reactive radicals are formed at higher ultrasonic frequencies, e.g., 300-1000 kHz, than at lower frequencies, e.g. 20-45 kHz [54, 68]. Therefore, higher REs for SDZ at 580 kHz and 22 W [97], and for AMP at 375 kHz and 24.4 W (actual ultrasonic powers, determined by calorimetric method) [46] have been observed. Al-Hamadani, *et al.* have investigated the degradation of SMX by

sonication in the absence of catalysts [71]. The removal of 10 μM SMX was higher at 1000 kHz sonication for 60 min (72%, 160 nmol/min of removal rate) than at 28 kHz sonication (33%, 55 nmol/min of removal rate), while all other experimental conditions remained the same (0.18 W/mL of US power density at pH 7 and 15 °C in 1000 mL solutions), because more •OH were generated at 1000 kHz than at 28 kHz [71]. In addition, 187.29 nmol (90%) SDZ was removed per minute in 250 mL of 0.1 mM aqueous SDZ solutions for 120 min under 580 kHz sonication at 30 °C and pH 5.5, whereas 41.7 nmol (82%) AMP was removed per minute in 250 mL of 0.03 mM aqueous AMP solutions after 180 min under 375 kHz sonication at 20 °C and pH 6.5.

Higher RE of antibiotics can be generally achieved at higher US energies and higher dissipated powers [31, 36, 41, 69, 94-100]. At higher input powers (400-600 W), however, a large number of gas bubbles exist in solution, which has been seen to scatter the US to the walls of the vessel or back to the transducer. Thus, less energy is dissipated into the liquid, as a result of cavitational activity, although the vessel was exposed to higher power [42]. In addition, changing the solution volume inside the reactor also changes the power density, which also significantly affects the degradation rate; increasing the solution volume will decrease the degradation rate [132].

2.3.2 Effect of Physicochemical properties of antibiotics

The physicochemical properties of antibiotics greatly affect their sonochemical degradation, with sonochemical eliminating showing significant selectivity for certain antibiotics in aqueous matrices [129]. Serna-Galvis, *et al.,* have studied the degradation of various antibiotics, including fluoroquinolones (CIP and NOR), penicillins (OXA and CLX) and cephalosporins (CPX and CPD) using 354 kHz sonication [129]. Different degradation rates, CLX > OXA > CPX > NOR > CIP > CDX, were observed under identical sonication conditions: 200 W; 375kHz; 300 mL of 40 μM of antibiotics, pH 6.5 [129]. Similarly, NAF was degraded faster than AMP by 375 kHz and 24.4 W sonication at pH 6.5 and 20 °C for 250 mL in 30 μM aqueous AMP solutions, and the rate constants of PFO (k_1) of NAF and AMP were calculated to be 0.5 min^{-1} and 0.4

314 min^{-1}, respectively [69].

315 It has been demonstrated that the initial degradation rate of pollutants exhibited
316 good correlation with LogP (Octanol-water partition coefficient, i.e., the
317 hydrophobicity). Thus, the fast elimination of penicillins is attributed to their high
318 hydrophobicity, leading to the accumulation of penicillins near cavitation bubbles,
319 compared to fluoroquinolones or cephalosporins [129]. In addition, Lastre-Acosta, *et*
320 *al.* have indicated that the sonochemical degradation mechanism of SDZ is directly
321 related to the *pKa*-dependent speciation of SDZ molecules [97]. Moreover, small-sized
322 molecules (molar volumes less than 130 mL/mol) more quickly diffuse to bubble
323 interfaces and are impacted most by pulsing US, resulting in a higher portion of the
324 antibiotic in and around cavitation bubbles. Large-sized molecules slowly diffuse to the
325 bubble surface, resulting in a higher portion of these personal care products (PPCPs)
326 degrading in bulk solution [70].

327 ### 2.3.3 Effect of pH value

328 The effect of pH value on antibiotic degradation is also related to the properties of
329 antibiotics (i.e., ionic species or molecule states). Some antibiotics are more
330 sophisticated, being zwitterions (a molecule containing both a basic and an acidic
331 group). For example, LEV has two different acid-dissociation constant values (*pKa* 5.7
332 and 7.9) [124]. De Bel, *et al.* have explored the effect of pH on CIP sonolysis at 520
333 kHz [38]. The k_1 value (0.021 min^{-1}) at pH 3 is almost 4-fold higher than those at pH 7
334 (0.0058 min^{-1}) and pH 10 (0.0069 min^{-1}). The solution can even be considered readily
335 biodegradable after sonication at pH 3 ($BOD_5/COD > 0.4$) [38]. Degradation is clearly
336 faster when the main part of the CIP molecules carries an overall positive charge. These
337 positively charged molecules will accumulate at the negatively charged liquid–bubble
338 interface, where the concentration of ROS and the reaction temperature are higher.
339 Hence, degradation is faster [38]. Similarly, Villegas-Guzman, *et al.* have found that
340 the highest sonolysis of DXC was achieved under 600 kHz sonication at pH=3 [96].
341 Acidic media also favour the sonochemical degradation of DXC (pH=3.0) [30], LEV

(pH =5.9) [42], SDZ (pH=5.5) [97], and TNZ (pH=3.0) [100], etc.

By contrast, Wang, *et al.* have reported that the TC degradation rate is highly pH-dependent, and that higher pH values favour TC degradation under sonication, due to the transformation of TC molecules at different pH values [99].

2.3.4 Effect of temperature

Generally, the degradation rate of antibiotics increases with increasing temperature [33, 40, 125]. The influence of temperature on the sonodegradation of antibiotics is complicated. As far as we know, high temperature usually results in a high solvent vapour pressure, followed by the formation of more water-vapour-containing cavitation bubbles, causing the cavitation bubbles to collapse less violently, which leads to reduced $^{\bullet}OH$ production. However, the reduction of the viscosity and surface tension at high temperatures leads to a low threshold intensity for cavitation, which can increase the number of cavitation bubbles, and then promote the generation of $^{\bullet}OH$ and $HOO^{\bullet}$. Moreover, the strengthened reactions of the hydroxyl radicals and mass transfer at high temperatures are favourable to the removal of antibiotics [33, 40, 111, 125]. According to De Bel *et al.*, increased temperature (15-45 °C) leads to faster CIP degradation (k_1 was increased from 0.0055 to 0.0105 min^{-1}). The low apparent activation energy (17.5 kJ/mol) suggests that the degradation of CIP is diffusion controlled (usually in the range of 12-15 kJ/mol) [125]. Higher temperature (in the range of 30-60 °C) facilitates the removal of FLU by the Sono/H_2O_2 process [111]. 3% of FLU was removed from 200 mL of 1 mM aqueous FLU solutions for 120 min under 40 kHz and 120W sonication at 60 °C and pH 4 in the presence of 20 mM H_2O_2. The activation energy for the degradation of FLU was 6.510 kJ/mol [111].

2.3.5 Effect of initial concentration of antibiotics

In general, low concentrations of antibiotics favour their sonochemical degradation; RE decreases with increasing initial concentration [30, 31, 36, 41, 69, 94-100]. The degradation of antibiotics is limited by the available surface at the bubble–

liquid interface. According to the Arrhenius law, for example, the apparent activation energy for the sonochemical degradation of CIP has been determined to be 17.5 kJ/mol, which suggests that the degradation of CIP is diffusion controlled. A Langmuir-type heterogeneous-reaction-kinetics model could be used to explain why the k_1 value increases with decreasing initial CIP concentration from 0.0204 min^{-1} (C_0: 0.15 mg/L) to 0.0009 min^{-1} (C_0: 150 mg/L). According to the model, the molecules at the interface region of the cavitation bubbles can be readily oxidized by the formed •OH [125].

2.3.6 Effect of additives

Antibiotics can be degraded to a certain degree by sonication alone, but the REs of non-volatile compounds are somewhat lower and degradation is really time consuming. For example, it has been observed that only 30% DXC was degraded after 8 h [96], and most antibiotics were converted into hydrophilic organics rather than CO_2 [17]. Although the BOD_5/COD ratio (biodegradability) noticeably increased, e.g., from 0 to 0.36, after the sonochemical degradation of CPX [127], the mineralization of antibiotics is challenging even after a long period of sonication [30, 98, 127, 128]. For example, 180 μM SMZ was almost fully removed, but only 8.31% TOC was reduced by sonication at 800 kHz and 100 W in 2 h [41]. Therefore, a great deal of effort has been devoted to enhancing sonolysis to increase the RE, with an eye on practical applications, using simple additives, such as noble gas Argon (Ar), anions, CCl_4, H_2O_2, etc. in the sonication system.

Due to Ar's physical properties (e.g. solubility, thermal conductivity and specific heat ratio), an Ar atmosphere favours sonolytic activity compared to diatomic gases [36, 109]. Gao, *et al.* have reported that the sonolytic degradation of SMZ is accelerated in the presence of Ar or O_2, but inhibited by N_2 [41]. Meanwhile, the SMZ degradation rate was slightly inhibited by NO_3^-, Cl^- and SO_4^{2-}, which is consistent with the sonochemical degradation of TC [99], but significantly improved by HCO_3^- and Br^- [41]. The enhancement of TC degradation by adding HCO_3^- has also been demonstrated [99], while a negligible influence was observed when adding mannitol or

calcium carbonate during the sonochemical degradation of OXA at a high frequency in wastewater (from a municipal wastewater treatment plant) [128]. In another sonication system, KI and H_2O_2 were used as an iodine source to enhance the RE of SMZ, and the RE value increased from 3.4 to 85.1 under 60 min sonication with 0.04 mM SMZ, 2.4 mM KI and 120 mM H_2O_2 at 195 W US under acidic conditions. $I^{\bullet}$ and $I^{2-\bullet}$ radicals were the most predominant active species. The activation energy of SMZ degradation was calculated to be 7.75 ± 0.61 kJ/mol (15–55 °C), which indicates that the reaction is potentially a diffusion-controlled process [98]. Furthermore, the addition of CCl_4 can also enhance sonochemical degradation, which is attributed mainly to the formation of chlorine-containing oxidizing species, such as HClO, Cl_2, $^{\bullet}Cl$, $^{\bullet}CCl_3$ and $^{\cdot}CCl_2$, from the sonolysis of CCl_4 [42, 133].

Zhang, *et al.* have investigated the degradation of sulfa antibiotics by potassium ferrate in combination with sonication (Sono/Fe(VI)) [75]. SDZ, SMR and SMX were all well degraded by sonication, and the reaction process was in accordance with pseudo-second order reaction kinetics; the REs of SDZ, SMR and SMX were 77.5, 82.5 and 82.5% for 30 min sonication, respectively. H_2O_2 was often added to the sonication system to enhance antibiotic degradation [36, 99, 100, 132]. Matouq, *et al.* have investigated AMX degradation at 2.4 MHz sonication, with the addition of H_2O_2 providing a great increase to the RE of AMX [132]. The effect of adding H_2O_2 to the sonochemical degradation of antibiotics has been summarized in Table 2.

As seen in Table 2, the sonolysis of TC, LEV, NOR, MTZ, OFX and FLU, etc., has been conducted in a US-frequency range of (20-2400 kHz) and a US-power range of (100-750 W). Their REs are located in the range of 1.88%-81.00%, under sonication alone, and 0-30%, under oxidation alone with 0.29-333.00 mM H_2O_2 for 30-240 min. In some cases, significantly higher REs (5.9-93%) were given by sono/H_2O_2 processes than in those performed with sonication alone, or oxidation with H_2O_2 alone. In addition, COD was slightly removed, leading to increasing ratio of BOD_5/COD.

Table 2 *Summary of sonochemical degradation of antibiotics in the presence of H_2O_2.*

Antibiotics	C_{H2O2} (mM)	F_{US}/P_E (kHz/W)	t (min)	C_0/V (mg/L)/mL	pH	RE_{H2O2} (%)	RE_{Sono} (%)	$RE_{Sono/H2O2}$ (%)	Refs.
TC	0.29	20/400	60	10/100	5.5	*~0*	*81.0*	*93.0*	[99]
LEV	5.0	20/195	150	20/100	7.1	6.7	1.9	*65.0*	[43]
NOR	20.0	20/240	30	5/200	7.0	~0	<5.0	5.9	[20]
MTZ	60.0	20/-	180	500/200	3.0	-	*42.0*	*68.0*	[41]
OFX	100.0	20/224	240	10/350	-	-	31.0	*50.0*	[36]
TNZ	333.0	120/750	150	80/100	3.0	-	*5.0*	*75.0*	[100]
CLM	1.0	130/500	150	45/-	3.0	~25.0	~30.0	~45.0	[21]
CIP	1.0	580/-	60	100/250	3.0	5.9	35.8	36.5	[32]
AMX	5.0 mL	2400/9.5	90	50/50	3.5-5.5	*~30.0*	-	70.0	[132]

Note: C_{H2O2}: H_2O_2 concentration; F_{US}: ultrasonic frequency; P_E: electrical power input; t: sonication time; C_0: initial antibiotic concentration; V: volume of solution; RE: removal efficiency; Refs.: references.

However, the addition of H_2O_2, used as a radical promoter, does not always promote sonication processes [20, 32]. When sonication was applied without H_2O_2, degradation and mineralization (35.8 and 22.6%, respectively) were similar to the results obtained in sono/H_2O_2 processes (36.5 and 24.4%, respectively) [32]. Therefore, excess H_2O_2 can act as a $^{\bullet}OH$ scavenger and decrease the RE of antibiotics, resulting in the presence of an optimal amount of H_2O_2 for the sonochemical degradation of the target compounds.

In addition, Serna-Galvis, *et al.* have reported the role of mechanical agitation in the removal of OXA (or AMP) via sonication [129], photo-Fenton, TiO_2 photo-electro [17, 69, 128], and sono-Fenton processes [46]. These results suggest that mechanical agitation is not required in the processes that involve sonication on the lab-scale [17, 46, 69, 128, 129]. The exception is the degradation of CIP in the US-assisted *Laccase* catalytic process, in which degradation increased from 8% to 50%, due to improved mass transfer, when the agitation speed was increased from 0 rpm to 200 rpm. However, no further enhancement in degradation efficiency was observed when the agitation speed was increased to 300 rpm [91].

Moreover, although the application of sonication has been shown to be feasible on small scales, its use in large-scale treatment process is still a challenge because of high

energy requirements [105]. Therefore, sonication has been combined with other additives (catalysts and persulfate) and other AOPs (Fenton reaction, photocatalysis, ozonation, etc.) to increase the RE, reduce reaction times and enhance mineralization [36, 38]. These hybrid methods are discussed below.

3 Degradation of antibiotics by sonocatalysis

The ability of sonication to enhance the heterogeneous catalytic degradation of antibiotics is discussed in this section, while the role of sonication in the homogeneous catalytic degradation of antibiotics, mainly Fenton reactions, will be discussed in the following section. In most cases, higher REs are obtained by sonocatalysis than the sum of those obtained under catalysis and sonication alone [40, 44, 71, 102, 103, 106, 109, 134, 135]. More importantly, antibiotics, such as TC, OTC, CTC and DTC, can be decomposed into a suite of non-toxic intermediates by sonocatalytic processes [136]. For example, GMF was first decomposed to aromatic and aliphatic intermediates in the early stage of reactions, and then mineralized to CO_2, H_2O and inorganic ions, leading to significant reductions in solution toxicity after the sonocatalytic degradation of GMF [103]. Similarly, a substantial reduction in the toxicity of an AMP solution has been observed after the sonocatalytic degradation of AMP with Zn(OH)F [101].

A bio-toxicity examination, using an inhibition test conducted on activated sludge, revealed diminishing oxygen-consumption-inhibition percentage [IOUR (%)], from 33.6 to 22.1%, during the sono/ZnO/nano-cellulose process. The utilization of the sono/ZnO/nano-cellulose process can convert TC molecules to less toxic compounds. However, longer reaction times are required for complete conversion into non-toxic substances [104].

3.1 Mechanisms of sonocatalysis

In sonocatalytic systems, $^{\bullet}OH$ radicals are the dominant reactive species that contribute to antibiotic degradation. The pronounced degradation effectiveness with the catalysts under sonication can be assigned to their synergetic ability to produce ROS

and subsequent radical reactions [109]. Sonocatalysis includes two reaction pathways (Figure 2): (1) catalytic degradation enhanced by sonication; (2) sonolysis enhanced by the catalyst.

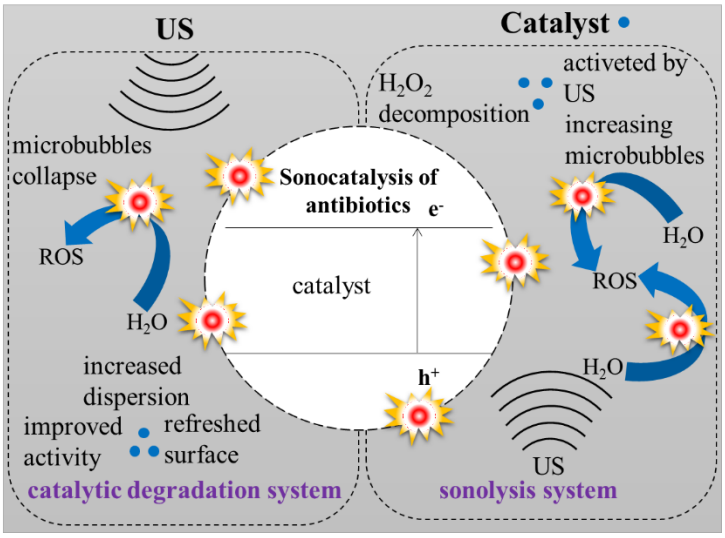

Figure 2 *The mechanisms of antibiotic removal by sonocatalysis.*

In an attempt to clarify the effects of sonication on heterogeneous catalysis, increased dispersion has been considered as a reason for the increased reaction rate. The removal of the passivating layer, the reduction of the catalyst particle size and enhanced interparticle collisions, all induced by cavitational shock waves and local turbulent microjets, may increase the number of active reaction sites on catalysts as well as increasing the contact area, improving mass transfer and minimizing fouling, which all result in increased catalytic activity [52].

In homogeneous systems, it is also critical to activate the catalyst and to keep it active during antibiotic degradation. Sonication can improve mass transfer, catalyst activation and the production of higher ROS concentrations, e.g., in Fenton reactions [77, 137]. Organometallic compounds are often used for the homogeneous catalysis of various reactions. The starting organometallic compound, however, is often catalytically inactive until it loses the metal-bonded ligands (such as carbon monoxide) from the metal. Sonication can induce ligand dissociation, making the initiation of homogeneous catalysis by sonication practical. The transient, coordinatively

unsaturated species produced from the sonolysis of metal carbonyls are likely candidates [37, 52].

On the other hand, solid catalyst particles may increase the density of microbubbles, meaning that more ROS will be produced during bubbles collapse. H_2O_2 formation is significantly increased due to the dispersion of catalysts under sonication, indicating that the dispersed catalyst particles can act as additional nuclei for the pyrolysis of water molecules and the formation of $^{\bullet}OH$ [40]. As a result, increased radical transfer from cavitation bubbles to the interface and bulk solution is promoted, and with it the RE of antibiotics [37, 52, 126]. In homogeneous systems, catalysts, such as Fe^{2+}, promote radical formation via the decomposition of H_2O_2, formed under sonication, to enhance and accelerate the degradation of antibiotics [137, 138]. For example, the sonolysis of SMZ was accelerated in the presence of ferrous ion. The synergetic effect was mainly attributed to the production of additional $^{\bullet}OH$ via Fenton chemistry [41].

3.2 Application of sonocatalysis in antibiotic degradation

To date, a great many catalysts, including single walled carbon nanotubes (SWNTs) [40, 71], novel Fe-Cu layered double hydroxide/biochar nanocomposites (Fe-Cu-LDH/biochar) [102], biochar-supported ZnO nanorods (ZnO-biochar) [103], ZnO nanostructures loaded on nano-cellulose (ZnO/NC) [104], cerium-substituted magnetite (CeO_2/Fe_3O_4) [106], and novel Z-scheme composites (mMBIP-MWCNT-In_2O_3) [107], etc., have been synthesized for the sonocatalytic degradation of antibiotics. Moreover, semiconductors, such as Ni powder, Raney Ni, Pd or Pt and metal oxides have recently been added to carbon to accelerate the degradation of antibiotics by sonication [52, 103].

Al-Hamadani, *et al.* have investigated the degradation of SMX via sonication at 1000 kHz in the presence of SWNTs [40]. The REs of SMX reached 92% and 70% at pH 7 for 60 min of treatment by sonocatalysis and sonication alone, respectively, with

519 the other conditions being constant (0.18 W/L of power density, 1 L of 2.5 mg/L SMX
520 solution), and 48% of RE was achieved by the SWNT alone [40]. Hoseini, *et al.* have
521 investigated the degradation of TC by sonocatalysis using TiO_2 nano-particles under 35
522 kHz US [105]. The efficacy of sonication alone in the removal of TC was negligible,
523 but the RE increased upon the addition of TiO_2.

524 The REs of various antibiotics under catalysis alone, sonication alone and
525 sonocatalysis have been compared and summarized in Table 3.

526 ***Table 3*** *Summary of sonocatalytic degradation of antibiotics in water.*

Antibiotics	**Catalyst**	**F_{US}/P_E (kHz/W)**	**t (min)**	**C_0/V (mg/L)/mL**	**pH**	**$RE_{Catal.}$ (%)**	**RE_{Sono} (%)**	**$RE_{Sono/Catal}$ (%)**	**SF**	**Refs.**
AMX	0.8 g/L ZnO@Fe_3O_4	20/60	120	10/100	3.0	47.0	9.6	90.0	1.6	[134]
CIP	0.2 g/L TiO_2/Montmorillonite	35/65	120	10/100	6.0	<25.0	8.1	65.0	~2.0	[135]
MOX	1 g/L NiFeLDH/rGO	36/150	60	20/100	8.0	33.8	8.2	72.4	1.7	[118]
TC	0.5 g/L ZnO/nano-cellulose	37/256	15	50/50	7.0	28.2	12.8	87.6	2.1	[104]
TC	0.5 g/L ZnO;	37/256	15	50/50	7.0	4.4	12.8	70.0	4.1	[104]
RIF	1.5 g/LZrO_2-pumice	40/300	90	20/100	5.0	~10.0	7.2	~95.3	15.5	[109]
RIF	1.5 g/L ZrO_2-tuff	40/300	90	20/100	5.0	~10.0	7.2	83.1	9.1	[109]
CFZ	1 g/L Fe-Cu layered double hydroxide	40/300	80	47.6/100	6.5	32.6	6.8	97.6	2.5	[102]
NOR	0.3 g/L multilayer ZnO nanoflowers	40/200	80	2.0/50	7.5	19.2	6.4	47.5	1.9	[140]
OTC	0.75 g/L $Fe_{2.8}Ce_{0.2}O_4$	40/300	120	50/150	4.7	37.0	17.0	64.0	1.2	[106]
GMF	1.5 g/L Nano-ZnO-biochar	40/300	45	20/100	5.5	15.1	10.4	96.1	3.8	[103]
SDZ	0.05 mM K_2FeO_4	100/800	30	5.1/100	7.0	~68.0	~52.0	~80.0	~0.7	[75]
SMR	0.05 mM K_2FeO_4	100/800	30	5.1/100	7.0	~70.0	~55.0	~82.0	~0.7	[75]
SMX	0.05 mM K_2FeO_4	100/800	30	5.1/100	7.0	~70.0	~56.0	~75.0	~0.6	[75]
SMX	45 mg/L SWCNs	1000/180	60	2.5/1000	7.0	48.0	70.0	92.0	1.1	[40]

527 Note: F_{US}: ultrasonic frequency; P_E: electrical power input; t: sonication time; C_0: initial antibiotic concentration;
528 V: volume of solution; RE: removal efficiency; SF: synergy factors = $\boldsymbol{RE_{Sono/Catal}/(RE_{Sono}+RE_{Catal})}$ [71, 81, 109];
529 Refs.: references.

530 As summarized in Table 3, the sonolysis of AMX, CIP, MOX, TC, TC and CIP,
531 etc., has been conducted by sonocatalysis. At low US frequency ranges (20-40 kHz)

and US power ranges (60-350 W), REs are located in the range of 2.5%-17.0% under sonication alone for 15-120 min. At high US frequency (100-1000 kHz) and power (180-800 W), high REs (52-70%) were observed for the removal of SDZ, SMR and SMX via sonication alone after 30-60 min. The adsorption by catalysts of these antibiotics was also performed at a dosage of 0.2-1.5 g/L, and the REs were observed to be in the range of 3.3-70%. The degradation of antibiotics by sonication was enhanced greatly by the addition of catalysts, due to the synergistic effect, and the REs reached a range of 47.5-95.3%.

In addition, most of the catalysts can be considered composite catalysts, in which both the effective component and support play important role. Khataee, *et al.* have investigated the sonocatalytic degradation of RIF using ZrO_2 nanoparticles on pumice (ZrO_2-pumice) and tuff (ZrO_2-tuff), which were synthesized using a modified sol-gel method [109]. About 95% and 83% of 20 mg/L RIF was removed by sonication at 40 kHz and 300 W using 1.5 g/L of ZrO_2-pumice or ZrO_2-tuff, respectively, under natural pH conditions [109].

A ZnO-biochar nanocomposite has exhibited better sonocatalytic performance than biochar and ZnO nanorods because of its huge surface area, narrow band gap and enhanced cavitational phenomenon [103]. The enhancement in the adsorption capacity of sonocatalyst is caused by reducing electron and hole recombination using fluorine and enhancing the oxidation potential of the valence band of ZF1 (ZnO with F/Zn molar ratio of 1:1) compared to ZnO. The prepared Z-scheme $KTaO_3/FeVO_4/Bi_2O_3$ sonocatalyst displayed much higher sonocatalytic activity in the sonocatalytic degradation of CEF sodium than Z-scheme $KTaO_3/Bi_2O_3$ [110]. This excellent sonocatalytic performance is attributed to the introduction of the $FeVO_4$ conductive channel in which the valence state changes of Fe and V provides driving force for e^- transfer, which obviously enhances the sonocatalytic activity of $KTaO_3/Bi_2O_3$ [110].

3.3 Role of effective factors

Similar to degradation by sonication alone, sonocatalytic efficiency is also affected by various factors, including initial substrate concentration [101, 105, 140], pH value [40, 141], temperature [40, 142], catalyst amount [139], US power/frequency [40, 71] and the presence of additives (IO_4^- [134], H_2O_2 [71, 102, 104, 134, 135, 139], and gases [103, 106]).

3.3.1 Effect of US frequency

Al-Hamadani, *et al.* have investigated the effect of US frequency on the degradation of SMX via sonocatalysis with glass beads (GBs) and SWCNs [71]. The removal of SMX was enhanced significantly in the presence of GBs at 28 kHz, whereas it was significantly reduced at 1000 kHz as the GB particle size was similar to or larger than that of the cavitation bubbles at high frequency, leading to interference between the US and GB particles that resulted in a reduction in H_2O_2 production [71]. Additionally, the presence of SWNTs was effective under low and high frequencies in both the sonochemical degradation mechanism and adsorption mechanism because the dispersed SWNT particles acted as additional nuclei for the pyrolysis of water molecules and the formation of more $^{\bullet}OH$. Moreover, the dispersion of SWNTs, due to sonication, enhanced the adsorption process by providing more adsorption sites, leading to increased adsorption capacity. However, maximum SMX removal was achieved at both frequencies when GBs and SWNTs were combined, as a result of enhanced sonochemical degradation via $^{\bullet}OH$ formation and the adsorption process resulting from SWNT dispersion [71].

3.3.2 Effect of pH value

Hoseini, *et al.* have investigated the effect of pH on TC degradation using sonocatalysis with TiO_2 nanoparticles, and it was found that an increase in pH attenuated TC degradation [105]. The relatively high *RE* values of sonocatalytic degradation for PG using MgO and SMX, with SWCNs nanoparticles, were also

obtained under acidic conditions at pH 3.0 and pH 3.5, respectively [40, 141]. Seid-Mohammadi, *et al.* have found that pH value clearly affects the removal of CPX in sono/H_2O_2/NiO hybrid process, and that process efficiency was reduced at pH 9, with pH 3 giving the highest RE (93.8%) [74].

3.3.3 Effect of temperature

The influence of increased temperature on the degradation of antibiotics is exerted via: i) the cavitational intensity; ii) changes in the physicochemical properties of the antibiotics; and iii) the type of cavities formed [40]. An increased k_1 was observed for SMX with increased temperature (15-55 °C) in a sono/SWNT system. The low apparent activation energy values (7.28 kJ/mol) for SMX indicate that the degradation of SMX is influenced by diffusion. This is presumably because the degradation rate reflects the fact that the SMX molecule in the bulk solution moves to the gas-liquid interface region, where temperatures and $^{\bullet}OH$ concentrations are high [40]. The removal rate for AZI increased with increasing temperature (20-40°C) in the sono/ZnO system, especially from 20 to 40 °C. However, a steady decrease in removal rate was observed at 40 to 60°C [142]. The removal of TYL was enhanced by increased temperature (10-40 °C). The k_1 values of the degradation of TYL were 0.0107, 0.0126, 0.0148 and 0.0165 min^{-1} at 10, 20, 30 and 40 °C, respectively [142].

3.3.4 Effect of initial concentration

Hoseini, *et al.* have investigated the effect of initial TC concentration on its degradation by sonocatalysis using TiO_2 nanoparticles, and it was found that an increase in initial TC concentration attenuated TC degradation [105]. Similarly, the *RE* values of NOR and AMP also decreased with increased initial concentrations [101, 107].

3.3.5 Effect of catalyst amount

Gao, *et al.* have found that increases in both the $MnSO_4$ concentration of the wet impregnation solution and the catalyst dosage enhanced the sonocatalytic degradation of TC with Mn-modified diatomite [139]. NOR degradation rate also increased with an

612 increase in ZnO dosage [140].

613 ### 3.3.6 Effect of additives

614 Adding noble gas Ar, CCl_4, or H_2O_2 to the sonocatalytic system can often enhance
615 RE, while the presence of inorganic and organic scavengers suppresses the performance
616 of the sonocatalytic removal of antibiotics [71, 102, 135]. Furthermore, the degradation
617 mechanisms, namely the interactions between $^{\bullet}OH$ and the antibiotics, can be
618 demonstrated [71]. For example, the presence of ethanol suppressed SSZ degradation
619 due to the quenching of $^{\bullet}OH$, while the addition of $K_2S_2O_8$ and H_2O_2 increased the RE
620 due to the formation of $SO_4^{\bullet-}$ and extra $^{\bullet}OH$, respectively [52, 54, 73, 74, 97, 111, 126,
621 128].

622 Seid-Mohammadi, *et al.* have investigated the removal of CFX from aqueous
623 solutions using sono/H_2O_2/NiO process at 40 kHz. Under optimum conditions (pH 3,
624 reaction time 90 min, 40 mg/L CEX, 7.5 mg/L NiO and 30 mL/L (30%, w/w) H_2O_2),
625 the REs of CEX, COD and TOC were 93.9, 72.5 and 54.6%, respectively. The pH value
626 is the most critical factor [74]. Yazdani, *et al.* have investigated the sonocatalytic
627 degradation of AZI with ZnO, finding that H_2O_2 addition significantly increased the RE
628 of AZI from 90.6% to 98.4% [142]. H_2O_2 addition also improved the sonocatalytic REs
629 of RIF [109]. However, Hoseini, *et al.* have reported that the addition of H_2O_2
630 attenuated the sonocatalytic degradation of TC with TiO_2 nano-particles [105].

631 In addition, Dehghan, *et al.* have investigated the effect of adding IO_4^- on the
632 sonocatalytic degradation of AMX with a ZnO@Fe_3O_4 magnetic nanocomposite. It was
633 observed that the degradation rate was accelerated in the presence of IO_4^-, showing the
634 greater oxidation potential compared to the other oxidant agents [134]. Moreover,
635 peroxydisulfate ($S_2O_8^{2-}$) has been extensively investigated as a means to enhance the
636 sonocatalytic degradation of antibiotics [109, 140], which is discussed particularly in
637 chapter 5.

638 Besides, Khataee, *et al.* have investigated the sonocatalytic degradation of OTC

639 with CeO_2/Fe_3O_4, and it was found that the addition of O_2 and Ar improved the RE of
640 OTC by up to 78 % and 76 %, respectively [106]. The enhancement of adding gases on
641 RE is attributed to an increase in the number of nucleation sites in aqueous media, and
642 enhancements in the pressure and temperature of collapsing cavitation bubbles [103].

643 On the other hand, inorganic and organic scavenging additives reduced the REs of
644 antibiotics in sonocatalytic systems, indicating that $^{\bullet}OH$-mediation oxidation is
645 responsible for the degradation of antibiotics, including SMX [71], CFZ [102], AMX
646 [134], CIP [135], and TC [104, 139]. For example, the RE of TC decreased by over 25%
647 in the presence of tert-butanol [104]. The presence of isopropanol, KBr and NaN_3
648 sharply quenched a series of reactive oxygen species [139]. Of these water matrix
649 components, chloride and sulfate anions had the highest and lowest inhibiting effects
650 on the RE of AMX, respectively [134].

651 ### 3.3.7 Reusability of catalysts

652 From the perspective of cost reduction and environmental protection, the
653 recyclability of catalysts is essential to promoting sonocatalytic processes. In many
654 cases, catalysts exhibited higher stability for the sonocatalytic degradation of antibiotics
655 due to the strong ultrasonic surface cleaning [108]. Under sonication, catalysts can
656 maintain their catalytic activity for antibiotic removal for 4-5 consecutive runs [73]. For
657 example, the RE of AMP was reduced by only 5% even after Zn(OH)F was reused for
658 four experiments [101]. Similarly, the REs of AMX with $ZnO@Fe_3O_4$ and CFZ with
659 Fe-Cu-LDH/biochar nanocomposite dropped by only 5-9 % after five successive runs
660 [102, 134]. Er^{3+}: $Y_3Al_5O_{12}$@Ni $(Fe_{0.05}Ga_{0.95})_2O_4$-Au-$BiVO_4$ coated composite also
661 exhibited excellent recyclability and sustainability for the sonocatalytic degradation of
662 SA for five repetitive cycles without any apparent deactivation [72].

663 Overall, sonocatalysis can significantly increase the RE of antibiotics compared
664 with catalysis or sonication alone, but this process is still highly energy demanding and
665 limited to laboratory-scale investigation at present. Thus, additional chemicals are

required in many cases to improve the RE. To overcome the drawbacks and reduce the operating costs, a combination of sonication and other AOPs has been proposed to exploit the benefits of the synergistic effects of the AOPs [37].

4 Degradation of antibiotics by sono/Fenton and sono/Fenton-like processes

4.1 Mechanisms of sono/Fenton processes

Fenton oxidation is one of the AOP techniques that has been most widely applied for antibiotic removal [17, 32-35]. So far, the Fenton processes that have been applied to the degradation of antibiotics can be divided into: classic homogeneous Fenton processes; and heterogeneous Fenton processes or Fenton-like processes. The classic Fenton reaction usually occurs in acidic homogeneous systems where Fe^{2+}, or other metal ions (Cu^{2+}, Zn^{2+}, etc.), and H_2O_2 exist simultaneously. By contrast, Fenton-like reactions generally occur in acidic heterogeneous systems where solid catalysts (Fe^0, Fe_3O_4, etc.) and H_2O_2 exist simultaneously.

As a green oxidant, H_2O_2 is frequently used to form ROS for organic removal [43]. In classic Fenton processes, Fenton's reagent is a mixture of H_2O_2 and ferrous iron [48], where the dissociation of the oxidant and the formation of highly reactive $^{\bullet}OH$ are included, as shown in Eq. (1) - (3) [47, 48].

$$Fe^{2+} + H_2O_2 \rightarrow Fe^{3+} + {}^{\bullet}OH + OH^- \quad (1)$$

$$Fe^{3+} + H_2O_2 \rightarrow Fe^{2+} + H^+ + {}^{\bullet}OOH^- \quad (2)$$

$$Fe^{3+} + {}^{\bullet}OOH \rightarrow Fe^{2+} + O_2 + H^+ \quad (3)$$

In sono/Fenton processes, the radical reactions near the hotspots and/or in the bulk liquid dominate the degradation of antibiotics [96]. One the one hand, sonication can improve mass transfer, thus enhancing the generation of $^{\bullet}OH$ and reducing the consumption of chemicals [47, 48]. On the other, adding the right amount of Fe^{2+} (e.g.,

1.0 mM) can also enhance •OH production via the reactions between Fe^{2+}/Fe^{3+} and H_2O_2, including H_2O_2 that is formed *in situ* [17, 30, 34, 41, 43, 46, 69, 95, 96, 97, 139].

Unfortunately, excessive H_2O_2 and Fe^{2+} negatively influence the degradation of antibiotics [30, 34, 96], since large doses of Fe^{2+} and H_2O_2 can act as scavengers for •OH in aqueous matrices [34, 41, 95, 96]. In addition, the pH value of solutions significantly affects the degradation of antibiotics [111]. For pH > 4, the total concentration of Fe^{2+} and Fe^{3+} decreases considerably as their complexes and hydroxides are formed in solution. At pH < 2, Fe^{2+} and Fe^{3+} exists as $[Fe(H_2O)_6]^{2+}$ and $[Fe(H_2O)_6]^{3+}$ respectively, and the regeneration of Fe^{2+} in the form of $[Fe(H_2O)_6]^{2+}$ from $[Fe(H_2O)_6]^{3+}$ is slow. Meanwhile, H_2O_2 forms oxonium ions ($H_3O_2^+$). These are more stable than H_2O_2 and their reactivity with ferrous ions decreases. In addition, the scavenging effect of •OH by H^+ is enhanced at pH < 2 [111]. Therefore, the optimal pH range for classic Fenton reactions is 2-4 [21, 22, 41,111]. Also, the pH value affects the chemical structures of the antibiotics, thus influencing REs in sono-Fenton process [96, 99].

4.2 Application of sono/Fenton processes on antibiotic degradation

Wang, *et al.* have reported the degradation of 50 mg/L TC via sonication at 20 kHz and 100 W US in 1 L solution at pH 6, in the presence of 0.2 mM Fe^{2+} and 2.0 mM H_2O_2 [34]. Consequently, an RE of 91.3% was achieved in 60 min using this sono/Fenton process, which is higher than the sum of those obtained under Fenton (70.2%) and sonication alone (6.7%). Meanwhile, mineralization reached 45.8% in the sono/Fenton process, resulting in the toxicity of the TC solution being significantly decreased [34].

Labrada, *et al.* have studied CIP degradation in wastewater using a homogeneous sono/Fenton process at high frequency [32]. 100 mg/L CIP was sonicated with 580 kHz and 30.6 W US in a 250 mL solution at pH 3, in the presence of 2.4 mM Fe^{2+} and 14.2 mM H_2O_2. An RE of about 98.4% was achieved using this sono/Fenton process in 15

718 min. However, the RE obtained by sono/Fenton is lower than the sum of those obtained
719 under Fenton and sonication alone (96.4% and 9.3%). However, the mineralization
720 reached 60% using the sono/Fenton process after 60 min [32]. Ammar *et al.* have
721 investigated the degradation of 500 mg/L MTZ by sonication at 20 kHz US in a 200
722 mL solution at pH 3.0 in the presence of 3 mM Fe^{2+} and 60 mM H_2O_2 [113]. The results
723 indicate that 98% of MTZ was removed using the sono/Fenton process in 180 min at
724 30 °C, which is higher than those obtained by sonication alone (42%) and Fenton
725 process alone (90.0%), but is lower than sum of REs of the two individual processes
726 [113]. At 40 kHz, 261.2 mg/L FLU was sonicated with 120 W US in a 200 mL solution
727 at pH 4.0 in the presence of 4 mM Fe^{2+} and 20 mM H_2O_2 [111] As a result, an RE of
728 93% was achieved using the sono/Fenton process in 120 min at 60 °C, which is
729 obviously higher than that (73%) obtained by the Fenton process alone [111]

730 Overall, this suggests that the synergistic effects of sonication and the Fenton
731 reaction for antibiotic degradation is dependent on the physicochemical properties of
732 the antibiotics and Fenton reagents rather than the character of the US used.

733 4.3 Mechanisms of sono/Fenton-like processes

734 The Fenton process requires a large amount of Fe^{2+} and acidic conditions, which
735 requires neutralization with alkaline, resulting in large-scale sedimentation and high
736 costs. With the development of Fenton-like technologies, the drawbacks of the
737 conventional Fenton process have been overcome to some extent [44]. Fe^0, Fe_3O_4
738 particles and their nanoparticles are important catalysts to promote the decomposition
739 of H_2O_2 for the formation of $^{\bullet}OH$ [21, 22, 33, 43, 44]. Unfortunately, the solid catalysts
740 may be poisoned during Fenton reactions, nano-catalysts particles can aggregate and
741 solid-catalyst passivation can occur, thus decreasing the degradation rate and limiting
742 potential applications [21, 22, 33, 119]. Therefore, sonication has been applied in the
743 Fenton-like process to maintain the activity of catalysts and improve antibiotic removal.
744 The mechanism of sono/Fenton-like processes is shown in Figure 3.

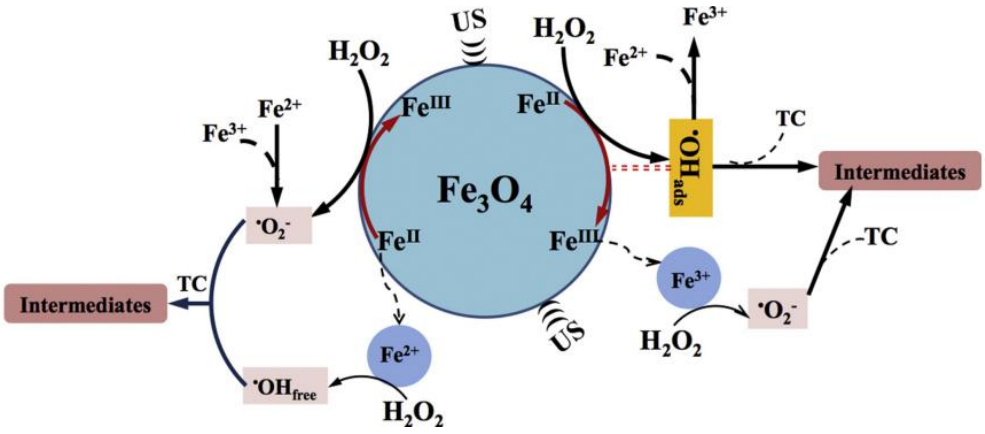

745

746 ***Figure 3*** *Mechanism schematic of sono/Fenton-like processes. Reprinted from ref. [33] Copyright (2016), with*
747 *permission from Elsevier.*

748 As shown in Figure 3, solid-liquid interfacial iron corrosion, bulk homogenous
749 oxygen activation and Fenton reactions are the main reaction pathways in sono/Fenton
750 processes, during which sonication plays both mechanical and chemical roles [35]. The
751 antibiotics and intermediates adsorbed onto the Fe_3O_4 surface are oxidized
752 preferentially [33]. $^{\bullet}OH$, $^{\bullet}O_2^-$ and H_2O_2, formed *in-situ* on the catalyst surface, have
753 been identified as the dominant reactive species in Fenton-like processes [21, 22, 33,
754 35, 44].

755 Figure S2 exhibits the LC/MS analysis of the intermediate formation during the
756 degradation of LEV in a sono/H_2O_2/Fe_3O_4 (magnetic nanoparticles) process [43]. The
757 degradation pathway of LEV is shown in Scheme 2. The formation of isatin and
758 anthranilic acid analogues is attributed to the oxidation of LEV by $^{\bullet}OH$. The
759 demethylation of the piperazinyl ring and the degradation at the oxazinyl group result
760 in the generation of the other two intermediates [43]. Unfortunately, this study does not
761 provide the mineralization data of LEV and toxicity variation of LEV solutions by the
762 treatment.

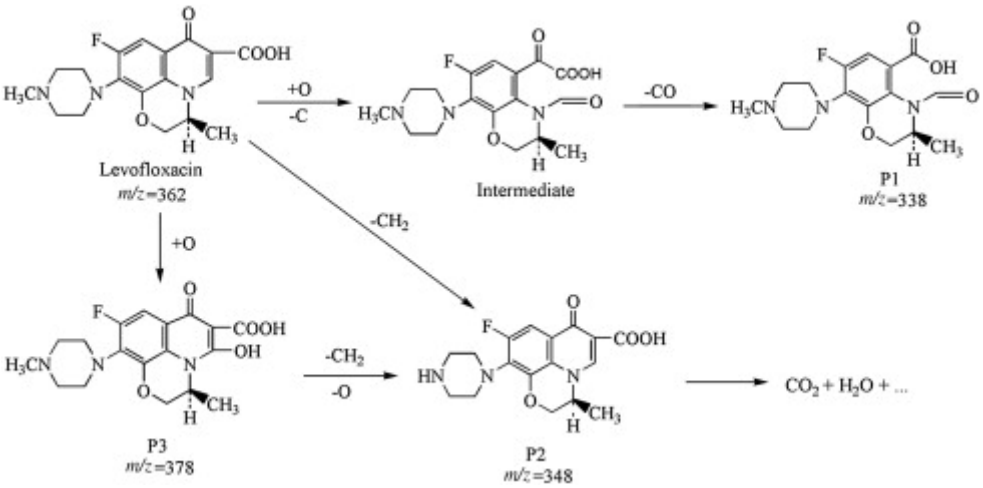

Scheme 2 *A tentative partial degradation pathway of LEV in a sono/H_2O_2/Fe_3O_4 (magnetic nanoparticles) system. Reprinted from ref. [43] Copyright (2015), with permission from Elsevier.*

4.4 Application of sono/Fenton-like processes on antibiotic degradation

So far, sono/Fenton-like processes have been used to remove some antibiotics, such as LEV, TC, NOR, CLA, RXM, TNZ, CLM, etc., and Fe_3O_4, nano-Fe^0, ZnS quantum dots/SnO_2, nano-Cu^0 and micro-Cu^0, etc. have been used as catalysts. The concentrations of H_2O_2 addition cover a wide range, 5-1000 mM, and degradations have been performed in the pH range of 3.0-7.1. In sono/Fenton-like systems, the three factors, sonication, Fenton catalyst and H_2O_2, act together to cause a strong synergistic effect for the degradation of antibiotics (such as MNZ [44]). The application of sono/Fenton-like processes on the degradation of antibiotics has been summarized in Table 4.

Table 4 *Summary of antibiotic degradation by sono/Fenton-like processes.*

Antibiotics	**Fenton reagents**	**F_{US}/P_E (kHz/W)**	**t (min)**	**C_0/V (mg/L)/mL**	**pH**	**RE Fenton-like (%)**	**RE Sono (%)**	**RE Sono/Fento-like (%)**	**SF**	**Refs.**
LEV	1 g/L Fe_3O_4, 5 mM H_2O_2	20/195	150	20/100	7.1	71.5	1.9	99.0	1.35	[43]
TC	1 g/L Fe_3O_4, 150 mM H_2O_2	20/80	60	100/200	3.7	72.2	-	93.6	-	[33]

CLA	0.3 g/L ZnS quantum dots/SnO_2, 6 mM H_2O_2	20/75	60	10/100	3.0	31.4	~8.0	61.2	~1.56	[119]
RXM	0.3 g/L ZnS quantum dots/SnO_2, 6 mM H_2O_2	20/75	60	10/100	3.0	36.4	~12.0	65.5	~1.35	[119]
NOR	0.25 g/L nano-Cu^0 or micro-Cu^0, 20 mM H_2O_2	20/240	30	5/200	7.0	46.7	<5.0	91.5	>1.77	[20]
CEX	7.5 mg/L NiO, 30 mL/L H_2O_2	40/-	90	40/<500	3.0	-	-	93.0	-	[74]
CLM	0.2 g /L Fe^0, 1 M H_2O_2	130/500	150	45/-	3.0	~40.0	~30.0	95.0	~1.36	[21]
TNZ	0.2 g /L Fe^0, 1 M H_2O_2	130/500	150	45/-	3.0	~20.0	-	93.0	-	[22]

Note: F_{US}: ultrasonic frequency; P_E: electrical power input; t: sonication time; C_0: initial antibiotic concentration; V: volume of solution; RE: removal efficiency; SF: synergy factors = $\boldsymbol{RE}_{\text{sono/Fenton-like}}/(\boldsymbol{RE}_{sono}+\boldsymbol{RE}_{\text{Fenton-like}})$ [71, 81, 109]; Refs.: references.

As shown in Table 4, the REs of most antibiotics are over 91.5% in 30-150 min, except for the degradation of CLA and RXM in the system with 0.3 g/L ZnS/quantum dots/SnO_2 and 6 mM H_2O_2, and the REs are obviously higher than the sum of those obtained using Fenton-like processes and sonication alone in most cases. In addition, the synergistic degradation of NOR in a heterogeneous sono/Fenton-like system with Fe^0/tetraphosphate has been reported [35]. 400 mL of a 10 mg/L NOR solution was sonicated at pH 7 with 1 g/L Fe^0 and 0.3 mM tetraphosphate. As a result, an RE of 90% was achieved in 60 min using this sono/Fenton-like process, which is obviously higher than the sum of those obtained using the Fenton-like process and sonication alone (50% and <5%) [35].

Ma, *et al.* have investigated the degradation of NOR via the ultrasound-enhanced nanosized zero-valent copper (Cu^0) activation of hydrogen [20]. Compared with the silent degradation system, significantly enhanced NOR removal was obtained in the sono/Fenton-like process. The Cu^+ released during Cu^0 dissolution was the predominant

copper species that activated H_2O_2, yielding $^{\bullet}OH$ in the sono/Cu^0/H_2O_2 system. According to radical quenching experiments and electron paramagnetic resonance technique, free $^{\bullet}OH$ in solution was verified as the primary reactive species, and superoxide anion radicals ($^{\bullet}O_2^-$) were regarded as the mediator for copper cycling, via the reduction of Cu^{2+} to Cu^+ [20].

Importantly, the toxicity of the solution increased during the first 60 min and then decreased with treatment time for the degradation of TC in a sono/Fenton-like process with a Fe_3O_4 catalyst [33]. In general, an increase in the biodegradability of wastewater has been demonstrated after antibiotic degradation by sono/Fenton and sono/Fenton-like processes [32], indicating that these processes are suitable for the treatment of wastewater that contains highly toxic and bio-recalcitrant compounds [113].

4.5 Role of effective factors

The factors influencing the RE of antibiotics using sono/Fenton-like processes includes the initial concentration of antibiotics, US power density, reaction temperature [33], etc. In general, lower antibiotic concentrations, higher temperature (up to 60 °C), higher US frequency and power are favourable for RE [21, 22]. The effects of the critical factors, dose of catalysts, the concentration of H_2O_2, and the pH value of the solution [21, 35, 43, 44, 74], are discussed below.

4.5.1 Effect of Fenton-Reagent dose

In general, a larger amount of catalyst increases the sites for H_2O_2 decomposition and the production of more ROS, resulting in higher antibiotic RE [21]. Gholami, *et al.* and Rahmani, *et al.* have investigated the effects of catalyst amount on the degradation of CLM and TNZ using sono/Fenton-like processes with nanoscale Fe^0, respectively [21, 22]. The REs increased with increasing Fe^0 nanoparticle dosage, and the highest REs (93%-95%) were observed in a 130 kHz sonochemical system with 0.2 g/L Fe^0 nanoparticles and 1 mM H_2O_2 [21, 22]. It was speculated that the increasing nano-Fe^0 dosage results in an increase in total surface area and therefore increased adsorption

822 onto active sites. Over 0.2 g/L Fe^0 nanoparticles, the RE values reached a plateau due
823 to the agglomeration of Fe^0 nanoparticles and the scavenging of •OH in undesirable
824 reactions [21, 22].

825 Wei, *et al.* have reported the effect of Fe_3O_4 magnetic-nanoparticle amount on the
826 removal of LEV in a sono/Fenton-like process [43]. As the amount of Fe_3O_4 magnetic
827 nanoparticles increased from 0 to 1.0 g/L, the k_1 value increased from 4.69×10^{-3} to
828 21.3×10^{-3} min^{-1} in the 20 kHz sonication system. The higher catalyst dose favoured
829 LEV removal due to higher number of nucleation sites for the generation of •OH [43].

830 ### 4.5.2 Effect of H_2O_2 concentration

831 Without H_2O_2 present initially, the RE of LEV was approximately 30%, which is
832 mostly attributed to the adsorption of LEV onto the catalyst. As H_2O_2 concentration
833 increased from 1.5 to 15.0 mM, the *RE* of LEV increased until it reached a peak. The
834 results are mainly related to the adsorption amount of H_2O_2 onto the catalyst [43].
835 During the degradation of CLM and TNZ in a sono/Fenton-like process with nanoscale
836 Fe^0, the RE increased with increasing H_2O_2 concentration due to the increase of •OH
837 formed. The system had the highest efficiency with 1 mM H_2O_2 [21, 22].

838 However, excessive amounts of H_2O_2 adversely affected the REs [82], as the
839 excess H_2O_2 consumes the •OH formed *in situ* and inhibits iron corrosion. In the
840 chemical reaction of •OH with the nanoparticle, hydroxyl ions are produced, which are
841 less active than •OH and reduced system efficiency [21, 22].

842 ### 4.5.3 Effect of pH value

843 In general, the pH value can affect the surface-charge properties, adsorption
844 behaviour and electron-transfer ability of the catalyst, which all affect catalytic
845 degradation. Thus, it is necessary to study the effect of the pH value on RE and
846 degradation kinetics in a wide range of pH conditions [44]. The acidic condition (pH 2-
847 4) has been demonstrated to be suitable for the Fenton reaction. Gholami, *et al.* and
848 Rahmani, *et al.* have investigated the effect of pH on the degradation of CLM and TNZ,

using a sono/Fenton-like process with nanoscale Fe^0 [21, 22]. Over the pH range of 3-9, the system had the highest efficiency under acidic conditions (pH 3), as Fe^0 corrosion and the reactivity of $^{\bullet}OH$ were greatly influenced by H^+ concentration [21, 22].

Guo, *et al.* have reported the effect of pH value on the degradation of LEV in a sono/Fenton-like process with Fe_3O_4 magnetic nanoparticles [43]. Over the pH range of 4-9, the k_1 values of LEV degradation were calculated to be 2.13×10^{-2}, 2.85×10^{-2} and 1.26×10^{-2} min^{-1} at pH 4, pH 8 and pH 9, respectively. It seems that pH 8 is the optimal condition. LEV exists as different species depending on pH value. At 5.7≤ pH≤ 7.9, LEV mainly exists in its zwitterion form in solution, while at pH > 7.9 and <5.7, LEV exists in its cationic or anionic form in solution, respectively. Therefore, the hydrophilicity and solubility of LEV at different pH values play the critical role in its oxidative degradation by $^{\bullet}OH$. In addition, pH value affects not only LEV adsorption onto the catalyst, but also the heterogeneous Fenton-like reaction on the catalyst surface. The enhanced degradation of LEV over the wide range $4.0 \leq pH \leq 8.0$ occurred due to nucleation sites on the catalyst for the formation of cavities. At pH 9.0, the decrease of RE was partly due to the decrease in H_2O_2 adsorption onto the catalyst, which was covered with $Fe(OH)_6^{3-}$, and the self-decomposition of H_2O_2, resulting in the low availability of H_2O_2 and a low yield of $^{\bullet}OH$ [43].

20 mg/L MNZ has been degraded with 157.4 mM H_2O_2 and 500 mg/L nano-Fe_3O_4 at 30 °C within a wide pH range, from 3 to 9, and the REs were considerably enhanced by sonication [44]. The RE reached its highest value (98%) after 5 h at pH 3, and the k_1 was 1.4×10^{-2} min^{-1}. k_1 decreased to 1.25×10^{-2}, 7×10^{-3}, 6×10^{-3} and 3.1×10^{-3} min^{-1} at pH 5.00, 5.79, 7.00 and 9.00, respectively. This dependence on pH is similar to that of the traditional Fenton reaction, and was attribute to a sharp decrease in the concentration of Fe in the oxidation state Fe^{2+} with increasing pH value, thus hindering the activity of the catalyst [44].

4.5.4 Effect of temperature

The k_1 of TC removal (0.04-0.12 min^{-1}) was enhanced by increased temperature (22-50 °C) in the sono/Fe_3O_4/H_2O_2 system. The chemical reaction was the dominant step during the degradation of TC, and the activation energy was 33.8 kJ/mol. The RE of TC was almost the same (> 90%) for all temperatures in 60 min, which indicates that a sufficient amount of $^{\bullet}OH$ was generated by the sono/Fe_3O_4/H_2O_2 process [33].

4.5.5 Stability of catalysts

The stability and recyclability of catalysts are important to the promotion of the sono/Fenton-like process [44]. Fortunately, the stability of the catalyst is significantly improved with sonication [33]. The reusability of Fe_3O_4 was evaluated 3 times under identical oxidation conditions, and the RE decreased slightly after 3 cycles. Moreover, these values were still much higher than those obtained in the simple catalytic process [33].

Fe^0 particles can be reused in the relative long-term and not lead to high concentration levels of dissolved iron in the treated effluents (<0.6 mg/L) [35]. A consecutive triplicate-repeated sono/Fe^0/tetrapolyphosphate experiment was conducted to examine the reusability of Fe^0 particles for NOR degradation. The k_1 for the three repeated runs were 0.039, 0.032 and 0.029 min^{-1}, respectively. This indicates that sonication is able to effectively clean and refresh the surface of used Fe^0 particles over a long-term treatment schedule. The Sono/Fe^0/tetrapolyphosphate system only led to acceptable levels of dissolved iron in the effluents even after repeated runs.

5 Degradation of antibiotics by sonication with peroxydisulfate (PS) and peroxymonosulfate (PMS)

5.1 Mechanisms of sono/PS and sono/PMS processes

Sulfate radical-based advanced oxidation processes (SR-AOP) are considered to be a promising technology for wastewater treatment [143]. In this technique, sulfate

radicals ($SO_4^{\bullet-}$, SR) can be formed by the activation of persulfate salts (PS, SO_5^{2-} or $S_2O_8^{2-}$) or peroxymonosulfate (PMS, HSO_5^-) via multiple approaches, including heat, UV, sonication, alkaline pH and transition metal ions [21, 119, 144-146]. The triple salt $KHSO_5 \cdot 0.5\ KHSO_4 \cdot 0.5\ K_2SO_4$ (Oxone) is a form with higher stability [147]. SR-AOP appears to be more advantageous, efficient and powerful than $^{\bullet}OH$-based AOPs [143, 145], as SR appears to be more stable than $^{\bullet}OH$ in reacting with target antibiotics and is able to oxidize antibiotics efficiently over a wide pH range of 2-8 [148, 149].

In general, $^{\bullet}OH$ is a powerful oxidant with a redox potential of 1.89-2.8 V [150, 151]. In comparison, SR has an equal or even higher redox potential (1.81–3.1 V), depending on activation method [113, 146, 150, 152]. SR is generated from PS, which has a higher standard redox potential (2.01 V) than PMS (1.81 V) [145, 150]. Therefore, the RE order of acid orange 7 by heat activation is PS $\gg$ PMS > H_2O_2, but by UV activation, the RE order of acid orange 7 becomes PS > H_2O_2 > PMS [153, 154]. Under sonication activation, the REs of 25 mg/L furfural with PS or PMS reached 95.3% or 58.4%, respectively [155]. However, the REs of SMX by UV activation were observed to follow a different order: PMS > PS > H_2O_2 [156]. Even with a TiO_2 catalyst, k_1 by UV activation still shows the same order: PMS > PS > H_2O_2 [157]. A similar order was observed during the degradation of rhodamine B by Fe^{2+}/PMS or PS/MoS_2 [158]. Therefore, the oxidation potential of PS and PMS was affected by the whole oxidation system rather than by one factor.

Sonication not only offers a new option for the removal of recalcitrant organic pollutants, but also promotes SR production from the reactions of PS and PMS with $^{\bullet}OH$ that is formed *in situ* during sonication, as shown in Eqs (4)-(9) [31, 34, 104, 131, 150, 159, 160]:

$$S_2O_8^{2-} + {}^{\bullet}OH \rightarrow HSO_4^- + SO_4^{\bullet-} + 0.5\ O_2 \quad (4)$$

$$HSO_5^- + US \rightarrow SO_4^{\bullet-} + {}^{\bullet}OH \quad (5)$$

$$HSO_5^- + SO_4^{\bullet-} \rightarrow SO_5^- + SO_4^{2-} + H^+ \quad (6)$$

928 $S_2O_8^{2-}$ + US/thermal → 2 $SO_4^{\bullet-}$ (7)

929 $SO_4^{\bullet-}$ + $^{\bullet}OH$ → HSO_4^- + 0.5 O_2 (8)

930 $S_2O_8^{2-}$ + $SO_4^{\bullet-}$ → SO_4^{2-} + $^{\bullet}S_2O_8^{2-}$ (9)

931 Therefore, the SR and $^{\bullet}OH$ that are formed from the activation of PS or PMS under
932 sonication have been considered the origins of antibiotic degradation [82, 131].
933 Subsequently, the cleavage of chemical bonds of antibiotic molecules, such as the S–N,
934 S–C and N–C of SMZ [82], or the removal of the N-methyl, hydroxyl and amino groups
935 of TC occurs via oxidation with SR and $^{\bullet}OH$ [131].

936 Figure S3 shows the LC-MS of the intermediates during the degradation of TC
937 using the sono/$S_2O_8^{2-}$ process [160]. Three new peaks, observed after 120 min of
938 reaction, were related to the formation of polar by-products. The protonated TC
939 molecular ion $[M+H]^+$ and the 4 main by-products generated are shown in the
940 degradation pathway of TC via the sono/$S_2O_8^{2-}$ process (Scheme 3) [160]. After 120
941 min sonication of 100 mL of 0.052 mM TC with 4 mM PS at pH 10, 35 kHz and 500
942 W, nearly 96.5% of TC, 74% of COD and 61.2% of TOC were removed, indicating that
943 the mineralization of TC was achieved to a certain degree, but incompletely.

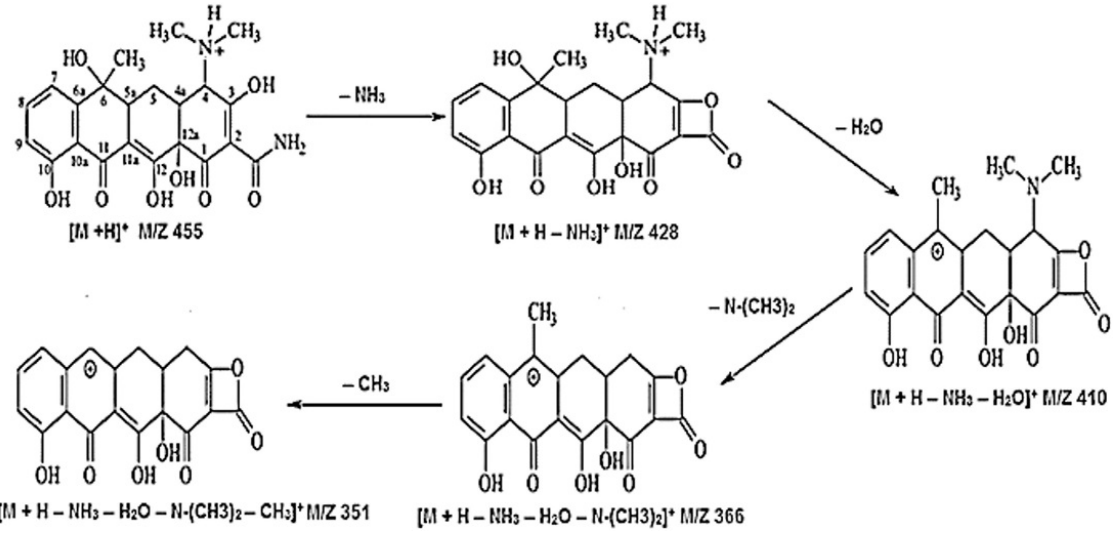

944

945 ***Scheme 3***. *Proposed degradation pathway for the TC antibiotic in a sono/$S_2O_8^{2-}$ process. Reprinted from ref.*
946 *[160] Copyright (2017), with permission from Elsevier.*

5.2 Application of Sono/PS or PMS on antibiotic degradation

Safari, *et al.* have reported that 95.0% of 30 mg/L TC was removed by sonication in the presence of PS in 100 mL of a TC solution under 35 kHz and 500 W at pH 10.0 after 120 min. Meanwhile, the REs of COD and TOC reached 72.8% and 59.7%, respectively [131]. Yin, *et al.* have reported that the REs of 50 mg/L SMZ reached 8.6%, 54.3% and 99.6% using sonication alone, PMS alone and Sono/PMS, respectively, under 20 kHz and 600 W at pH 7.5 for 30 min (Figure 4) [82].

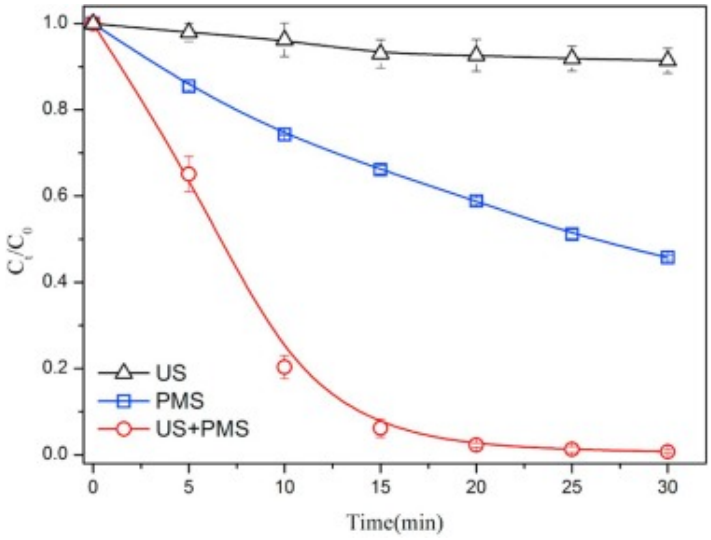

Figure 4 *SMT degradation by different processes: US, PMS and US/PMS systems. Reprinted from ref. [82] Copyright (2018), with permission from Elsevier.*

So far, the sonochemical degradation of antibiotics, such as CAP, CIP, TC, SMZ, SDZ, etc., with PS in aqueous solution have been studied. 5-100 mg/L of antibiotics has been sonicated for 30-240 min with 1-200 mM PS or Oxone in 50-1000 mL of aqueous solution. The application of sonication for the degradation of antibiotics with PS or Oxone has been summarized in Table 5.

Table 5 *Summary of the degradation of antibiotics by sonication with PS or Oxone.*

Antibiotics	**C_{PS} (mM)**	**F_{US}/P_E (kHz/W)**	**t (min)**	**C_0/V (mg/L)/mL**	**pH**	**RE_{PS} (%)**	**RE_{Sono} (%)**	**$RE_{Sono/PS}$ (%)**	***SF***	**Refs.**
TC	2	20/100	60	50/1000	3.0	-	6.7	91.3	-	[34]
TC	200	20/80	90	100/200	3.7	~20.0	~0	51.5	~2.60	[149]
TC	5	35/500	120	23/100	10.0	57.3	26.9	88.5	1.05	[160]

CAP	4	22/200	240	20/50	1.0	<5.0	37.3	62.4	>1.47	[145]
CIP	4.4	40/350	60	50/<1000	4.5	7.5	2.5	18.5	1.85	[19]
SDZ	1.84	20/-	60	-/400	3.0–7.0	-	9.7	13.7	-	[76]
SMZ	1	40/60	60	5/500	7.0	-	1.6	7.2	-	[161]
SMZ	Oxone 2	20/600	30	50/<100	7.5	54.3	8.6	99.6	1.58	[82]

Note: C_{PS}: PS concentration; F_{US}: ultrasonic frequency; P_E: electrical power input; C_0: initial concentration of antibiotic solution; V: the volume of antibiotic solution; RE: removal efficiency; SF: synergy factors = $\boldsymbol{RE_{sono/PS}/(RE_{sono}+RE_{PS})}$ [71, 81, 109]; Refs.: references.

As summarized in Table 5, the dosage of PS or Oxone was in the range of 2-5 mM. Combined sonication with PS or Oxone exhibits higher degradation of antibiotics than sonication alone or oxidation alone under the given conditions. Meanwhile, mineralization can be achieved to a certain degree [34, 162]. For example, the RE of TC reached 96.5% using sono/PS, and 74% of COD removal and 61.2% of TOC removal were achieved [160]. However, some antibiotics, such as CAP, are difficult to degraded using such combined process, even after long treatment times (240 min).

5.3 Mechanism of sono/PS and sono/PMS in the presence of catalysts

To effectively remove antibiotics from aqueous solutions using sono/PS, PMS or Oxone, catalysts have been added to enhance RE [149, 163]. For example, Fe^0 or PS alone cannot cause significant SDZ degradation, and sonication alone only led to marginal degradation of SDZ after 1 h treatment (9.7% RE). Moreover, the RE of SDZ reached only 9.8% and 13.7% in 1 h using a combination of two factors, such as sono/Fe^0 and sono/PS, respectively. By contrast, 45.5% of SDZ was removed in 1 h using the Fe^0/PS combination due to the catalytic decomposition of PS by Fe^0 and higher SR formation. However, surface passivation prevented the dissolution of Fe^0 and the release of Fe^{2+}, hampering the continuous degradation of SDZ. Therefore, sonication was used to remove the passivation film and improve mass transfer, inducing an SDZ RE of 95.7% in 1 h in the sono/Fe^0/PS reaction system [76]. Similarly, it is also

986 difficult to remove TC by sonication alone, or PS alone. Furthermore, little TC was
987 removed with only the Fe_3O_4 catalyst and even the catalyst with sonication due to the
988 insignificant adsorption of TC onto Fe_3O_4 and the inadequate formation of active
989 radicals. However, the RE of TC increased greatly and reached 50.5% and 51.5% in 90
990 min using the Fe_3O_4/PS and sono/PS combinations, respectively, due to the activation
991 of PS by the catalyst or sonication; the formation of more SR and •OH on the surface
992 of catalyst. More significantly, the RE of TC reached 89% with sono/Fe_3O_4/PS since
993 the activity of Fe_3O_4 was maintained by sonication and PS was activated by Fe_3O_4 and
994 sonication simultaneously to produce more SR [149].

995 Fe^0 [76, 161], ZnO [104], Fe^{2+} [111, 113], Co^{2+} [145, 162], Ag [150], Fe_3O_4 [163],
996 etc. can enhance the activation of PS, PMS or Oxone in sonication systems. Obviously,
997 transition metals or their ions and oxides were the important catalysts for the activation
998 of PS, PMS or Oxone to generate SR [19, 76, 140, 145, 149, 150, 159, 161, 162]. The
999 cavitation effects mean that sonication not only induces the release of SR from PS or
1000 PMS, but also enhances mass transfer in the solid-liquid interphases, and removes the
1001 passivated films, while continuously keeping the catalyst surface active. The
1002 degradation mechanisms of SDZ by sono/Fe^0/PS are shown in Scheme 4 [76].

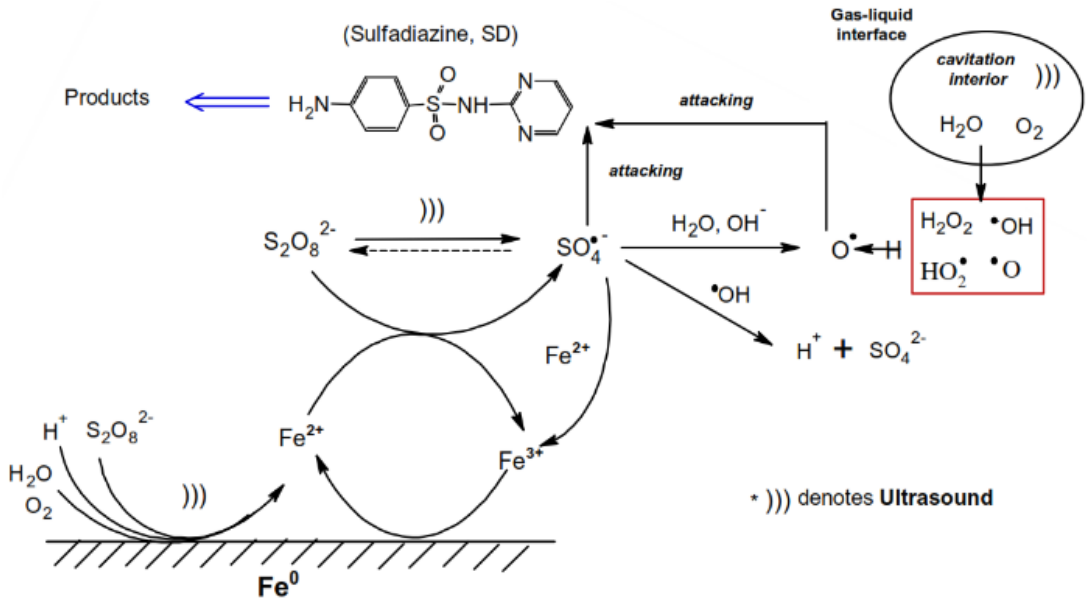

1003

1004 ***Scheme 4*** *The degradation mechanism of SDZ by sono/Fe^0/PS. Reprinted from ref. [76] Copyright (2014), with*

permission from Elsevier.

As shown in Scheme 4, sonication played important roles in the Fe^0/PS system, including producing radicals, enhancing iron-corrosion reactions and accelerating the radical reactions in the bulk liquid [76, 149]. The microstreaming or microjets, shockwaves, and turbulence generated by sonication promoted mixing at the solid-liquid interfaces and the continuous cleaning of the solid catalyst surface, which favour the above reactions [149].

Based on an HPLC-ESI-MS examination, oxidation by SR was the main SDZ degradation pathway, as shown in Scheme 5 [76]. The main degradation step was the oxidation of the amine group (α-position in the benzene ring) by SR to generate the nitro-SD derivatives. SR then further attacks the nitro-SD derivatives (the C–N bonds on the γ-position in the heterocyclic ring), leading to ring opening. Another degradation pathway was the direct oxidative cleavage of the S–N bond, and then the intermediate (4-[2-iminopyr-imidine-1(2H)-yl]aniline), which was formed via reaction between the products, 2-aminopyrimidine and sulfanilic acid. Furthermore, the low molecular weight organic acids (formate and acetate), inorganic ions (nitrate, nitrite and sulfate) were examined using an ion chromatograph, which demonstrated the mineralization of SDZ [76]. Unfortunately, this study does not provide the variation of TOC and toxicity of the SDZ solutions by the treatment.

Pan, *et al.* have investigated SMZ degradation in a pre-magnetized Fe^0/PS process enhanced by sonication [161]. The stronger signals of the DMPO–SO_4 and DMPO–OH adducts illustrated that more SR and $^{\bullet}OH$ radicals were produced in the system and that this occurred more quickly. Similarly, $^{\bullet}OH$ played important roles in the degradation of TC by sonication with Fe_3O_4 and PS. The oxidation of TC mainly took place on the surface of Fe_3O_4 and the concentration of leaching iron during the reaction could be neglected [149].

Moreover, Hu, *et al.* have demonstrated that the sonocatalytic degradation of NOR is principally induced by $^{\bullet}OH$ and SR in the system with PS and multilayer flower-like

ZnO [140]. Soltani, *et al.* have also demonstrated that •OH-mediated oxidation was the main mechanism in the decomposition of TC, and that PMS led to the more significant enhancing effect on the removal of TC, compared with percarbonate, PS and periodate [104]. Guo, *et al.* have reported that the reactive radicals were generated through the Co_3O_4-mediated activation of PMS during the sonocatalytic degradation of AMX using Co_3O_4-catalyzed PMS [159]. Furthermore, the sonocatalytic degradation of CAP was accelerated remarkably by adding PS and Co^{2+} simultaneously [145].

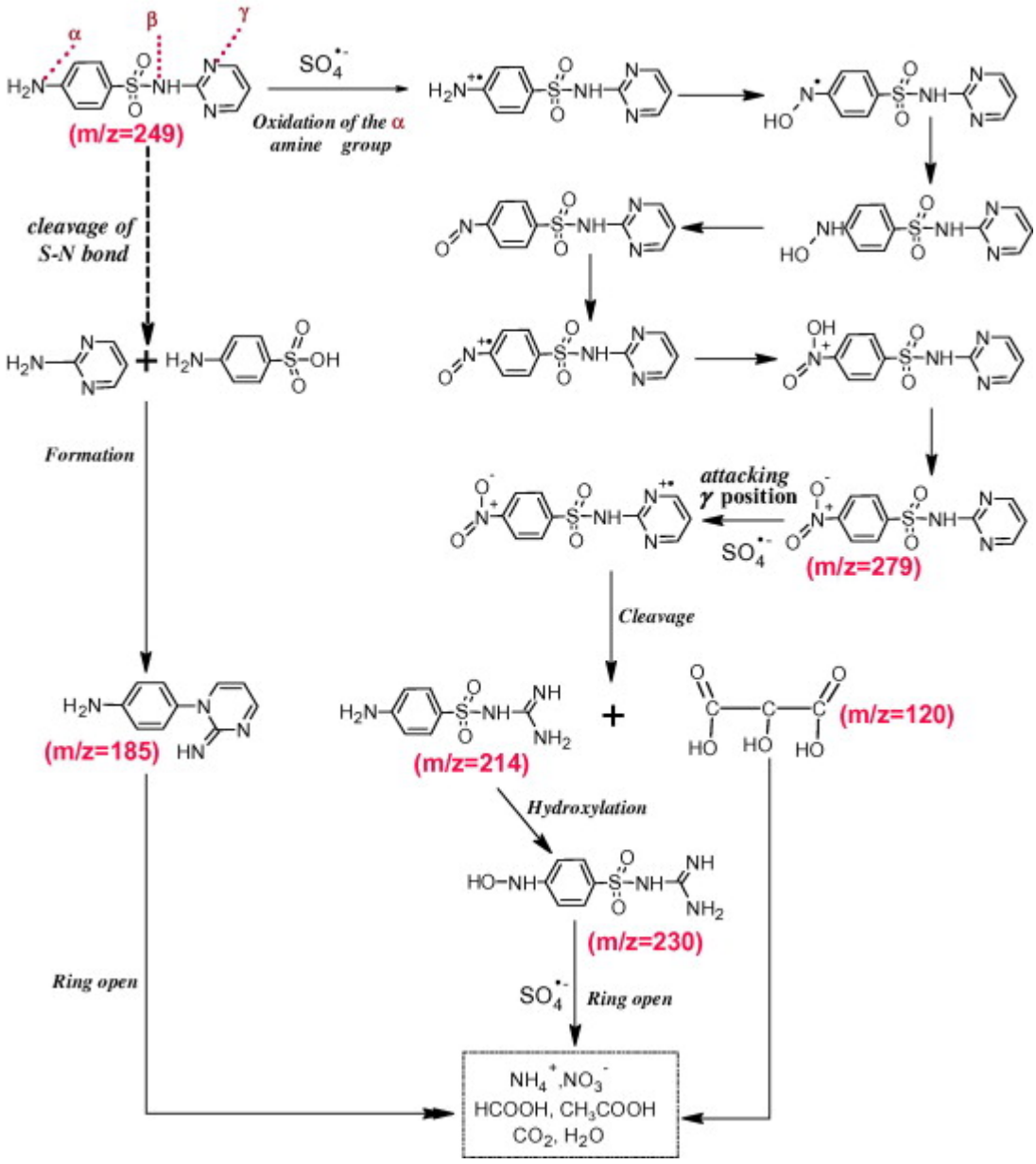

Scheme 5 *Proposed SDZ degradation pathways in the sono/Fe^0/PS system. Reprinted from ref. [76] Copyright (2014), with permission from Elsevier.*

5.4 Application of sono/PS and PMS/catalyst in antibiotic degradation

So far, the sono/PS and PMS/catalyst processes have been extensively applied in antibiotic degradation. For example, the elimination of FLU was significantly accelerated and the RE increased when 1.0 mM PS was added to a sono/Fenton system. As a result, 98% of FLU elimination was achieved in 80 min [111]. Roy, *et al.* have investigated SDZ degradation in a sono/Fenton-like process with PS and yolk-shell Fe_3O_4@hollow@$mSiO_2$ nanoparticles [164]. The faster leaching of Fe^{2+}/Fe^{3+} ions from the metal core of the Fe_3O_4@hollow@$mSiO_2$ particles, due to micro-convection generated by sonication, enhanced SDZ degradation [164].

Rahmani, *et al.* have reported the sonocatalytic degradation of CIP associated with PS and Zn^0 under 40 kHz and 350 W sonication [19]. With 4.4 mM PS and 1.84 mM Zn^0 at pH 4.5 for 60 min, the RE of CIP reached 55% under sono/Zn^0/PS in 1 L of a 50 mg/L CIP solution, which was much higher than those (39.7, 18.5, 9.9, 7.5, 3.3 and 2.5%) obtained by PS/Zn^0, sono/PS, sono/Zn^0, PS, Zn^0 and sonication alone, respectively [19]. This indicates that the production of $^{\bullet}OH$, activation of PS and Zn^0 dispersion in solution were enhanced by sonication [19]. In the presence of 10 mM PMS, periodate, PS and percarbonate, the sonocatalytic RE of TC reached 99.6, 94.2, 90.4 and 98.2% in 50 mL of 50 mg/L TC solutions with 0.5 g/L ZnO/nano-cellulose at pH 4.0 for 30 min, respectively, under 37 kHz and 256 W sonication, which are higher than that of the sono/ZnO/nano-cellulose process (87.6%) [104].

Besides the removal of antibiotics, the mineralization of antibiotic solutions can be significantly enhanced by sonication with PS, PMS and catalysts. Su, *et al.* have investigated the sonocatalytic degradation of AMX and the removal of COD with Co^{2+} and Oxone [162]. The REs of COD were in the order of: Oxone < Oxone/Co^{2+} < Sono/Oxone < Sono/Oxone/Co^{2+}. More than 98% of COD removal was achieved by sonication with 20 kHz and 200 W at 24 °C for 60 min in the presence of 0.095 mM

AMX and 0.025 mM Co^{2+} [162]. Consequently, sonication reduced the energy barrier of the reaction and enhanced the COD removal of antibiotics [162]. The degradation of antibiotics by sonication with PS or PMS and catalysts has been summarized in Table 6. As shown in Table 6, 20-40 kHz US has usually been used to enhance the degradation of antibiotics via oxidation with a PS/Catalyst. CIP, NOR and CAP are difficult to oxidize, and their REs only reached 55.0%-68.5% under sono/PS/Catal after 60-240 min of treatment. By contrast, the REs of SDZ, TC and SMZ reached higher values (95.7%-98.3%) after 15-60 min of treatment. Importantly, all synergy factors fall over the range from 1.3-1.9. Meanwhile, mineralization can be achieved to a certain degree by sono/PS/Catal. For example, 50 mL of 0.1 mM AMX was sonicated with 20 kHz and 300 W US in the presence of 5 mM Oxone and 0.25 mM Co^{2+} at pH 7 for 60 min, giving a RE of COD of 85%, which is higher than that (51%) of oxidation with 5 mM Oxone and 0.25 mM Co^{2+} without sonication [162]. In addition, 89% of COD was removed as the RE of TC reached 93% under sono/PS/Fe_3O_4 nanoparticles [163].

Table 6 *The degradation of antibiotics by sonication with PS and catalysts.*

Antibiotics	**PS/Catal. (mM/mM)**	**F_{US}/P_E (kHz/W)**	**t (min)**	**C_0/V (mg/L) /mL**	**pH**	**$RE_{PS/Catal.}$ (%)**	**RE_{Sono} (%)**	**$RE_{/Sono/PS/Catal.}$ (%)**	***SF***	**Refs.**
CIP	PS/Zn^0 4.4/1.84	40/350	60	100/<1 000	4.5	39.7	2.5	55.0	1.3	[19]
NOR	PS/Zn^0 0.42/6.14	40/200	80	2.0/50	7.5	-	6.4	66.8	-	[140]
CAP	PS/Co^{2+} 5.0/0.1	22/200	240	20/50	1.0	<5.0	37.3	68.5	1.6	[145]
SDZ	PS/Fe^0 1.84/0.92	20/40	60	20/400	3.0–7.0	45.5	9.7	95.7	1.7	[76]
TC	PMS/ZnO/NC 10.0/0.5 g/L	37/256	15	50/50	7.0	-	12.8	96.4	-	[104]
SMZ	PS/Fe^0 1.0/0.1	40/60	60	5/500	7.0	49.3	1.6	98.3	1.9	[161]

Note: F_{US}: ultrasonic frequency; P_E: electrical power input; C_0: initial antibiotic concentration; V: the volume of antibiotic solution; RE: removal efficiency; *SF*: synergy factors = $\boldsymbol{RE_{Sono/PS/Catal}/(RE_{Sono}+RE_{PS/Catal})}$ [71, 81, 109]; Refs.: references.

5.5 Role of effective factors

As shown in Table 5 and Table 6, the removal of antibiotics is highly pH dependent and acidic conditions favour the degradation of antibiotics by sono/PS and sono/PS/Catal [76, 149, 145]. Other factors, including US frequency, initial concentration of antibiotics, concentration of PS or PMS, contact time and temperature [76, 131, 159, 160, 162], are also important. Additives are also critical for antibiotic degradation under sonication with PS, PMS, Oxone, or/and catalyst [19, 34, 76, 82, 104, 111, 112, 113, 131, 140, 145, 148, 149, 150, 160, 161, 162, 163].

The sonocatalytic degradation of antibiotics, such as TC [31], AMX [159, 162], etc., with PS or PMS generally follows PFO kinetics [131]. For example, a k_1 value for 20 mg/L SDZ in a 400 mL solution was measured to be about 0.057 min^{-1} at pH 7 and room temperature under 20 kHz and 40 W sonication with 0.92 mM Fe^0 and 1.84 mM PS [76]. In general, initial antibiotic concentration, catalyst dosage, PS and PMS concentration, and the initial pH value of the solution, temperature and US frequency and power affect the degradation kinetics [112, 131, 149, 160]. At lower US power ranges, the RE increased with increased US power [76, 112, 148, 149, 161], but the benefits of increasing US power over an optimal power value were not observed [149]. In addition, RE increased with an increase in temperature [131, 160, 162], while RE decreased with an increase of the initial antibiotic concentration [76, 131, 140, 149, 162, 163]. However, the amount of antibiotics removed increased with increasing initial concentration. For example, 45.9, 88.9 and 121.9 mg/L TC were oxidized by sonication with Fe_3O_4/PS when its initial concentrations were 50, 100 and 200 mg/L, respectively [149]. The effects of catalyst dosage, PS or PMS concentration, pH value, and other additives, on the degradation of antibiotics using sono/PS or PMS/ and catalyst are discussed below.

5.5.1 Effect of catalyst dosage

Ammar, *et al.* have investigated the effect of Fe^{2+} concentration on the degradation

of MTZ in a sono/Fenton/PS process [113]. The results revealed that the Fe^{2+} concentration was low enough to make the treated solution directly compatible with a safe environment, and the combination is an efficient method for the high elimination of MTZ [113].

Based on the sonocatalytic degradation of SMZ with pre-magnetized Fe^0/PS, Pan, *et al.* have demonstrated that the degradation rate of SMZ is mainly determined by the amount of Fe^{2+} produced from Fe^0 [161]. The SMZ removal at 60 min was 84.8%, 96.1%, 97.8%, 100% and 99.3% at 0.05, 0.1, 0.2, 0.4 and 0.8 mM Fe^0, respectively. Thus, the removal of SMZ increased with increasing Fe^0 doses over the above range. Meanwhile, k_1 value increased from 0.028 min^{-1}, at 0.05 mM Fe^0, to 0.176 min^{-1} at 0.40 mM Fe^0, but slightly decreased at 0.80 mM Fe^0 (0.143 min^{-1}) due to the consumption of SR by excess Fe^{2+}. Thus, 0.40 mM Fe^0 was noted to be the optimum dosage and the optimum ratio of Fe^0/PS was denoted as 2/5 [161].

Hou, *et al.* have concluded that initial degradation rates increase with various doses of Fe_3O_4, in the range from 0 to 2.0 g/L, in the sonocatalytic degradation of TC with Fe_3O_4/PS [149]. As an initiator, Fe_3O_4 activates PS to generate SR, and then accelerates the decomposition of TC. However, the final RE was similar, as a result of the same concentration of PS, since the SR yield is dependent on PS concentration [149]. In addition, the degradation rate of TC increases with increasing martite nanoparticle dosage, and the sonocatalytic RE of 100 mg/L TC reached 87% with 0.5 g/L martite (Fe_2O_3)/3 mM Oxone at pH 4 for 60 min [112].

5.5.2 Effect of PS or PMS concentration

In general, the degradation rate of antibiotics increases with increased initial PS concentration [149, 160]. During the sonocatalytic degradation of TC with Fe_3O_4/PS, the RE of TC increased with increasing PS concentration from 20 to 200 mM [149]. However, when the PS concentration was over 200 mM, the RE decreased as excessive amounts of PS produced sulfate anions rather than active SR. It is also speculated that

the SR formed could be scavenged by excess PS, thus inhibiting the generation of •OH, meaning that it is sufficient to provide SR with 200 mM PS [149].

Soltani, *et al.* have demonstrated the similar effect of lower Oxone concentration on the sonocatalytic degradation of TC with martite nanoparticles and Oxone [112]. The results revealed that increasing the Oxone dosage from 1 to 7 mM increases the decomposition rate from 0.0282 to 0.0588 min^{-1}. Similarly, excessive amounts of Oxone (5 and 7 mM) led to insignificant improvements in the decomposition rate of TC. It was assumed that the excessive amounts of HSO_5^- react with SR to form $SO_5^{\bullet-}$, which has lower oxidation potential than $SO_4^{\bullet-}$, leading to poorer decomposition of TC. In addition, the reaction between sulfate radicals intensified when the Oxone concentration was excessive, leading to the generation of PS ions. Subsequently, the addition of extra amounts of Oxone not only causes the scavenging of SR, but also generates the less reactive species [112].

5.5.3 Effect of pH value

The pH value of a solution not only affects the leaching of metal and their oxides, but also influences the dissociation of antibiotics, and the adsorption of antibiotics onto the catalysts, thus manipulating the sonocatalytic degradation of antibiotics with PS or PMS.

5.5.3.1 RE decreased under alkaline conditions.

In homogeneous systems, antibiotics such as TC exist in the molecular form under acidic conditions, resulting in higher affinity to the cavitation bubbles where oxidation with higher concentration •OH and the pyrolysis of molecules can occur [34]. Thus, higher RE has been achieved under acidic conditions. For example, 90.5%-91.3% of 50 mg/L TC degradation and 25.7%-28.3% of TOC removal were achieved in 1 L solutions at pH 3 to pH 6 in 60 min under 20 kHz and 100 W sonication with 2 mM Fe^{2+} and 2 mM PS. However, the differences in the REs at the various pH values under acidic conditions are not significant. Therefore, it is not necessary to adjust the initial pH to a very low level, and an initial pH of 6 is an optimal pH condition [34]. Similarly, the

sonocatalytic degradation of 20 mg/L CAP has been carried out in 50 mL solutions by 22 kHz and 200 W sonication for 240 min with 5 mM PS and 0.1 mM Co^{2+} [145]. The results revealed that the RE of CAP decreases with increasing pH value, while k_1 values are higher under acidic solutions (pH 1.0-3.3) than those obtained in neutral or basic solutions (pH 5.0-10.0) [145].

In heterogeneous systems, such as sono/Fe^0/PS, the efficient degradation of SDZ (95.7%–98.4%) has been achieved at a pH range of 3.0–7.0 [76], but the performance was greatly slowed (35.7%) at pH 10.0. Acidic conditions favour the corrosion of Fe^0 and produce more soluble Fe^{2+}, while alkaline conditions cause the precipitation of soluble iron ions and the passivation of the Fe^0 surface, resulting in a low production of oxidative radicals, both $SO_4^{\bullet-}$ and $^{\bullet}OH$. Moreover, the $SO_4^{\bullet-}$ formed reacts with H_2O and OH^- under neutral or alkaline conditions, and also inhibits the reactivity of $^{\bullet}OH$. [76].

Furthermore, a gradual decrease in solution pH was observed during the degradation of antibiotics at an initial pH 3.0–7.0; the formation of carboxyl acid products and the decomposition of PS led to this pH decrease. At an initial pH of 10.0, the pH value decreased to 6.5 by the end of degradation [76]. Pan *et al.* have found that pH value decreases faster with reaction time during the degradation of SMZ in a sono/premagneted-Fe^0/PS system than in other systems [161]. As pH dropped quickly, Fe^{2+} was produced faster, leading to the formation of more $SO_4^{\bullet-}$, a higher RE of SMZ, and better synergistic effects in the sono/premagnated-Fe^0/PS system [161].

5.5.3.2 Insignificant effect of pH value

Hou, *et al.* have found that the TC degradation rate increases with decreasing pH value in a system of Sono/Fe_3O_4/PS, but the REs were all similar after 1.5 h sonication [149]; the finial REs were 89%, 86% and 85% at pH 3.7, 7.0 and 9.0, respectively. This indicates that pH value had an insignificant effect on the RE of TC.

Carboxyl acids, such as acetic acid and sulfate acid, are produced during the reaction. Therefore, the final pH value decreased from initial pH values of 3.70, 7.00

and 9.00 to 2.66, 2.63 and 2.68 after 1.5 h reaction, respectively. This is probably the reason why similar REs were achieved by the end of the reactions at various initial pH values [149]. Similarly, the pH value decreased from 4.0 to 3.4, from 7.0 to 5.8 and from 10.0 to 7.3 during TC degradation via sono/PS in the absence of a buffer solution [160].

5.5.3.3 RE increased under alkaline conditions.

The TC degradation rate under sono/PS is highly dependent on the initial pH value. After 120 min of reaction, the TC degradation rates were 77.4%, 62.5% and 88.5% at pH 4, 7 and 10, without adding any buffer solution, respectively [160].

TC is an amphoteric molecule with *pKa* values of 3.3, 7.7 and 9.7. TC molecules are predominantly neutral and positively charged at pH = 4 and negatively charged at pH= 9. The negatively charged TC molecules tend to attract reactive species such as $^{\bullet}OH$ because of the high electrical density on ring system, which resulted in an acceleration in the degradation of TC [160, 165]. Moreover, alkaline-activated PS is primarily responsible for the production of $SO_4^{\bullet-}$, $O_2^{\bullet-}$ and $^{\bullet}OH$ at pH ≥ 10. Furthermore, SR can react with OH^- to generate $^{\bullet}OH$ under alkaline conditions [160, 165]. Therefore, increasing pH enhances the decomposition of PS to form $^{\bullet}OH$ and SR.

$$S_2O_8^{2-}+2H_2O \xrightarrow{OH^-} HO_2^-+2SO_4^{2-}+3H^+ \quad (10)$$

$$HO_2^-+S_2O_8^{2-} \rightarrow SO_4^{\bullet-}+SO_4^{2-}+H^++O_2^{\bullet-} \quad (11)$$

$$SO_4^{\bullet-}+OH^- \rightarrow SO_4^{2-}+{}^{\bullet}OH \quad (12)$$

SR is the predominant species responsible for TC degradation at pH 4, whereas TC degradation was caused by both $SO_4^{\bullet-}$ and $^{\bullet}OH$ at pH 7. Thus, the competing reactions between SR and $^{\bullet}OH$, and TC reduce the TC degradation rate at pH 7 [160].

Similarly, TC degradation under a sono/martite/oxone process has been studied at initial pH values of 4, 7 and 9, and the k_1 values were 0.0481, 0.0545 and 0.0641 min^{-1}, respectively [112]. On the one hand, the scavenging of SR and disintegration of the

active species by H^+ was thought to cause slight decreases in the TC degradation rate under acidic conditions. The increased degradation rate with increased initial pH can be explained by the conversion of $SO_4^{\bullet-}$ and $^{\bullet}OH$ in the presence of OH^- under alkaline conditions. On the other hand, the reaction between $^{\bullet}OH$ and SR leads to the production of HSO_4^- in the bulk solution, and then the dissociation of HSO_4^- into sulfate ions releases H^+ ions, decreasing the pH of the solution [166]. Therefore, an insignificant increase in the degradation rate was observed with increasing initial pH value [112].

5.5.4 Effect of temperature

Increasing temperature dramatically improved the cavitational activity and chemical effects, resulting in higher degradation rates of antibiotics under sono/$S_2O_8^{2-}$ [131, 160] or Sono/Oxone [162] processes. PS activation can be performed by heat to produce SR, as shown in Eq. (13) [131, 160].

$$S_2O_8^{2-} \xrightarrow{\text{Thermal-cavitation}} 2SO_4^{\bullet-} \quad (13)$$

The k_{obs} of SDZ increased (3.56-27.39 h^{-1}) with increased bulk temperature (10-50 °C) in the sono/Fe^0/PS system. The pseudo activation energy was 38.2 kJ/mol, demonstrating that higher temperature was beneficial to the removal of SDZ and verifying that thermal treatment can also be a persulfate activator. The activation energy obtained in sono/Fe^0/PS was approximately one order of magnitude lower than that obtained in the heat/PS system and Fe^0/PS system, which indicates that the effective removal of SDZ can also be achieved by sono/Fe^0/PS processes even at a low bulk temperature (10 °C) [76]. Upon increasing the temperature from 25 to 65 °C, the degradation rate constant increased from 0.0229 to 0.1042 min^{-1} under the sono/$S_2O_8^{2-}$ process [131]. Complete TC degradation occurs after 40, 60 and 75 min of reaction at 65, 55 and 45 °C respectively. The low activation energy (32.01 kJ/mol) indicates that the degradation of TC by sono/$S_2O_8^{2-}$ is thermodynamically feasible [131]. Increasing temperature (25-65 °C) enhanced the TC degradation rate constant (0.0175 to 0.1573 min^{-1}) during the sono/$S_2O_8^{2-}$ process. TC was completely removed after 60, 90 and

120 min of reaction at 65, 55 and 45 °C respectively. An activation energy value of 42.66 kJ/mol was obtained [160]. Su *et al.* have observed an insignificant enhancement in COD removal in AMX solution by temperature (24 to 40 °C) during a sono/Co^{2+}/Oxone process (the RE of COD reached more than 85% in 60 min at ambient temperature) [162].

5.5.5 Effect of other additives

5.5.5.1 Addition of H_2O_2.

H_2O_2 is a common oxidant and also the precursor to producing $^{\bullet}OH$, which is frequently used to accelerate the degradation of organic pollutants [113]. Under sonication, the formation of extra $^{\bullet}OH$, from H_2O_2 decomposition, enhanced MTZ removal [113]. In a homogenous Fe^{2+}/PS (3 mM/1 mM) system, the RE of 500 mg/L MTZ in 200 mL solution reached 97% at pH 3 in 90 min of sonication with 20 kHz and the addition of 60 mM H_2O_2, as compared to an RE of 72% in the absence of PS [113]. In another homogenous Fe^{2+}/PS (4 mM/1 mM) system, the RE of 261 mg/L FLU in 200 mL solution reached 98% at pH 4 after 80 min of sonication with 40 kHz and the addition of 20 mM H_2O_2, compared to an RE of 73% in sono/H_2O_2 [111].

In a heterogeneous martite/Oxone /(0.5 g/L/3 mM) system, the RE of 100 mg/L TC in 100 mL solution reached 87% at pH 4 in 60 min under 37 kHz and 320 W sonication with martite-nanoparticle-activated Oxone, compared to an RE of 78% in unmilled martite (sono/unmilled martite/Oxone) [112]. Only 6.5% of TC was removed by the adsorption process, while the decomposition of TC by Oxone alone was lower than 44%. As a result, when the H_2O_2 concentration rose from 10 to 40 mM, the k_1 value increased from 0.0533 to 0.0907 min^{-1}. However, increasing H_2O_2 concentration up to 50 mM caused a substantial drop in the decomposition rate of TC [112].

5.5.5.2 Addition of scavengers.

The quenching effect of t-BuOH, EtOH and 1,4-benzoquinone is a signal for verifying the roles of $^{\bullet}OH$, $O_2^{\bullet-}$ and $SO_4^{\bullet-}$ in TC degradation by sono/Fe_3O_4/PS processes [149]. The results revealed that TC degradation is suppressed with the addition of 1.05

M EtOH. This indicates that $SO_4^{\bullet-}$ and $^{\bullet}OH$ are the major radicals for the degradation of TC. In theory, EtOH is a scavenger of $SO_4^{\bullet-}$ and can also react with $^{\bullet}OH$, and the reaction constants of EtOH with $SO_4^{\bullet-}$ and OH are $1.6–7.7\times10^7$ and $1.2–2.8\times10^9$ $M^{-1}S^{-1}$, respectively [149].

In order to investigate the role of $O_2^{\bullet-}$, 1,4-benzoquinone was used as an $O_2^{\bullet-}$ quencher in a TC degradation via a sono/Fe_3O_4/PS process [149]. The addition of 0.021 M 1,4-benzoquinone did not significantly affect the TC degradation in the initial stages. However, the suppression became significant after 30 min, indicating the delayed formation of $O_2^{\bullet-}$ during the reaction [149].

t-BuOH is generally used as an OH scavenger and the reaction constant is $3.8–7.6\times10^8$ $M^{-1}S^{-1}$. Excess t-BuOH (1.05 M) was added to the solution to check the contribution percentage of $^{\bullet}OH$ [149].

Zhou, *et al.* have demonstrated that SDZ degradation is inhibited by SO_4^{2-}, NO^{3-}, HCO^{3-}/CO_3^{2-} and $H_2PO_4^-$ to different extents in a sono/Fe^0/PS system [148]. Such inorganic anions would mainly react with $SO_4^{\bullet-}$ and/or $^{\bullet}OH$ to form sub-radicals of less oxidative potential, which was also proven by the sonocatalytic degradation of SDZ in a sono/yolk-shell Fe_3O_4@ hollow@ $mSiO_2$ nanoparticle/PS system [164]. The inhibition effect was revealed to be probably due to the stronger metal ion complexation and radical scavenging in the hollow core of the yolk-shell nanoparticles [164]. Moreover, the presence of carbonate and even persulfate ions suppressed the sonocatalytic degradation of TC with martite nanoparticles and Oxone [112]. However, Cl^- enhanced the SDZ degradation with a low dose (5 mM), but inhibited it at a high dosage (100 mM) [148]. Moreover, the enhanced effects of chloride and carbon tetrachloride have also been demonstrated in the sonocatalytic degradation of TC [112].

At pH 3 and 5 with a buffer solution, the REs of SDZ reached 54.6% and 58.4%, respectively, which were lower than in the un-buffered systems. It was also speculated that the additional phosphate species (mainly HPO_4^{2-} and $H_2PO_4^-$ at pH 3.0–5.0) play

the scavenging role for SR via complexion of the phosphate species. It also indicates that the soluble iron ions inhibit SDZ degradation. As the predominant oxidant under stable neutral or alkaline conditions, •OH was strongly scavenged by phosphate species, and significant inhibition of SDZ degradation was therefore found at pH 7 and 10 with a buffer solution [76].

Finally, the addition of humic acid in concentrations above 10 mg/L also reduced the degradation rate of TC in a sono/PS process, although the effect could be compensated using higher concentrations of PS [160]. The low RE of TOC is due to the generation of recalcitrant products during TC degradation [160]. Therefore, a longer exposure time is required for the efficient mineralization of antibiotics [112].

5.5.6 Stability of catalysts

In the heterogonous sonocatalytic system with martite nanoparticles and Oxone, the decomposition rate of TC dropped by only 10.8% after four consecutive experimental runs, indicating the appropriate reusability potential of martite nanoparticles [112]. In a sonocatalytic system with Fe_3O_4 and PS, the RE of TC reached 89% in 1.5 h in the primary experiment, and then the RE decreased to 73.5% after three repetitive experiments. A low dissolved iron concentration (<0.2 mM) was detected in the solution. It was speculated that Fe(III)-bearing iron oxides formed on the surface of the catalyst, which may be more soluble, less active and stable, and thus cause the RE decline. As for effect of sonication on the catalyst particle size distribution, the particle size distribution of the used catalysts is similar to that of the fresh catalysts, indicating that Fe_3O_4 is stable under sonication [149].

6 Degradation of antibiotics by sonophotocatalysis (sonication/photocatalysis)

6.1 Mechanism of sonophotocatalysis

Photocatalysis that are based on semiconductors provide favourable results,

compared to other AOPs, in the destruction of persistent organics. In recent years, conventional photocatalytic processes have exhibited some problems, such as difficulty in the separation and recovery of catalysts, the production of secondary pollution, and the high consumption of catalysts and energy, etc. [31]. Furthermore, the lack of efficient photoactivity under solar-light, the high recombination rate of photo-induced electron-hole (e_{CB}^--h_{VB}^+) pairs, and low resistance to photo-corrosion has limited their practicality in environmental applications [84]. To overcome these obstacles, photocatalysis is usually combined with sonication, chemical oxidants or microwave techniques [31].

Sonophotocatalysis has attracted much attention because it is generally considered to be an applicable and environmentally friendly process [114]. The synergistic effect of sonocatalysis and photocatalysis generates a large number of ROS, and thus enhances the oxidation process to remove organic contaminants [84]. The cavitation effects induced by sonication eliminate the defects of photocatalysis, including the decrease in UV-available sites, mass transfer limitations and the blocking of the catalyst surface by contaminants [84]. The degradation mechanisms of TC by sonophotocatalysis are shown in Figure 5.

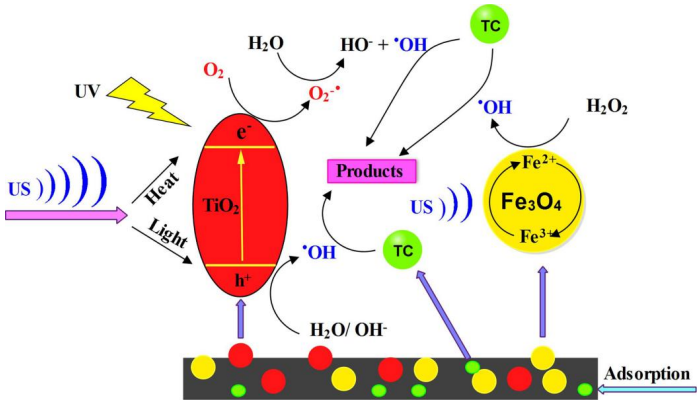

Figure 5 *Degradation mechanisms of TC by sonophotocatalysis. Reprinted from ref. [31] Copyright (2019), with permission from Elsevier.*

6.2 Application of sonophotocatalysis in antibiotic degradation

Vinesh, *et al.* have investigated the degradation of TC by sonophotocatalysis under simulated visible light with a reduced graphene-oxide (rGO) supported electron-deficient B-doped TiO_2 (Au/B-TiO_2/rGO) nanocomposite synthesized via the hydrothermal method [117]. The RE of TC under sonolysis, photocatalysis and sonophotocatalysis was found to be 25, 65 and 100%, respectively, when the reaction was performed in the presence of sonolysis and photocatalysis under 40 kHz, 600 W US, 300 W of visible light power with 0.25 g/L Au/B-TiO_2/rGO in 60 min (40 mL, 15 mg/L). The enhanced sonophotocatalytic activity (SF: ~1.3) observed was attributed to the generation of more ROS by the combination of sonication and photocatalysis [117]. According to trapping tests, holes, $^{\bullet}OH$ and $^{\bullet}O_2^-$ contributed to the degradation process [31].

The application of sonophotocatalysis for the degradation of antibiotics ha sbeen summarized in Table 7.

Table 7 *Degradation of antibiotics by sonophotocatalysis.*

ABX	**Catalysts**	**$\lambda_{UV/vis}$/$P_{UV/vis}$ (nm/W)**	**F_{US}/P_E (kHz/W)**	**t (min)**	**C_0/V (mg/L)/mL**	**pH**	**RE_{Photo} (%)**	**RE_{Sono} (%)**	**$RE_{Sono/Photo}$ (%)**	***SF***	**Refs.**
OFX	1 g/L TiO_2	350–400 /3.2 W/m^2	20/192*	120	10/300	6.0	85.0	15.0	~100.0	~1.0	[85]
TC	0.3 g/L TiO_2/MAC@T	254/6	20/40	60	30/<500	5.5	47.4	2.1	59.2	1.2	[31]
TC	0.25 g/L Au/B-TiO_2	-300	40/600	60	15/40	-	65.0	25.0	100.0	1.3	[117]

	/rGO										
CLA	0.3 g/L ZnS QDs/SnO_2	254/4	20/75	60	10/100	3.0	68.2	~8.0	86.7	1.7	[119]
RXM	0.3 g/L ZnS QDs/SnO_2	254/4	20/75	60	10/100	3.0	72.6	~12.0	90.3	~1.1	[119]
AMX	1.0 g/L gC_3N_4-20@Ni−Ti LDH	420-470/400	20/200	150	-/100	-	87.0	53.0	99.0	0.7	[39]
MOX	1 g/L NiFe-LDH/rGO	-/10	36/150	60	20/100	8.0	62.7	8.2	90.4	1.3	[118]

Note: ABX: Antibiotics; $\lambda_{UV/vis}$: wavelength of light; P_{UV}:light power; W/m^2: light power intensity; F_{US}: ultrasonic frequency; P_E: electrical power input; C_0: initial antibiotic concentration ; V: the volume of antibiotic solution; RE: removal efficiency; synergy factors = $\boldsymbol{RE_{Sono/Photo}/(RE_{Sono}+RE_{Photo})}$ [71, 81, 109]; Refs.: references.

As listed in Table 7, TiO_2 and its composites, as well as transition metal oxides, have usually been used as the catalysts for the degradation of antibiotics by sonophotocatalysis. The applications of sonophotocatalysts in the degradation of antibiotics are discussed below.

6.2.1 TiO_2 and its composites

TiO_2 is a common catalyst for promoting the photocatalytic degradation of organic contaminants. Hapeshi, *et al.* have investigated the degradation of OFX by sonophotocatalysis with TiO_2 (Conditions: 300 mL of 10 mg/L OFX, pH 6.0, 1.0 g/L catalysts, 20 kHz, 640 W/L US power, 350-400 nm UV, 3.2 W/m^2 UV power, 120 min treatment at 27 ± 2 °C) [85]. The working solution, containing 10 mg/L OFX, was prepared by spiking the appropriate mass of the compound in the secondary treated wastewater (collected from the urban wastewater treatment plant (UWTP) of Limassol, Cyprus) and then performing the necessary dilutions. The results revealed that the sonophotocatalytic degradation of OFX follows PFO kinetics. The k_1 values were 0.1054, 0.0713, 0.0203 and 0.0131 min^{-1} for sono/Photo/TiO_2, photo/TiO_2, sono/TiO_2 and sonication alone, respectively. The REs of OFX for 120 min reached 15, 62, 85 and

~100% for sonication, sono/TiO_2, photo/TiO_2 and sono/photo/TiO_2, respectively. Therefore, degradation by sonophotocatalysis was generally faster than all the individual processes, presumably due to the enhanced formation of reactive radicals. Additionally, the presence of the TiO_2 catalyst significantly increased the RE of OFX by sonication. It was assumed that the increase is attributed to the additional cavitation activity, which is used as an alternative energy source for TiO_2 to generate positive holes [85].

Kakavandi *et al.* have investigated the degradation of TC by sonophotocatalysis using TiO_2 that was decorated on magnetic activated carbon (MAC@T), where MAC was fabricated via the magnetization of AC using Fe_3O_4 nanoparticles [31]. The REs of TC for 60 min under various sonocatalytic and photocatalytic processes are listed in Table 8.

Table 8 *REs of TC for 60 min under various sonication and photocatalytic processes (Conditions: <500 mL of 30 mg/L TC, pH 5.5, 0.3 g/L catalysts, 20 kHz, 40 W US power, 6 W UV power, 60 min treatment at 25 ± 2 °C,).*

Process	Photo*	Sono*	Sono/Photo*	MAC@T	Sono/MAC@T	Photo/MAC@T	Photo/TiO_2	Sono/Photo/MAC@T
RE(%)	2.1	4.0	7.4	36.8	38.5	47.4	44.9	59.2

* Without catalysts [31].

As listed in Table 8, it was assumed that the negligible REs of TC are caused by very low generation efficiencies of free radicals in photolysis or sonication alone. The increased RE value using the sono/photo process indicates the synergistic effect between sonication and photolysis [31]. 36.8% of RE obtained by MAC@T composite indicated the RE by adsorption onto the catalyst, while an RE of 47.4% by photo/MAC@T is comparable with that (44.9%) obtained by traditional photo/TiO_2 due to the synergistic effect of adsorption and photocatalytic degradation. The highest RE (59.2%) was obtained using the sonophotocatalysis process with MAC@T. This is because the catalyst played roles for adsorption, photocatalysis and sonocatalysis simultaneously. Furthermore, the synergistic effect is associated with a contribution by

sonication and the subsequent production of ROS in the system, while the surface of the catalyst was cleaned by sonication continuously to maintain the activity of catalyst [31].

6.2.2 Fenton and Fenton-like reactions

Zhou, *et al.* have compared the degradation kinetics and REs of SMZ using 5 different sonocatalytic and photocatalytic systems with Fe_3O_4 [116]. The SMZ degradation in the sono/photo/Fe_3O_4/OA system follows PFO kinetics under the conditions used - 25 mg/L SMZ, 0.4 g/L Fe_3O_4, 0.8 mM oxalic acid (OA), UV (365 nm, 9 W), US (20 kHz, 330 W), initial pH 3, 20 °C, and the k_1 value reached 3.5×10^{-2} min^{-1}, which is about 10-times higher than that obtained in the sono/Fe_3O_4/OA system (k_1 =0.36 $\times 10^{-2}$ min^{-1}). However, the degradation of SMZ in the photo/Fe_3O_4/OA system does not follow PFO kinetics, because there was an initial degradation lag period. Thus, sonication was used to reduce the initial lag period of SMZ degradation [116].

The high stability of the SMZ molecule meant that lower REs (ca. 10–20%) were observed after 60 min in the sono/Fe_3O_4, sono/photo/Fe_3O_4 and sono/Fe_3O_4/OA systems, but higher SMZ REs were achieved in the photo/Fe_3O_4/OA system and sono/photo/Fe_3O_4/OA system [116]. It was speculated that the rapid release of dissolved iron species in the initial reaction phases, induced by Fenton-like reactions, resulted in the efficient production of ROS. Moreover, in the sono/photo/OA and sono/Fe_3O_4/OA systems, oxalate mostly acts as a competitive reactant. By contrast, in the Photo/Fe_3O_4/OA and Sono/Photo/Fe_3O_4/OA systems OA acts as both a reactant and an ROS initiator [116]. The synergistic degradation of SMZ has also been demonstrated in a Sono/Photo/Gothite- Fe^{3+}/OA system by integrating *in-situ* H_2O_2 generation under UV illumination and efficient Fe^{2+} species regeneration (Initial parameters: 25 mg/L SMZ , 0.5 g/L goethite, 0.8 mM OA, 330W US and pH 3, initial Fe^{3+} concentration of 250 μM) [115]. The cleavage of the S–N bond in the SMZ molecule was dominant under $^{\bullet}OH$ attack. Meanwhile, organic mineralization and wastewater detoxification

were achieved.

Transition metal oxide (ZnO) or sulfide (ZnS and SnO_2) have been used to accelerate the degradation of antibiotics in sono/photo/Fenton-like processes [83, 119]. After pretreatment, the degradation of antibiotics becomes possible using biological treatment processes. The degradation of 10 mg/L RXM and CLA was studied in a sono/photo/Fenton-like system with ZnS quantum dots decorated onto SnO_2 nanosheets prepared using the hydrothermal method [119]. Without catalysts, REs were low using the Photo method alone, sonication alone, photo/H_2O_2, sono/H_2O_2 and sono/photo/H_2O_2, due to the insufficient formation of $^{\bullet}OH$. With 0.3 g/L catalyst and 6 mM H_2O_2, only 31.4% of 10 mg/L CLA and 36.4% of 10 mg/L RXM were removed from 100 mL aqueous solutions at pH 3 after 60 min. When sonication (20 kHz, 75 W) was used to enhance the degradation in the above system, the REs of CLA and RXM increased to 61.2% and 65.5%, while higher REs (68.2% and 72.6%) were obtained in the same system, but in the presence of UV (254 nm, 4 W). Surprisingly, The REs of CLA and RXM reached 86.7% and 90.3% in the sono/photo/Fenton process [119]. Consequently, the superior performance and synergistic effects of the sono/photo/catalyst process were attributed to the promotion of $^{\bullet}OH$ generation [119].

6.2.3 Other nano-composites

Khataee, *et al.* have investigated the degradation of MOX by the sonophotocatalytic method using a NiFe-layered double hydroxide/reduced graphene oxide (NiFe-LDH/rGO) nanocomposite [118]. The RE of MOX (90.4%) by sonophotocatalysis under the used conditions - 100 mL of 20 mg/L MOX, pH 8.0, 1.0 g/L catalysts, 36 kHz, 150 W US power, 10 W UV power, 60 min treatment - was higher than the REs of sonocatalysis (72.4%) and photocatalysis (62.7%), but lower than their sum. The results revealed that $^{\bullet}OH$ and $^{\bullet}O_2^-$ radicals play the dominant role in MOX degradation.

Abazari, *et al.* have investigated the degradation of AMX by sonophotocatalysis

with nanocomposites of g-C_3N_4@Ni-Ti layered double hydroxides (g-C_3N_4@Ni−Ti LDH) synthesized using the hydrothermal method with NH_4F [39]. The conditions - 100 mL AMX, pH 8.0, 1.0 g/L catalysts, 20 kHz, 200 W US power, 420-470 nm, 400 W UV power and 150 min treatment – allowed the following RE order to be determined: sonocatalysis < photocatalysis < sonophotocatalysis. The formation of $^{\bullet}OH$ on the surface of the g-C_3N_4-20@Ni−Ti LDH particles was approved using the terephthalic acid probe in photoluminescence spectroscopy [39]. Thus, the observed enhancement in the sonophotocatalytic activity of the nanocomposites can be related to their higher specific surface areas, the intimacy of the contact interfaces of their individual components, i.e., pristine g-C_3N_4 and Ni−Ti LDH, the synergistic effect between these components and restriction of electron−hole recombination.

Ghoreishian, *et al.* have investigated the degradation of TC by sonophotocatalysis with flower-like rGO/$CdWO_4$ hierarchical structures that were synthesized using a facile wet-chemistry method without any calcination [84]. rGO/$CdWO_4$ exhibited significant photoelectrochemical performance under the conditions used - 500 mL of 13.54 mg/L AMX, 0.432 g catalysts, 60 min treatment - and demonstrated superior sonophotocatalytic activity and mineralization efficiency compared with $CdWO_4$ [84]. Thus, the higher catalytic activity of rGO/$CdWO_4$ is attributable to rGO, which catches TC residuals from aqueous solution and acts as a charge acceptor to promote the separation of photo-generated carriers via its π-π conjugated structure.

6.3 Other concerning issues

6.3.1 Effective factors

Due to the emerging nature of sonophotocatalysis, little has been reported on the effects of critical factors. The performance of sonophotocatalytic systems is influenced by various parameters, such as US and UV conditions, catalyst dosage, pH value, initial antibiotic concentration, additives, etc. [31, 83-85]. In general, the RE of antibiotics increases with increasing US intensity, UV intensity [39] and catalyst dosage [20, 31,

85, 118, 119, 167], and acidic conditions favour degradation [20, 116]. For example, Tavasol, *et al.* have designed a photocatalyst of sea sediment/titanate to remove CPX from aqueous media in the presence of sono/photo/H_2O_2 [26]. Under the conditions - 150 mL of 100 mg/L CPX, pH 6.8, 40 kHz US, 15 W UV power, 100 min treatment - the removal of antibiotics was achieved with increasing titanium content loaded onto the sediments (1.5 g/L catalysts), due to higher surface area and higher photocatalytic activity that it provides [26].

In some cases, the ratio of catalyst and acid (e.g., Fe_3O_4/OA) is also an important factor for the degradation of antibiotics [116]. As discussed above, sonocatalysis or photocatalysis alone are not adequate to effectively remove antibiotics from aqueous solutions, but the addition of either H_2O_2 or PS significantly enhances the RE, while RE increases with increasing concentration of additives [20, 163]. For example, OFX degradation increases slightly upon increasing the H_2O_2 concentration, but with an optimum level of H_2O_2 concentration at 0.14 mM. [85]. Zeng, *et al.* have investigated the degradation of LEV by visible-light-driven sonophotocatalysis and PS activation over 3D urchin-like MoS_2/C nanoparticles [100]. The radical species $^{\bullet}OH$ and $SO_4^{\bullet-}$ were accelerated, while $^{\bullet}O_2^-$ was limited in this coupled system, which largely facilitates its excellent degradation performance with a synergistic effect [167].

By contrast, the addition of inhibitors decreases the degradation of antibiotics as a means to probe the role of $^{\bullet}OH$ that is formed *in situ*. For example, the inhibitory effect of different inorganic salts on NOR degradation in a sono/nano-Cu^0/H_2O_2 system followed the sequence: Na_2SO_4 > $NaNO_3$ >≈ no salt > NaCl > $NaHCO_3$ [20]. However, a contradictory result has been observed, in which a decreasing sequence of the inhibitory effect of anions towards TC degradation in a sono/photo/MAC@T process was observed to be: Cl^- > HCO_3^- > PO_4^{3-} > NO_3^- > SO_4^{2-} [31].

6.3.2 Mineralization and detoxification

Because of the significant synergy in the sonophotocatalysis of antibiotics, the

mineralization and detoxification of aqueous antibiotics solution have been improved [115, 116]. For example, under the conditions used - 40 mL of 15 mg/L TC, 0.25 g/L catalysts, 40 kHz, 600 W US power, 300 W UV power, 60 min treatment - 12.1, 45.7 and 73.6 % TOC removal have been achieved by sonolysis, photocatalysis and sonophotocatalysis, respectively [117].

The significant synergistic degradation of SMZ can be further evidenced by the results of mineralization and detoxification of treated water samples. 78% of TOC was removed in a sono/photo/Fe_3O_4/OA system after 1 h of reaction time, with an increase of the corresponding EC 50 from 17% (the raw sample) to 89%. The efficiencies of mineralization and detoxification were much higher than those achieved in the other six systems [116]. Montoya-Rodríguez *et al.* have observed 100% removal of AMP after 75 min of treatment with the sonochemical process. Moreover, the antimicrobial activity of AMP significantly decreased, which was related to attacks of $^{\bullet}OH$ on the active nucleus [46]. In addition, the highest mineralization of the pollutant (40% of TOC removal) was achieved after 180 min of treatment with a sono/photo/Fenton process [46].

Toxicity depends on the chemical properties and concentration of not only the OFX that was initially present, but also of its transformation products (TPs). Interestingly, the by-products formed during the dissolved organic matter (DOM) oxidation seem to play a similar role with regards to the toxicity changes as that of the by-products formed during OFX degradation [85]. Antimicrobial activity (AA) has been assessed by the Kirby-Bauer method using *Staphylococcus aureus* as the indicator microorganism. As a result, 100% of AA was removed after 60 and 20 min for AMP and NAF by the sono/photo/Fenton process, respectively [69].

6.3.3 Stability and reusability of catalysts

The stability and reusability of catalysts used in sonophotocatalysis are critical to the promotion of the degradation of antibiotics. Evaluations have revealed that some

catalysts are robust. For example, insignificant loss was observed in the sonophotocatalytic activity of the nanocomposites of g-C_3N_4-20@Ni−Ti LDH even after five consecutive runs [39]. Both Fe leaching and loss of decontamination were slight after reuse, indicating that MAC@T has high stability and reusability [31]. The rapid degradation of SMZ and the decomposition of oxalate could still be achieved in the heterogeneous sonophotolytic Fenton-like system using goethite over five consecutive reaction cycles [115]. Besides, wastewater treatment is plausible using a reusable synthesized NiFe-LDH/rGO nanocomposite [118].

7 Degradation of antibiotics by sonozonation (Sonication/Ozonation)

7.1 Mechanisms of sonozonation

Ozone is a powerful oxidant that can directly react with contaminants or decompose into more powerful oxidants - free radicals. Ozonation has usually been used to remove refractory organics, including antibiotics, and improve biodegradability. However, high costs, poor gas-liquid mass transfer and selective oxidation have limited its use. Due to the cavitation effects, such as hotspots, microjets, shockwaves, turbulence, etc., sonication enables the mass transfer and $^{\bullet}OH$ production to be improved, leading to significantly high degradation rates for antibiotics [78, 79, 80, 120, 121]. It was speculated that cavitation effects reduce the liquid-film thickness of gas bubbles containing O_3, and increase the gas/liquid specific surface area. Meanwhile, the diffusion of free radicals, generated in the vapour phase of cavitation bubbles and O_3/O_2 bubbles, into the bulk solution is enhanced under sonication to oxidize hydrophilic antibiotics [79].

For example, AMX cannot be efficiently oxidized through sonication alone, but can be removed efficiently using ozonation or sonozonation [78]. Moreover, the oxidative degradation efficiency of AMX using the above methods has been identified by intermediate analysis with GC-MS, mineralization analysis and the Microtox

toxicity test [78]. In ozonation processes, six products, formed via the hydroxylation of AMX, demethylation, decarboxylation and the opening of beta-lactam and thiazole rings with ROS, have been observed under alkaline conditions. The degradation pathway of AMX by sonozonation is similar to that of ozonation. Scheme 6 shows the pathway of intermediate formation during the degradation of AMX by the sonication, ozonation and sonozonation processes. Meanwhile, the mineralization degrees reached 10% by sonication alone, 32% by ozonation alone and 45% by sonozonation under optimized conditions.

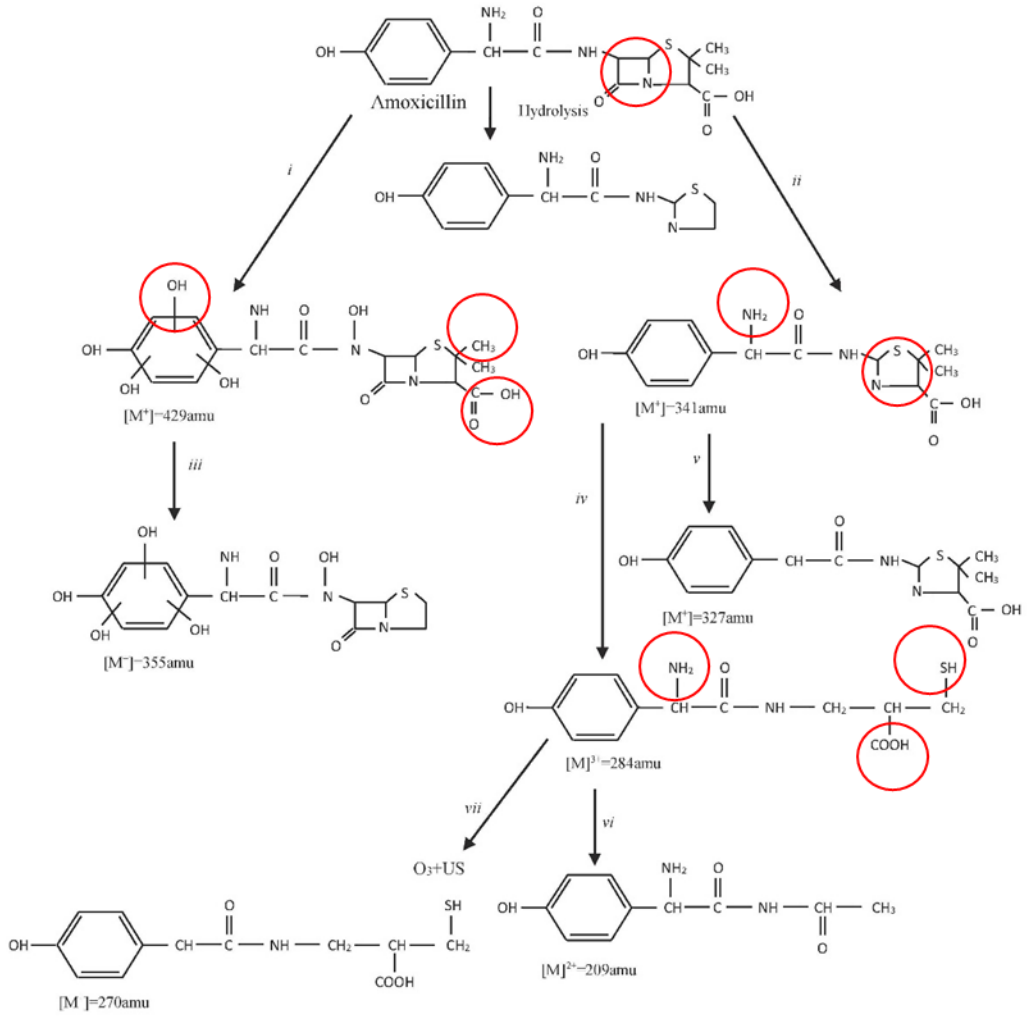

***Scheme 6**. Pathway of intermediate formation during the degradation of AMX by sonication alone, ozonation alone and sonozonation at pH 10, 575 kHz, 75 W, 15 mg/L O_3(aq). Reprinted from ref. [78] Copyright (2012), with permission from Elsevier.*

Figure S4 shows the LC-APCI-MS of five major intermediates formed during the

degradation of TC by sonozonation, indicating the degradation pathway of TC (Scheme 6) [80]. As shown in Scheme 7, Product 1 was generated by an initial 1,3-dipolar cycloaddition towards the C_{11a}–C_{12} double-bond and a rearrangement with the hydroxyl at position C_{12}. Subsequently, Product 2 was formed via the further oxidization of the double-bond C_2–C_3 in Product 1. Product 3 was finally synthesized by O_3 or •OH by successively attacking ring D (bearing hydroxyl group) of Product 2. Therefore, •OH dominates the degradation of TC in the sonozonation system [80].

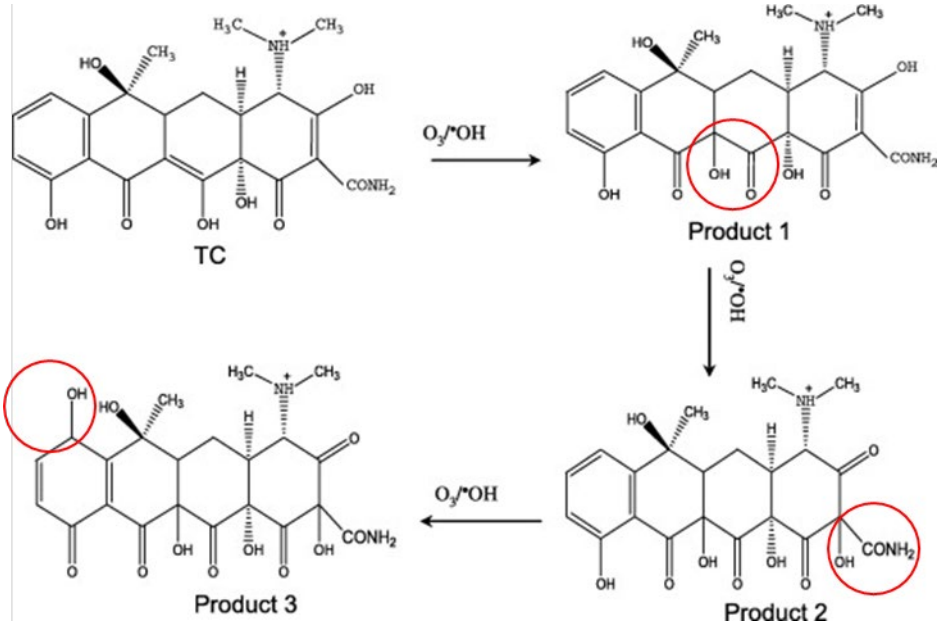

Scheme 7. *The degradation pathway of TC in the sonozonation system. Reprinted from ref. [80] Copyright (2012), with permission from Elsevier.*

Recently, we have reported the mechanisms, reactors and effective factors of sonozonation for organic degradation [81]. In this review, the applications of sonozonation and the roles of effective factors on antibiotic degradation are discussed.

7.2 Application of sonozonation on antibiotic degradation

Kıdak *et al.* have investigated the degradation of AMX by sonozonation at 575 kHz US [78]. Under the optimized sonozonation conditions - 250 mL of 25 mg/L AMX solution, 0.13 mg/L O_3, 575 kHz, 75 W, pH 10, 90 min treatment - the highest degradation rate constant (k_1 = 2.5 min^{-1}), highest mineralization (45% of TOC removal) and reduced toxicity (EC_{50}% = 67.5) were achieved, compared with those obtained by

sonication alone (k_1 = 0.04 min^{-1} and 10% of TOC removal) and ozonation alone (k_1=1.97 min^{-1} and 32% of TOC removal and EC_{50}%= 13.6) [78]. Based on the k_1 values obtained by the various processes, the synergistic factor of sonozonation for AMX degradation was calculated to be 1.24.

Naddeo *et al.* have investigated the degradation of SMX using sonozonation with 20 kHz and 370W/L US [120]. 61% of SMX was removed from 200 mL of a 10 mg/L SMX solution, with 3.3 g/h of O_3 dose, after 40 min in the sonozonation system, while 51% SMX was removed by ozonation alone [120]. The enhancement of SMX degradation by sonozonation can reduce the consumption of chemicals, which is particularly interesting for performing the scale-up of sonozonation process [120].

Guo *et al.* have also investigated the degradation of SMX by sonozonation with 20 kHz and 600W/L US [121]. A 100 mg/L (0.5 mM) SMX solution was treated in a 1.5 L-reactor with 3.0 g/h of O_3 dose, and about 95% of SMX was removed after 5 min treatment in the sonozonation system, while only 3% and about 85% SMX was removed by sonication alone and ozonation alone [121].

7.3 Role of effective factors

The RE of antibiotics by sonozonation is influenced by various parameters, including O_3 concentration/flow rate [79, 80, 120], pH value [78, 79, 80, 120, 121], initial antibiotic concentration [79, 80], US power/frequency [79, 80], and additives [78, 79, 80], as discussed below.

7.3.1 Effect of gaseous O_3 concentration, flowrate and dosage

In general, O_3 concentration in a gas increases with the yield or dosage of O_3 production under an identical gas flowrate. Naddeo *et al.* have noted that the degradation of SMX was enhanced by increasing ozone flows in the sonozonation system, which was attributed to improved O_3 mass transfer [120]. Guo *et al.* have found that the RE of SMX doubled as O_3 dosage increased from 2 to 5 g/h, because the increasing ozone concentration was able to improve the mass transfer of O_3 from the

gas to liquid phase [79]. In addition, the increasing O_3 concentration increase the amount of O_3 molecules and $^{\bullet}OH$ that were available to react with antibiotics in solution [79].

Wang *et al.* have also demonstrated that the RE of TC increases with increasing gaseous O_3 concentration and gas flowrate in a sonozonation system [80]. On the one hand, k_1 values were 0.42, 0.66, 0.85 and 1.34 min^{-1} at 30, 35, 40 and 50 L/h of gas flowrate, respectively. The increasing gas flowrate increases the net surface area and improved O_3 mass transfer from the gas phase to aqueous phase, thus increasing the volumetric mass transfer coefficient of O_3 [80]. On the other hand, k_1 values reached 0.66, 0.77, 0.84 and 1.04 min^{-1} at 35.8, 44.5, 45.6 and 47 mg/L of gaseous O_3 concentration, respectively. This suggests that the increasing gaseous O_3 concentration increased the equilibrium O_3 concentration in the aqueous phase, according to Henry's law. The increasing equilibrium O_3 concentration also improved O_3 mass transfer from the gas phase to the liquid phase [80].

7.3.2 Effect of pH value

The pathways of ozonation generally include direct oxidation by O_3 molecules, which is more selective and predominant under acidic conditions, and the indirect oxidation by $^{\bullet}OH$ that is formed *in situ*, which is non-selective and predominant under alkaline conditions [79, 80]. Therefore, the predominant reaction and reaction rate during ozonation can be controlled by adjusting pH value, which is also considered a critical factor for the efficiency of sonozonation [79]. The increase of reaction rate means that a shorter reaction time is required to complete the degradation of antibiotics, while O_3 consumption and operation costs are reduced [121].

Guo *et al.* have found that the degradation rate of SMX increases with increasing pH value. SMX has two *pKa* values, of 1.6 and 5.7, resulting in protonated, non-protonated and deprotonated forms at different pH values. The amino groups are possible reaction centres that are most susceptible to O_3 electrophilic attack. The non-

protonated form is the predominant form at pH < 7, and is less susceptible to O_3 attack than the deprotonated form, leading to lower k_1 values under acidic conditions (0.29 min^{-1} at pH 3; 0.30 min^{-1} at pH 5). At pH 7, SMX molecules were converted into the completely deprotonated form, which had a higher reactivity towards O_3 molecules. Under basic conditions, the oxidation of SMX was enhanced due to the generation of numerous $^{\bullet}OH$ species (0.42 min^{-1} at pH 7; 0.50 min^{-1} at pH 9). Consequently, the degradation rate of SMX under basic conditions was higher than under acidic conditions [79].

Furthermore, the enhancement of sonication on SMX degradation by ozonation varied by 6–26% under different pH values, and the highest enhanced effect was observed at pH 5 [121]. This suggests that sonication promoted the diffusion of O_3 molecules in water under acidic conditions and increased the contact area between O_3 and SMX, resulting in increased RE of SMX by direct-oxidation with O_3 molecules. Under neutral and alkali conditions, sonication increased the degradation rates of SMX by only 6-7%. This indicates that sonication slightly enhanced O_3 decomposition and the yield of $^{\bullet}OH$, which is responsible for the indirect-oxidation [121].

TC degradation rate has also increased as the pH value increased from 3 to 9 in a sonozonation process [80]. Similarly, there are four different species of TC molecule, TCH_3^+, TCH_2, TCH^- and TC^{2-} , in which the protonation-deprotonation reactions depend on pH value. The deprotonated TC with a positively charged group at higher pH values is more easily attacked by O_3 molecules and/or $^{\bullet}OH$ than TC itself. Thus, the TC degradation rate increases with increasing pH [80]. Likewise, AMX is a hydrophilic and weak polyprotic acid with three *pKa* values of 2.67, 7.11 and 9.55 at 37 °C. At pH 10, dissolution is favoured for the more degradable forms of AMX when the amine is deprotonated and a pair of electrons is available for electrophilic attack, while the increased solubility of AMX at pH 10 leads to higher reaction rates in the presence of the readily abundant radicals formed in the 575 kHz US field [78].

7.3.3 Effect of initial antibiotic concentration

Since the concentrations of O_3 and $^{\bullet}OH$ available are almost identical under the same operation conditions in a sonozonation system, and are independent of the initial antibiotic concentrations, the degradation rate decreases mostly with increasing antibiotic concentration. For example, the k_1 value of SMX degradation decreased three-fold (from 0.37 to 0.09 min^{-1}) as SMX concentration increased from 50 to 400 mg/L in a sonozonation system. The additional reason for this is the fact that the competing reactions between SMX and its degradation products gradually turned predominant with the increasing initial SMX concentration. Such competing reactions reduced the reaction rates of SMX with O_3 and $^{\bullet}OH$ [79]. Similarly, the TC degradation rate also decreased with increasing initial TC concentration in a sonozonation system, and the k_1 value decreased from 0.92 to 0.59 min^{-1} when TC concentration increased from 200 to 800 mg/L [80].

7.3.4 Effect of power density of US

Increasing US power density can generally enhance the turbulence effect, resulting in increased antibiotic degradation rates, as the enhanced turbulence favours O_3 mass transfer from the gas to liquid phase [79]. It has been speculated that powerful sonication enhances mechanical mixing, making O_3-containing bubbles smaller and reducing the thickness of liquid films [80]. In addition, more O_3 molecules can be decomposed to generate more ROS under more powerful sonication. For example, the k_1 values of SMX degradation reached 0.25, 0.26 and 0.30 min^{-1} at 400, 600 and 800 W/L of power density in a sonozonation system, respectively [79]. Moreover, the TC degradation rate increased with increasing power density, and the k_1 values of TC degradation reached 0.57, 0.71, 0.90, 1.04, 1.74 and 2.60 min^{-1} at 0, 85.3, 125.4, 142.8, 169.8 and 218.6 W/L of power density, respectively [80].

7.3.5 Other concerning issues

The chemical structures and hydrophobicity of antibiotics generally influence their

degradation kinetics and efficiency [120]. Little competitive oxidation of SMX, diclofenac and carbamazepine has been observed in a mixing solution under sonozonation, showing that the simultaneous presence of SMX, diclofenac and carbamazepine is not an obstacle for degradation via sonozonation [120].

This indicates that the oxidation of TC by •OH that are generated *in situ* dominates the degradation of TC by sonozonation. By contrast, the addition of the radical scavenger *t*-butanol can accelerate the SMX degradation rate [79], and it has been speculated that the direct oxidation of SMX by O_3 molecules is the dominant pathway in the sonozonation system. The presence of H_2O_2 improved the TC degradation rate when the H_2O_2 concentration did not exceeded 10 mM, while the presence of t-butanol inhibited the TC degradation rate to some extent [80].

Alkalinity and humic acid species reduced the RE (50% decrease) by sonication alone as radical reactions control the degradation of AMX [78]. However, the addition of alkalinity, humic acid and both did not significantly change the removal rate of AMX during both ozonation and sonozonation, since, in this case, the reaction of AMX with O_3 molecules controls the degradation [78].

Besides enhancing the degradation of antibiotics by ozonation, sonication can simultaneously promote the mineralization and detoxification of antibiotics in aqueous solutions. The Microtox toxicity test has been used to find the concentration value of the treated effluents that affects 50% of the microorganisms in a solution (EC50), and thus to assess the toxicity of solutions. The initial AMX solution shows high toxicity with a EC50 value of 14% [78]. Under sonozonation (250 mL of 25 mg/L AMX, 575 kHz, 75 W/L US power, 0.13 mg/L O_3, pH 10.0, 90 min treatment), the EC50 value decreased to 10.87% and 13.59% after treatment with sonication and ozonation alone, respectively, showing that the intermediates with higher toxicity were formed during the degradation of AMX. By contrast, the EC50 value increased to 67.48% under sonozonation, indicating that fewer intermediates were formed with a higher mineralization degree [78]. For the degradation of 100 mg/L SMX by sonozonation,

with 20 kHz, 600 W/L US and 5.0 g/h O_3 at pH 7.0 for 30 min, the BOD_5/COD ratio increased from 0 to 0.54 after sonozonation treatment and the biological toxicity of the solution was reduced [79].

During the degradation of 400 mg/L TC by sonozonation with 20 kHz and 142.8 W/L of US at pH 7, Wang *et al.* found that the COD removal reached 91% after 90 min treatment, while very low COD removal was obtained by sonication alone, due to the lower production of free radicals by sonication at 20 kHz. 76% of COD removal was achieved by ozonation alone at a gas flow rate of 35 L/h, which contained 45.6 mg/L O_3 [80]. The initial TC solution resulted in 24% death of the crustaceans after 24 h of exposure. However, the acute toxicity reached its maximum after 10 min of sonozonation treatment, and the mortality was as high as 95%. The acute toxicity then gradually decreased to 80% in 70 min and 60% in 90 min of treatment [80].

Finally, it should be mentioned that most of the reported work, whether it used sonication alone or hybrid processes, made use of standard solutions and simulated wastewater to investigate the removal of antibiotics. Only a few studies have focused on the comparison of simulated and actual wastewater. Higher degradation rates (Rd) have been found for AMP in simulated urine than in distilled water (ρ>1, ρ= Rd in matrix/Rd in distilled water), which indicates that sonochemical processes are suitable for the removal of antibiotics in complex matrices [46]. OXA was difficult to mineralize (360 min) under sonication, while it can be completely mineralized using non-adapted microorganisms from a municipal wastewater treatment plant, which demonstrates that the sonication process transformed the antibiotic into substances that are bio-treatable using a typical aerobic biological system [128]. Furthermore, the highest (the most hydrophobic, i.e., CLX) and lowest (the most hydrophilic, i.e., CPD) Rd of antibiotics were observed in simulated hospital wastewater and seawater. A higher degradation rate for CLX was obtained in simulated hospital wastewater and seawater than in distilled water (ρ>1), probably due to the salting-out effect exerted by matrix components. The moderate inhibition of CPD removal in hospital wastewater and seawater, compared to

distilled water, has been attributed to competition by $^{\bullet}OH$ with the other substances in the matrices [129]. Compared with synthetic water, the RE of CIP for 15 min and mineralization for 60 min in real wastewater from a municipal wastewater treatment plant was decreased by 13.6 and 18.9% respectively, which illustrates that the treatment of CIP and TOC by the sono/Fe^{2+}/H_2O_2 process is significantly hampered in a real matrix [32].

Another important factor to consider is the fact that almost all research on the the removal of antibiotics by US involves processes that are performed on a bench scale, thus further pilot-scale investigations are recommended. Factors that should be considered when using pilot-scale systems include energy consumption by US, mass transfer, pH adjustment and application in real wastewater samples, temperature controls, *et al.*

Declaration of Competing Interest

The authors declare that they have no known competing financial interests or personal relationships that could have appeared to influence the work reported in this paper.

Acknowledgments

This research was supported by Fondazione CRT "*Sviluppo di tecnologie integrate per l'eliminazione dei residui di antibiotici dal latte vaccino*" and also by the China Scholarship Council. Pengyun Liu was supported by the China Scholarship Council (No. 201909505008).

8 References

[1] S.A. Waksman, What is an antibiotic or an antibiotic substance?, Mycologia. 39 (1947) 565-569.

[2] S. Suzuki, P.T.P. Hoa, Distribution of quinolones, sulfonamides, tetracyclines in aquatic environment and antibiotic resistance in Indochina, Front. Microbiol. 3 (2012) 67.

[3] R. Gothwal, T. Shashidhar, Antibiotic pollution in the environment: a review, Clean–Soil Air Water. 43 (2015) 479-489.

[4] K. Kümmerer, Antibiotics in the aquatic environment–a review–part I, Chemosphere. 75 (2009) 417-434.

[5] V. Homem, L. Santos, Degradation and removal methods of antibiotics from aqueous matrices–a review, J. Environ. Manage. 92 (2011) 2304-2347.

[6] S. Thiele-Bruhn,, Pharmaceutical antibiotic compounds in soils–a review, J. Plant. Nutr. Soil Sc. 166 (2003) 145-167.

[7] J. Wang, Z. Run, L. Chu, The occurrence, distribution and degradation of antibiotics by ionizing radiation: an overview, Sci. Total Environ. 646 (2019) 1385-1397.

[8] D. Ghernaout, N. Elboughdiri, Antibiotics Resistance in Water Mediums: Background, Facts, and Trends, Appl. Eng. 4 (2020) 1.

[9] X. Liu, G. Zhang, Y. Liu, S. Lu, P. Qin, X. Guo, B. Bi, L. Wang, B. Xi, F. Wu, W. Wang, T. Zhang, Occurrence and fate of antibiotics and antibiotic resistance genes in typical urban water of Beijing, China, Environ. Pollut. 246 (2019) 163-173.

[10] P .Grenni, V. Ancona, A.B. Caracciolo, Ecological effects of antibiotics on natural ecosystems: A review, Microchem. J. 136 (2018) 25-39.

[11] S. Li, W. Shi, M. You, R. Zhang, Y. Kuang, C. Dang, W. Sun, Y. Zhou, W. Wang, J. Ni, Antibiotics in water and sediments of Danjiangkou Reservoir, China: Spatiotemporal distribution and indicator screening, Environ. pollut. 246 (2019) 435-442.

[12] K. Chen, J. Zhou, Occurrence and behavior of antibiotics in water and sediments from the Huangpu River, Shanghai, China, Chemosphere. 95 (2014) 604-612.

[13] W. Li, Y. Shi, L. Gao, J. Liu, Y. Cai, Occurrence of antibiotics in water, sediments, aquatic plants, and animals from Baiyangdian Lake in North China, Chemosphere. 89 (2012) 1307-1315.

[14] Y. Huang, Y. Liu, P. Du, L. Zeng, C. Mo, Y. Li, H. Lü, Q. Cai, Occurrence and distribution of antibiotics and antibiotic resistant genes in water and sediments of urban rivers with black-odor water in Guangzhou, South China, Sci. total environ. 670 (2019) 170-180.

[15] L. Huang, Y. Mo, Z. Wu, S. Rad, X. Song, H. Zeng, S. Bashir, B. Kang, Z. Chen, Occurrence, distribution, and health risk assessment of quinolone antibiotics in water, sediment, and fish species of Qingshitan reservoir, South China, Sci. Rep-UK. 10 (2020) 1-18.

[16] V. Yargeau, C. Leclair, Impact of operating conditions on decomposition of antibiotics during

ozonation: a review, Ozone-Sci. Eng. 30 (2008) 175-188.

[17] E.A. Serna-Galvis, J. Silva-Agredo, A.L. Giraldo, O.A. Flórez, R.A. Torres-Palma, Comparison of route, mechanism and extent of treatment for the degradation of a β-lactam antibiotic by TiO_2 photocatalysis, sonochemistry, electrochemistry and the photo-Fenton system, Chem. Eng. J. 284 (2016) 953-962.

[18] Z. Fang, J. Chen, X. Qiu, X. Qiu, W. Cheng, L. Zhu, Effective removal of antibiotic metronidazole from water by nanoscale zero-valent iron particles, Desalination. 268 (2011) 60-67.

[19] A.R. Rahmani, H. Rezaei-Vahidian, H. Almasi, F. Donyagard, Modeling and optimization of ciprofloxacin degradation by hybridized potassium persulfate/zero valent-zinc/ultrasonic process, Environ. Processes. 4 (2017) 563-572.

[20] X. Ma, Y. Cheng, Y. Ge, H. Wu, Q. Li, N. Gao, J. Deng, Ultrasound-enhanced nanosized zero-valent copper activation of hydrogen peroxide for the degradation of norfloxacin, Ultrason. Sonochem. 40 (2018) 763-772.

[21] M. Gholami, K. Rahmani, A. Rahmani, H. Rahmani, A. Esrafili, Oxidative degradation of clindamycin in aqueous solution using nanoscale zero-valent iron/H_2O_2/US, Desalin. Water Treat. 57 (2016) 13878-13886.

[22] H. Rahmani, M. Gholami, A.H. Mahvi, M. Ali-Mohammadi, K. Rahmani, Tinidazol antibiotic degradation in aqueous solution by zero valent iron nanoparticles and hydrogen peroxide in the presence of ultrasound radiation, J. Water Chem. Techno+. 36 (2014) 317-324.

[23] M. Magureanu, D. Piroi, N.B. Mandache, V. David, A. Medvedovici, C. Bradu, V.I. Parvulescu, Degradation of antibiotics in water by non-thermal plasma treatment, Water Res. 45 (2011) 3407-3416.

[24] C. Adams, Y. Wang, K. Loftin, M. Meyer, Removal of antibiotics from surface and distilled water in conventional water treatment processes, J. Environ. Eng. 128 (2002) 253-260.

[25] O.A. Alsager, M.N. Alnajrani, H.A. Abuelizz, I.A. Aldaghmani, Removal of antibiotics from water and waste milk by ozonation: kinetics, byproducts, and antimicrobial activity, Ecotox. Environ. Safe. 158 (2018) 114-122.

[26] F. Tavasol, T. Tabatabaie, B. Ramavandi, F. Amiri, Design a new photocatalyst of sea sediment/titanate to remove cephalexin antibiotic from aqueous media in the presence of sonication/ultraviolet/hydrogen peroxide: Pathway and mechanism for degradation, Ultrason. Sonochem. (2020) 105062.

[27] K.S. Suslick, D.A. Hammerton, R.E. Cline, Sonochemical hot spot, J. Am. Chem. Soc. 108 (1986) 5641-5642.

[28] X. Ge, Z. Wu, M. Manzoli, Z. Wu, G. Cravotto, Feasibility and the Mechanism of Desorption of Phenolic Compounds from Activated Carbons, Ind. Eng. Chem. Res. 59 (2020) 12223-12231.

[29] X. Ge, Z. Wu, M. Manzoli, L. Jicsinszky, Z. Wu, A.E. Nosyrev, G. Cravotto, Adsorptive Recovery of Iopamidol from Aqueous Solution and Parallel Reuse of Activated Carbon: Batch and Flow Study, Ind. Eng. Chem. Res. 58 (2019) 7284-7295.

[30] Z. Fang, J. Chen, X. Qiu, X. Qiu, W. Cheng, L. Zhu, Effective removal of antibiotic metronidazole from water by nanoscale zero-valent iron particles, Desalination. 268 (2011) 60-67.

[31] B. Kakavandi, N. Bahari, R.R. Kalantary, E.D. Fard, Enhanced sono-photocatalysis of tetracycline antibiotic using TiO_2 decorated on magnetic activated carbon (MAC@T) coupled with US and UV: A new hybrid system, Ultrason. sonochem. 55 (2019) 75-85.
[32] K. González Labrada, D.R. Alcorta Cuello, I. Saborit Sánchez, M. García Batle, M.H. Manero, L. Barthe, U.J. Jáuregui-Haza, Optimization of ciprofloxacin degradation in wastewater by homogeneous sono-Fenton process at high frequency, J. Environ. Sci. Heal. A. 53 (2018) 1139-1148.
[33] L. Hou, L. Wang, S. Royer, H. Zhang, Ultrasound-assisted heterogeneous Fenton-like degradation of tetracycline over a magnetite catalyst, J. Hazard. Mater. 302 (2016) 458-467.
[34] C. Wang, J. Jian, Feasibility of tetracycline wastewater degradation by enhanced sonolysis, J. Adv. Oxid. Technol. 18 (2015) 39-46.
[35] T. Zhou, X. Zou, X. Wu, J. Mao, J. Wang, Synergistic degradation of antibiotic norfloxacin in a novel heterogeneous sonochemical Fe^0/tetraphosphate Fenton-like system, Ultrason. Sonochem. 37 (2017) 320-327.
[36] E. Hapeshi, A. Achilleos, A. Papaioannou, L. Valanidou, N.P. Xekoukoulotakis, D. Mantzavinos, D. Fatta-Kassinos, Sonochemical degradation of ofloxacin in aqueous solutions, Water Sci. Technol. 61 (2010) 3141-3146.
[37] R.J. Wood, J. Lee, M.J. Bussemaker, A parametric review of sonochemistry: control and augmentation of sonochemical activity in aqueous solutions, Ultrason. sonochem. 38 (2017) 351-370.
[38] E. De Bel, J. Dewulf, B. De Witte, H. Van Langenhove, C. Janssen, Influence of pH on the sonolysis of ciprofloxacin: biodegradability, ecotoxicity and antibiotic activity of its degradation products, Chemosphere. 77 (2009) 291-295.
[39] R. Abazari, A.R. Mahjoub, S. Sanati, Z. Rezvani, Z. Hou, H. Dai, Ni–Ti layered double hydroxide@graphitic carbon nitride nanosheet: a novel nanocomposite with high and ultrafast sonophotocatalytic performance for degradation of antibiotics, Inorg. Chem. 58 (2019) 1834-1849.
[40] Y.A.J. Al-Hamadani, C. Jung, J.K. Im, L.K. Boateng, J. R.V. Flora, M. Jang, J. Heo, C. Min Park, Y. Yoon, Sonocatalytic degradation coupled with single-walled carbon nanotubes for removal of ibuprofen and sulfamethoxazole, Chem. Eng. Sci. 162 (2017) 300-308.
[41] Y. Gao, N. Gao, Y. Deng, J. Gu, Y. Gu, D. Zhang, Factors affecting sonolytic degradation of sulfamethazine in water, Ultrason. Sonochem. 20 (2013) 1401-1407.
[42] W. Guo, Y. Shi, H. Wang, H. Yang, G. Zhang, Sonochemical decomposition of levofloxacin in aqueous solution, Water Environ. Res. 82 (2010) 696-700.
[43] H. Wei, D. Hu, J. Su, K. Li, Intensification of levofloxacin sono-degradation in a US/H_2O_2 system with Fe_3O_4 magnetic nanoparticles, Chinese J. Chem. Eng. 23 (2015) 296-302.
[44] Y. Hu, G. Wang, M. Huang, K. Lin, Y. Yi, Z. Fang, P. Li, K. Wang, Enhanced degradation of metronidazole by heterogeneous sono-Fenton reaction coupled ultrasound using Fe_3O_4 magnetic nanoparticles, Environ. Technol. (2017) 1-22.
[45] H.C. Yap, Y.L. Pang, S. Lim, A.Z. Abdullah, H.C. Ong, C.H. Wu, A comprehensive review on state-of-the-art photo-, sono-, and sonophotocatalytic treatments to degrade emerging contaminants, Int. J. Environ. Sci. Te. 16 (2019) 601-628.
[46] D.M. Montoya-Rodríguez, E.A. Serna-Galvis, F. Ferraro, R.A. Torres-Palma, Degradation of the emerging concern pollutant ampicillin in aqueous media by sonochemical advanced oxidation

processes-Parameters effect, removal of antimicrobial activity and pollutant treatment in hydrolyzed urine, J Environ. Manage. 261 (2020) 110224.
[47] S.G. Cetinkaya, M.H. Morcali, S. Akarsu, C.A. Ziba, M. Dolaz, Comparison of classic Fenton with ultrasound Fenton processes on industrial textile wastewater, Sustain. Environ. Res. 28 (2018) 165-170.
[48] E. Neyens, J. Baeyens, A review of classic Fenton's peroxidation as an advanced oxidation technique, J. Hazard. Mater. 98 (2003) 33-50.
[49] Z. Wu, M. Franke, B. Ondruschka, Y. Zhang, Y. Ren, P. Braeutigam, W. Wang, Enhanced effect of suction-cavitation on the ozonation of phenol, J. Hazard Mater. 190 (2011) 375-380.
[50] Z. Wu, H. Shen, B. Ondruschka, Y. Zhang, W. Wang, D.H. Bremner, Removal of blue-green algae using the hybrid method of hydrodynamic cavitation and ozonation, J. Hazard Mater. 235 (2012) 152-158.
[51] Y.G. Adewuyi, Sonochemistry: environmental science and engineering applications, Ind. Eng. Chem. Res. 40 (2001) 4681-4715.
[52] K.S Suslick, Sonochemistry, Science. 247 (1990) 1439-1445.
[53] L.H. Thompson, L.K. Doraiswamy, Sonochemistry: science and engineering, Ind. Eng. Chem. Res. 38 (1999) 1215-1249.
[54] C. Petrier, M.F. Lamy, A. Francony, A. Benahcene, B. David, V. Renaudin, N. Gondrexon, Sonochemical degradation of phenol in dilute aqueous solutions: comparison of the reaction rates at 20 and 487 kHz, J. Phys. Chem. A. 98 (1994) 10514-10520.
[55] E.B. Flint, K.S. Suslick , The temperature of cavitation, Science. 253 (1991) 1397-1399.
[56] K.S. Suslick, S.B. Choe, A.A. Cichowlas, M.W. Grinstaff, Sonochemical synthesis of amorphous iron, Nature. 353 (1991) 414-416.
[57] W.B. McNamara, Y.T. Didenko, K.S. Suslick, Sonoluminescence temperatures during multi-bubble cavitation, Nature. 401 (1999) 772-775.
[58] K.S. Suslick, E.B. Flint, Sonoluminescence from non-aqueous liquids, Nature. 330 (1987) 553-555.
[59] Y.T. Didenko, W.B. McNamara III, K.S. Suslick, Molecular emission from single-bubble sonoluminescence, Nature. 407 (2000) 877-879.
[60] N.C. Eddingsaas, K.S. Suslick , Light from sonication of crystal slurries, Nature. 444 (2006) 163-163.
[61] S.J. Doktycz, K.S. Suslick , Interparticle collisions driven by ultrasound, Science. 247 (1990) 1067-1069.
[62] P. Sathishkumar, R.V. Mangalaraja, S. Anandan, Review on the recent improvements in sonochemical and combined sonochemical oxidation processes–A powerful tool for destruction of environmental contaminants, Renew. Sust. Energ. Rev. 55 (2016) 426-454.
[63] K. Kümmerer, Antibiotics in the aquatic environment–a review–part II, Chemosphere. 75 (2009) 435-441.
[64] R. Daghrir, P. Drogui, Tetracycline antibiotics in the environment: a review, Environ. Chem. Lett. 11 (2013) 209-227.
[65] Z. Wu, B. Ondruschka, Roles of hydrophobicity and volatility of organic substrates on sonolytic kinetics in aqueous solutions, J. Phys. Chem. A. 109 (2005) 6521-6526.

[66] Z. Wu, B. Ondruschka, A. Stark, Ultrasonic cleavage of thioethers, J. Phys. Chem. A. 109 (2005) 3762-3766.
[67] Z. Wu, G. Cravotto, M. Adrians, B. Ondruschka, W. Li, Critical factors in sonochemical degradation of fumaric acid, Ultrason. Sonochem. 27 (2015) 148-152.
[68] Z. Wu, J. Lifka, B. Ondruschka , Comparison of energy efficiency of various ultrasonic devices in aquasonochemical reactions, Chem. Eng. Technol. 29 (2006) 610-615.
[69] D.M. Montoya-Rodríguez, Y. Ávila-Torres, E.A. Serna-Galvis, R.A. Torres-Palma, Data on treatment of nafcillin and ampicillin antibiotics in water by sonochemistry, Data Br. (2020) 105361.
[70] R. Xiao, D. Diaz-Rivera, L.K. Weavers, Factors influencing pharmaceutical and personal care product degradation in aqueous solution using pulsed wave ultrasound, Ind. Eng. Chem. Res. 52 (2013) 2824-2831.
[71] Y.A.J. Al-Hamadani, K.H. Chu, J.R.V. Flora, D.H. Kim, M. Jang, J. Sohn, W. Joo, Y. Yoon, Sonocatalytical degradation enhancement for ibuprofen and sulfamethoxazole in the presence of glass beads and single-walled carbon nanotubes, Ultrason. Sonochem. 32 (2016) 440-448.
[72] G. Wang, S. Li, X. Ma, J. Qiao, G. Li, H. Zhang, J. Wang, Y. Song, A novel Z-scheme sonocatalyst system, Er^{3+}: $Y_3Al_5O_{12}$@Ni($Fe_{0.\ 05}Ga_{0.95}$)$_2O_4$-Au-$BiVO_4$, and application in sonocatalytic degradation of sulfanilamide, Ultrason. Sonochem. 45 (2018) 150-166.
[73] A. Khataee, S. Fathinia, M. Fathinia, Production of pyrite nanoparticles using high energy planetary ball milling for sonocatalytic degradation of sulfasalazine, Ultrason. Sonochem. 34 (2017) 904-915.
[74] A. Seid-Mohammadi, G. Asgarai, Z. Ghorbanian, A. Dargahi, The removal of cephalexin antibiotic in aqueous solutions by ultrasonic waves/hydrogen peroxide/nickel oxide nanoparticles (US/H_2O_2/NiO) hybrid process, Sep. Sci. Technol. 55 (2020) 1558-1568.
[75] K. Zhang, Z. Luo, T. Zhang, N. Gao, Y. Ma, Degradation effect of sulfa antibiotics by potassium ferrate combined with ultrasound (Fe (VI)-US), Biomed Res. Int. (2015).
[76] X. Zou, T. Zhou, J. Mao, X. Wu, Synergistic degradation of antibiotic sulfadiazine in a heterogeneous ultrasound-enhanced Fe^0/persulfate Fenton-like system, Chem. Eng. J. 257 (2014) 36-44.
[77] Z. Wu, F.J. Yuste-Córdoba, P. Cintas, Z. Wu, L. Boffa, S. Mantegna, G. Cravotto, Effects of ultrasonic and hydrodynamic cavitation on the treatment of cork wastewater by flocculation and Fenton processes, Ultrason. Sonochem. 40 (2018) 3-8.
[78] R. Kıdak, Ş. Doğan , Medium-high frequency ultrasound and ozone based advanced oxidation for amoxicillin removal in water, Ultrason. Sonochem. 40 (2018) 131-139.
[79] W. Guo, R. Yin, X. Zhou, H. Cao, J. Chang, N. Ren, Ultrasonic-assisted ozone oxidation process for sulfamethoxazole removal: impact factors and degradation process, Desalin. Water Treat. 57 (2016) 21015-21022.
[80] Y. Wang, H. Zhang, L. Chen, S. Wang, D. Zhang, Ozonation combined with ultrasound for the degradation of tetracycline in a rectangular air-lift reactor, Sep. Purif. Technol. 84 (2012) 138-146.
[81] Z. Wu, A. Abramova, R. Nikonov, G. Cravotto, Sonozonation (sonication/ozonation) for the degradation of organic contaminants-a review, Ultrason. Sonochem. (2020) 105195.
[82] R. Yin, W. Guo, H. Wang, J. Du, X. Zhou, Q .Wu, H. Zheng, J. Chang, N. Ren, Enhanced peroxymonosulfate activation for sulfamethazine degradation by ultrasound irradiation: performances and mechanisms, Chem. Eng. J. 335 (2018) 145-153.

[83] A. Almasi, M. Mohammadi, F. Baniamerian, F. Baniamerian, Z. Berizi, M.H. Almasi, Z. Pariz, Modeling of antibiotic degradation in sonophotocatalytic process, increasing biodegradability and process optimization by response surface methodology (RSM), Int. J. Environ. Sci. Te. 16 (2019) 8437-8448.
[84] S.M. Ghoreishian, G.S.R. Raju, E. Pavitra, C.H. Kwak, Y.K. Han, Y.S. Huh, Ultrasound-assisted heterogeneous degradation of tetracycline over flower-like rGO/$CdWO_4$ hierarchical structures as robust solar-light-responsive photocatalysts: Optimization, kinetics, and mechanism, Appl. Surf. Sci. 489 (2019) 110-122.
[85] E. Hapeshi, I. Fotiou, D. Fatta-Kassinos, Sonophotocatalytic treatment of ofloxacin in secondary treated effluent and elucidation of its transformation products, Chem. Eng. J. 224 (2013) 96-105.
[86] R.D.C. Soltani, M. Mashayekhi, A. Khataee, M.J. Ghanadzadeh, M. Sillanpää, Hybrid sonocatalysis/electrolysis process for intensified decomposition of amoxicillin in aqueous solution in the presence of magnesium oxide nanocatalyst, J. Ind. Eng. Chem. 64 (2018) 373-382.
[87] Y. Ren, Z. Wu, M. Franke, P. Braeutigam, B. Ondruschka, D.J. Comeskey, P.M. King, Sonoelectrochemical degradation of phenol in aqueous solutions, Ultrason. Sonochem. 20 (2013) 715-721.
[88] Y. Ren, Z. Wu, B. Ondruschka, P. Braeutigam, M. Franke, H. Nehring, U. Hampel, Oxidation of Phenol by Microbubble‐Assisted Microelectrolysis, Chem. Eng. Technol. 34 (2011) 699-706.
[89] Z. Wu, , B. Ondruschka, G. Cravotto, Degradation of phenol under combined irradiation of microwaves and ultrasound, Environ. Sci. Technol. 42 (2008) 8083-8087.
[90] Franke, Marcus, *et al.*, Enhancement of chloroform degradation by the combination of hydrodynamic and acoustic cavitation, Ultrason. Sonochem. 18 (2011) 888-894.
[91] R.S. Sutar, V.K. Rathod, Ultrasound assisted Laccase catalyzed degradation of Ciprofloxacin hydrochloride, J. Ind. Eng. Chem. 31 (2015) 276-282.
[92] A.K. Subramani, P. Rani, P.H. Wang, B.Y. Chen, S. Mohan, C.T. Chang, Performance assessment of the combined treatment for oxytetracycline antibiotics removal by sonocatalysis and degradation using Pseudomonas aeruginosa, J. Environ. Chem. Eng. 7 (2019) 103215.
[93] R. Pulicharla, R.K. Das, S.K. Brar, P. Drogui, R.Y. Surampalli, Degradation kinetics of chlortetracycline in wastewater using ultrasonication assisted laccase, Chem. Eng. J. 347 (2018) 828-835.
[94] W. Yan, Y. Xiao, W. Yan, R. Ding, S. Wang, F. Zhao, The effect of bioelectrochemical systems on antibiotics removal and antibiotic resistance genes: a review, Chem. Eng. J. 358 (2019) 1421-1437.
[95] M.S. Saghafinia, S.M. Emadian, M. Vossoughi, Performances evaluation of Photo-Fenton process and sonolysis for the treatment of Penicillin G formulation effluent, Procedia Environ. Sci. 8 (2011) 202-208.
[96] P. Villegas-Guzman, J. Silva-Agredo, A.L. Giraldo-Aguirre, O. Flórez-Acosta, C. Petrier, R.A. Torres-Palma, Enhancement and inhibition effects of water matrices during the sonochemical degradation of the antibiotic dicloxacillin, Ultrason. Sonochem. 22 (2015) 211-219.

[97] A.M. Lastre-Acosta, G. Cruz-González, L. Nuevas-Paz, U.J. Jáuregui-Haza, A.C.S.C. Teixeira, Ultrasonic degradation of sulfadiazine in aqueous solutions, Environ. Sci. Pollut. R. 22 (2015) 918-925.
[98] X. Yang, H. Wei, K. Li, Q. He, J. Xie, J. Zhang, Iodine-enhanced ultrasound degradation of sulfamethazine in water, Ultrason. Sonochem. 42 (2018) 759-767.
[99] X. Wang, Y. Wang, D. Li, Degradation of tetracycline in water by ultrasonic irradiation, Water Sci. Technol. 67 (2013) 715-721.
[100] H. Rahmani, M. Gholami, A.H. Mahvi, M. Alimohammadi, G. Azarian, A. Esrafili, K. Rahmani, M. Farzadkia, Tinidazole removal from aqueous solution by sonolysis in the presence of hydrogen peroxide, B. Environ. Contam. Tox. 92 (2014) 341-346.
[101] A. Mirzaei, F. Haghighat, Z. Chen, L. Yerushalmi, Sonocatalytic removal of ampicillin by Zn(OH)F: Effect of operating parameters, toxicological evaluation and by-products identification, J. Hazard Mater. 375 (2019) 86-95.
[102] P. Gholami, L. Dinpazhoh, A. Khataee, A. Hassani, A. Bhatnagar, Facile hydrothermal synthesis of novel Fe-Cu layered double hydroxide/biochar nanocomposite with enhanced sonocatalytic activity for degradation of cefazolin sodium, J. Hazard Mater. 381 (2020) 120742.
[103] P. Gholami, L. Dinpazhoh, A. Khataee, Y. Orooji, Sonocatalytic activity of biochar-supported ZnO nanorods in degradation of gemifloxacin: synergy study, effect of parameters and phytotoxicity evaluation, Ultrason. Sonochem. 55 (2019) 44-56.
[104] R.D.C. Soltani, M. Mashayekhi, M. Naderi, G. Boczkaj, S. Jorfi, M. Safari, Sonocatalytic degradation of tetracycline antibiotic using zinc oxide nanostructures loaded on nano-cellulose from waste straw as nanosonocatalyst, Ultrason. Sonochem. 55 (2019) 117-124.
[105] M. Hoseini, G.H. Safari, H. Kamani, J. Jaafari, M. Ghanbarain, A.H. Mahvi, Sonocatalytic degradation of tetracycline antibiotic in aqueous solution by sonocatalysis, Toxicol. Environ. Chem. 95 (2013) 1680-1689.
[106] A. Khataee, R. Hassandoost, S.R. Pouran, Cerium-substituted magnetite: Fabrication, characterization and sonocatalytic activity assessment, Ultrason. Sonochem. 41 (2018) 626-640.
[107] Li, Siyi, *et al.*, Sonocatalytic degradation of norfloxacin in aqueous solution caused by a novel Z-scheme sonocatalyst, mMBIP-MWCNT-In_2O_3 composite, J. Mol. Liq. 254 (2018) 166-176.
[108] Y. He, Z. Ma, L.B. Junior, Distinctive binary g-C_3N4/MoS_2 heterojunctions with highly efficient ultrasonic catalytic degradation for levofloxacin and methylene blue, Ceram. Int. (2020).
[109] A. Khataee, P. Gholami, B. Kayan, D. Kalderis, L. Dinpazhoh, S. Akay, Synthesis of ZrO_2 nanoparticles on pumice and tuff for sonocatalytic degradation of rifampin, Ultrason. Sonochem. 48 (2018) 349-361.
[110] J. Qiao, M. Lv, Z. Qu, M. Zhang, X. Cui, D. Wang, C. Piao, Z. Liu, J. Wang, Y. Song, Preparation of a novel Z-scheme $KTaO_3$/$FeVO_4$/Bi_2O_3 nanocomposite for efficient sonocatalytic degradation of ceftriaxone sodium, Sci. Total Environ. 689 (2019) 178-192.
[111] M. Harrabi, H.B. Ammar, K. Mbarki, I. Naifar, C. Yaiche, F. Aloulou, B. Elleuch, Ultrasonic power improvement of flumequine degradation effectiveness in aqueous solution via direct and indirect action of mechanical acoustic wave, Ultrason. Sonochem. 48 (2018) 517-522.
[112] R.D.C. Soltani, M. Mashayekhi, S. Jorfi, A. Khataee, M.J. Ghanadzadeh, M. Sillanpää, Implementation of martite nanoparticles prepared through planetary ball milling as a heterogeneous

activator of oxone for degradation of tetracycline antibiotic: Ultrasound and peroxy-enhancement, Chemosphere. 210 (2018) 699-708.
[113] Ammar, Hafedh Belhadj, Sono-Fenton process for metronidazole degradation in aqueous solution: effect of acoustic cavitation and peroxydisulfate anion, Ultrason. Sonochem. 33 (2016) 164-169.
[114] A. Almasi, A. Dargahi, M. Mohamadi, H. Biglari, F. Amirian, M. Raei, Removal of Penicillin G by combination of sonolysis and Photocatalytic (sonophotocatalytic) process from aqueous solution: process optimization using RSM (Response Surface Methodology), Electron. Physician. 8 (2016) 2878.
[115] T. Zhou, X. Wu, Y. Zhang, J. Li, T.T. Lim, Synergistic catalytic degradation of antibiotic sulfamethazine in a heterogeneous sonophotolytic goethite/oxalate Fenton-like system, Appl. Catal. B Environ. 136 (2013) 294-301.
[116] T. Zhou, X. Wu, J. Mao, Y. Zhang, T.T. Lim, Rapid degradation of sulfonamides in a novel heterogeneous sonophotochemical magnetite-catalyzed Fenton-like (US/UV/Fe_3O_4/oxalate) system, Appl. Catal. B Environ. 160 (2014) 325-334.
[117] V. Vinesh, A.R.M. Shaheer, B. Neppolian, Reduced graphene oxide (rGO) supported electron deficient B-doped TiO_2 (Au/B-TiO_2/rGO) nanocomposite: an efficient visible light sonophotocatalyst for the degradation of Tetracycline (TC), Ultrason. Sonochem. 50 (2019) 302-310.
[118] A. Khataee, T.S. Rad, S. Nikzat, A. Hassani, M.H. Aslan, M. Kobya, E. Demirbaş, Fabrication of NiFe layered double hydroxide/reduced graphene oxide (NiFe-LDH/rGO) nanocomposite with enhanced sonophotocatalytic activity for the degradation of moxifloxacin, Chem. Eng. J. 375 (2019) 122102.
[119] M. Hosseini, M.R.R. Kahkha, A. Fakhri, S. Tahami, M.J. Lariche, Degradation of macrolide antibiotics via sono or photo coupled with Fenton methods in the presence of ZnS quantum dots decorated SnO_2 nanosheets, J. Photochem. Photobio. B Biol. 185 (2018) 24-31.
[120] V. Naddeo, C.S. Uyguner-Demirel, M. Prado, A. Cesaro, V. Belgiorno, F. Ballesteros, Enhanced ozonation of selected pharmaceutical compounds by sonolysis, Environ. Technol. (United Kingdom). 36 (2015) 1876-1883.
[121] W. Guo, R. Yin, X. Zhou, J. Du, H. Cao, S. Yang, N. Ren, Sulfamethoxazole degradation by ultrasound/ozone oxidation process in water: kinetics, mechanisms, and pathways, Ultrason. Sonochem. 22 (2015) 182-187.
[122] Y.H. Huang, H.T. Su, L.W. Lin, Degradation of furfural in aqueous solution using activated persulfate and peroxymonosulfate by ultrasound irradiation, J. Environ. Sci. 266 (2020) 110616.
[123] H. Zhang, L. Duan, D. Zhang , Decolorization of methyl orange by ozonation in combination with ultrasonic irradiation, J. Hazard Mater. 138 (2006) 53-59.
[124] R. Xiao, Z. He, D. Diaz-Rivera, G.Y. Pee, L.K. Weavers, Sonochemical degradation of ciprofloxacin and ibuprofen in the presence of matrix organic compounds, Ultrason. Sonochem. 21 (2014) 428-435.
[125] E. De Bel, C. Janssen, S. De Smet, H. Van Langenhove, J. Dewulf, Sonolysis of ciprofloxacin in aqueous solution: Influence of operational parameters, Ultrason. Sonochem. 18 (2011) 184-189.
[126] K.S. Suslick, J.J. Gawienowski, P.F. Schubert, H.H. Wang, Alkane sonochemistry, J. Phys. Chem. 87 (1983) 2299-2301.

[127] W. Guo, H. Wang, Y. Shi, G. Zhang, Sonochemical degradation of the antibiotic cephalexin in aqueous solution, Water SA. 36 (2010).
[128] E.A. Serna-Galvis, J. Silva-Agredo, A.L. Giraldo-Aguirre, O.A. Flórez-Acosta, R.A. Torres-Palma, High frequency ultrasound as a selective advanced oxidation process to remove penicillinic antibiotics and eliminate its antimicrobial activity from water, Ultrason. Sonochem. 31 (2016) 276-283.
[129] E.A. Serna-Galvis, D. Montoya-Rodríguez, L. Isaza-Pineda, M. Ibáñez, F. Hernández, A. Moncayo-Lasso, R.A. Torres-Palma, Sonochemical degradation of antibiotics from representative classes-Considerations on structural effects, initial transformation products, antimicrobial activity and matrix, Ultrason. Sonochem. 50 (2019) 157-165.
[130] P. Villegas-Guzman, J. Silva-Agredo, O. Florez, A.L. Giraldo-Aguirre, C. Pulgarin, R.A. Torres-Palma, Selecting the best AOP for isoxazolyl penicillins degradation as a function of water characteristics: Effects of pH, chemical nature of additives and pollutant concentration, J. Environ. Manage. 190 (2017) 72-79.
[131] G.H. Safari, S. Nasseri, A.H. Mahvi, K. Yaghmaeian, R. Nabizadeh, M. Alimohammadi, Optimization of sonochemical degradation of tetracycline in aqueous solution using sono-activated persulfate process, J. Environ. Health Sci. Eng. 13 (2015) 76.
[132] M. Matouq, T. Tagawa, S. Nii, High frequency ultrasound waves for degradation of amoxicillin in the presence of hydrogen peroxides for industrial pharmaceutical wastewater treatment, Glob. NEST J. 16 (2014) 805-813.
[133] W. Guo, Y. Shi, H. Wang, H. Yang, G. Zhang, Intensification of sonochemical degradation of antibiotics levofloxacin using carbon tetrachloride, Ultrason. Sonochem. 17 (2010) 680-684.
[134] S. Dehghan, B. Kakavandi, R.R. Kalantary, Heterogeneous sonocatalytic degradation of amoxicillin using ZnO@Fe_3O_4 magnetic nanocomposite: influential factors, reusability and mechanisms, J. Mol. Liq. 264 (2018) 98-109.
[135] A. Hassani, A. Khataee, S. Karaca, C. Karaca, P. Gholami, Sonocatalytic degradation of ciprofloxacin using synthesized TiO_2 nanoparticles on montmorillonite, Ultrason. Sonochem. 35 (2017) 251-262.
[136] J. Qiao, H. Zhang, G. Li, S. Li, Z. Qu, M. Zhang, J. Wang, Y. Song, Fabrication of a novel Z-scheme $SrTiO_3/Ag_2S/CoWO_4$ composite and its application in sonocatalytic degradation of tetracyclines, Sep. Purif. Technol. 211 (2019) 843-856.
[137] A.A. Pradhan, P.R. Gogate, Degradation of p-nitrophenol using acoustic cavitation and Fenton chemistry, J. Hazard Mater. 173 (2010) 517-522.
[138] D.H. Bremner, S. Di Carlo, A.G. Chakinala, G. Cravotto, Mineralisation of 2, 4-dichlorophenoxyacetic acid by acoustic or hydrodynamic cavitation in conjunction with the advanced Fenton process, Ultrason. Sonochem. 15 (2008) 416-419.
[139] Y. Guo, X. Mi, G. Li, X. Chen, Sonocatalytic degradation of antibiotics tetracycline by Mn-modified diatomite, J. Chem. (2017).
[140] S. Hu, L. Li, M. Luo, Y. Yun, C. Chang , Aqueous norfloxacin sonocatalytic degradation with multilayer flower-like ZnO in the presence of peroxydisulfate, Ultrason. Sonochem. 38 (2017) 446-454.

[141] S. Rahdar, C.A. Igwegbe, A. Rahdar, S. Ahmadi, Efficiency of sono-nano-catalytic process of magnesium oxide nano particle in removal of penicillin G from aqueous solution, Desalin. Water Treat. 106 (2018) 330-335.
[142] A. Yazdani, M.H. Sayadi, Sonochemical degradation of azithromycin in aqueous solution, Environ. Health. Eng. Manag. J. 5 (2018) 85-92.
[143] Y. Deng, C.M. Ezyske, Sulfate radical-advanced oxidation process (SR-AOP) for simultaneous removal of refractory organic contaminants and ammonia in landfill leachate, Water Res. 45 (2011) 6189-6194.
[144] N. Yousef Tizhoosh, A. Khataee, R. Hassandoost, R. Darvishi Cheshmeh Soltani, E. Doustkhah, Ultrasound-engineered synthesis of WS_2@CeO_2 heterostructure for sonocatalytic degradation of tylosin, Ultrason. Sonochem. (2020) 105114.
[145] X. Meng, Y. Chu , Enhancement of chloramphenicol sonochemical degradation by sodium peroxydisulfate, Adv. Mater. Res. (2013) 33-36
[146] J. Wang, S. Wang, Activation of persulfate (PS) and peroxymonosulfate (PMS) and application for the degradation of emerging contaminants, Chem. Eng. J. 334 (2018) 1502-1517.
[147] J.K. Crandall, Y. Shi, C.P. Burke, Potassium monoperoxysulfate, in: Encyclopedia of Reagents for Organic Synthesis, John Wiley & Sons, Ltd. (2001).
[148] T. Zhou, X. Zou, J. Mao, X. Wu, Decomposition of sulfadiazine in a sonochemical Fe^0-catalyzed persulfate system: parameters optimizing and interferences of wastewater matrix, Appl. Catal. B: Environ. 185 (2016) 31-41.
[149] L. Hou, H. Zhang, X. Xue, Ultrasound enhanced heterogeneous activation of peroxydisulfate by magnetite catalyst for the degradation of tetracycline in water, Sep. Purif. Technol. 84 (2012) 147-152.
[150] A. Eslami, A. Asadi, M. Meserghani, H. Bahrami, Optimization of sonochemical degradation of amoxicillin by sulfate radicals in aqueous solution using response surface methodology (RSM), J. Mol. Liq. 222 (2016) 739-744.
[151] S. Wang, J. Wang , Carbamazepine degradation by gamma irradiation coupled to biological treatment, J. Hazard. Mater. 321 (2017) 639-646.
[152] A. Ghauch, A.M. Tuqan, Oxidation of bisoprolol in heated persulfate/H2O systems: kinetics and products, Chem. Eng. J. 183 (2012) 162-171.
[153] S. Yang, P. Wang, X. Yang, L. Shan, W. Zhang, X. Shao, R. Niu, Degradation efficiencies of azo dye Acid Orange 7 by the interaction of heat, UV and anions with common oxidants: persulfate, peroxymonosulfate and hydrogen peroxide, J. Hazard. Mater. 179 (2010) 552-558.
[154] N. Gao, Q. Wang, P. Rao, G. Li, L. Dong, X. Zhang, Y. Shao, W. Chu, B. Xu, N. An, J. Deng, Degradation of imidacloprid by UV-activated persulfate and peroxymonosulfate processes: Kinetics, impact of key factors and degradation pathway, Ecotox. Environ. Safe. 187 (2020) 109779.
[155] M. Kermani, M. Farzadkia, M. Morovati, M. Taghavi, S. Fallahizadeh, R. Khaksefidi, S. Norzaee, Degradation of furfural in aqueous solution using activated persulfate and peroxymonosulfate by ultrasound irradiation, J. Environ. Manag. 266 (2020) 110616.
[156] X. Ao, W. Liu, Degradation of sulfamethoxazole by medium pressure UV and oxidants: peroxymonosulfate, persulfate, and hydrogen peroxide, Chem. Eng. J. 313 (2017) 629-637.

[157] M. Ahmadi, F. Ghanbari, M. Moradi, Photocatalysis assisted by peroxymonosulfate and persulfate for benzotriazole degradation: effect of pH on sulfate and hydroxyl radicals, Water Sci. Technol. 72 (2015) 2095-2102.
[158] A. Rastogi, S.R. Al-Abed, D.D. Dionysiou, Sulfate radical-based ferrous–peroxymonosulfate oxidative system for PCBs degradation in aqueous and sediment systems, Appl. Catal. B. 85 (2009) 171-179.
[159] W. Guo, S. Su, C. Yi, Z. Ma, Degradation of antibiotics amoxicillin by Co_3O_4-catalyzed peroxymonosulfate system, Environ. Prog. Sustain. Energy. 32 (2013) 193-197.
[160] S. Nasseri, A.H. Mahvi, M. Seyedsalehi, K. Yaghmaeian, R. Nabizadeh, M. Alimohammadi, G.H. Safari, Degradation kinetics of tetracycline in aqueous solutions using peroxydisulfate activated by ultrasound irradiation: effect of radical scavenger and water matrix, J. Mol. Liq. 241 (2017) 704-714.
[161] Y. Pan, Y. Zhang, M. Zhou, J. Cai, X. Li, Y. Tian, Synergistic degradation of antibiotic sulfamethazine by novel pre-magnetized Fe^0/PS process enhanced by ultrasound, Chem. Eng. J. 354 (2018) 777-789.
[162] S. Su, W. Guo, C. Yi, Y. Leng, Z. Ma, Degradation of amoxicillin in aqueous solution using sulphate radicals under ultrasound irradiation, Ultrason. Sonochem. 19 (2012) 469-474.
[163] M. Malakotian, S.N. Asadzadeh, M. Khatami, M. Ahmadian, M.R. Heidari, P. Karimi, N. Firouzeh, S.V. Rajender, Protocol encompassing ultrasound/Fe_3O_4 nanoparticles/persulfate for the removal of tetracycline antibiotics from aqueous environments, Clean Techn. Environ. Policy. 21 (2019) 1665-1674.
[164] K. Roy, C. Agarkoti, R.S. Malani, B. Thokchom, V.S. Moholkar, Mechanistic study of sulfadiazine degradation by ultrasound-assisted Fenton-persulfat esystem using yolk-shell Fe_3O_4@hollow@$mSiO_2$ nanoparticles, Chem. Eng. Sci. 217 (2020) 115522.
[165] S. Jiao, S. Zheng, D. Yin, L. Wang, L. Chen, Aqueous photolysis of tetracycline and toxicity of photolytic products to luminescent bacteria, Chemosphere. 73 (2008) 377-382.
[166] Wikipedia, the free encyclopedia n.d., Beta-lactam core structures. Available from: https://en.wikipedia.org/wiki/File:Beta-lactam_core_structures.svg. 25 February 2021.
[167] Wikipedia, the free encyclopedia n.d., Tetracycline. Available from: https://de.wikipedia.org/wiki/Tetracycline. 25 February 2021.
[168] T.D. Pham, Z.M. Ziora, M.A. Blaskovich, Quinolone antibiotics, MedchemComm. 10 (2019) 1719-1739.
[169] M.I. Andersson, A.P. MacGowan, Development of the quinolones, J. Antimicrob. Chemoth. 51 (2003) 1-11.
[170] B. Schnyder, W.J. Pichler, Allergy to sulphonamides, J. allergy clin. immun. 131 (2013) 256-257.
[171] S. Mutak, Azalides from azithromycin to new azalide derivatives, J. antibiot. 60 (2007) 85-122.